

# **PTFE- and PEEK-Matrix Composites for Tribological Applications at Cryogenic Temperatures and in Hydrogen**

von der Fakultät III  
– Prozesswissenschaften –  
der Technischen Universität Berlin  
zur Erlangung des akademischen Grades

Doktor der Ingenieurwissenschaften  
– Dr.-Ing. –  
genehmigte Dissertation

vorgelegt von  
Géraldine Theiler  
aus Rennes, Frankreich

Tag der wissenschaftlichen Aussprache: 6. Mai 2005

Promotionsausschuss:

Vorsitzender:

Prof. Dr. rer. nat. H. Schubert

Gutachter:

Prof. Dr.-Ing. M. H. Wagner

Prof. Dr.-Ing. K. Friedrich

Die vorliegende Arbeit entstand an der Bundesanstalt für Materialforschung und -prüfung (BAM).

Impressum

BAM-Dissertationsreihe – Band 14

**PTFE- and PEEK-Matrix Composites  
for Tribological Applications at  
Cryogenic Temperatures and in Hydrogen**

2005

Herausgeber:

Bundesanstalt für Materialforschung und -prüfung (BAM)

Unter den Eichen 87

12205 Berlin

Telefon: +49 30 8104-0

Telefax: +49 30 8112029

E-mail: [info@bam.de](mailto:info@bam.de)

Internet: [www.bam.de](http://www.bam.de)

Copyright © 2005 by Bundesanstalt für  
Materialforschung und -prüfung (BAM)

Verlag und Vertrieb:

Wirtschaftsverlag NW

Verlag für neue Wissenschaft GmbH

27568 Bremerhaven

Telefon: +49 471 94544-0

Telefax: +49 471 94544-77/-88

Layout: BAM-Arbeitsgruppe Z.67

ISSN 1613-4249

ISBN 3-86509-378-7

## Acknowledgement

This work is based on a joined project between the Federal Institute for Materials Research and Testing, BAM, Berlin, and the Institute for Composite Materials, IVW, Kaiserslautern. My first thank goes to the German Science Foundation (DFG) for its financial support.

Thermophysical and mechanical tests were performed thanks to a EU sponsorship at the Aerospace Materials Technology Testhouse (AMTT) of the Austrian Research Centers Seibersdorf (ARCS).

The thesis has been elaborated in the Division VIII.1 of BAM, Tribology and Wear Prevention, under the direction of Prof. Erich Santner. Sincere thanks are due to him, who gave me the opportunity to work with experienced tribology specialists. My gratitude goes to the whole Division VIII.1 for their great help and cooperation. A special thank is due to Dr. Wolfgang Hübner, who initiated this project and provided precious advice, fruitful discussions and encouragement throughout my work. Also, I would like to express my sincere gratitude to Dr. Thomas Gradt for his great assistance, as well as Dipl.-Ing. Helmut Börner, Mr. Matthias Heidrich, Mr. Olaf Berndes and Mrs. Sigrid Binkowski for their technical support. Many thanks are due to Dr. Kerstin Meine and Dr. Thomas Schneider for the AFM analyses.

Furthermore, I greatly appreciate the contributions of the laboratory VIII.23 of BAM, in particular Dr. Wolfgang Unger, Dr. Thomas Gross, Mrs. Sigrid Benemann and Mr. Dieter Treu, for SEM, EDX and XPS analyses.

Also, many thanks to our project partners at IVW, Kaiserslautern, in particular to Prof. K. Friedrich for the good cooperation, his precious discussions and expertise for this thesis.

In additions, my sincere thanks go to Prof. M.H. Wagner (TU Berlin), major professor of the thesis, for his grateful assistance throughout this work, as well as Prof. H. Schubert (TU Berlin) for chairing the examination.

Finally, I would like to thank my husband André for his constructive comments and great encouragement. I dedicate this work to him and our daughter Océane.

A handwritten signature in black ink, reading "Geraldine Heitel". The signature is written in a cursive style with a large initial "G" and a long horizontal stroke extending to the right.

Berlin, May 2005



## Abstract

Many new technologies are based on applications in extreme conditions, such as at low temperatures or in hydrogen environment. This involves new requirements on material properties, in particular regarding their operability and reliability. To fulfil this demand, the tribological behaviour of PTFE- and PEEK-matrix composites filled with carbon fibres were investigated at cryogenic temperatures and in hydrogen by means of surface analyses.

For a better understanding of the tribological behaviour, and because of the temperature-dependent characteristics of polymer materials, thermal and mechanical properties of selected composites were initially investigated at low temperatures. Thermal shock experiments as well as cryo- and hydrogen treatments were carried out. Different coefficients of thermal expansion within the composite lead to debondings of particles, particularly in the case of PTFE materials.

Tensile tests indicate that the YOUNG's modulus increases at  $T = 77$  K compared to room temperature. However, this improvement at low temperatures is moderate for PEEK composite which is already under its glass transition at room temperature.

In the main investigation, tribological experiments were carried out at first at  $T = 77$  K to observe the influence of the matrix, fillers and fibres on the material behaviour comparing to room temperature. The reduction of the friction coefficient and wear at low temperatures has been attributed to the low temperature properties of the polymer in particular due to the higher YOUNG's modulus at  $T = 77$  K. Whereas at room temperature friction and wear depend strongly of the CF content, the quantity of fillers and fibres does not have a significant effect on the tribological behaviour at low temperatures. At  $T = 77$  K, the tribological behaviour of PTFE and PEEK composites is mainly influenced by the matrix. PEEK composites have a better tribological performance than PTFE materials especially regarding the wear resistance.

Furthermore, the influence of the cryogenic medium was determined with experiments carried out in LN<sub>2</sub> ( $T = 77$  K), LH<sub>2</sub> ( $T = 20$  K) and LHe ( $T = 4.2$  K), as well as in helium at  $T = 77$  K and hydrogen at room temperature. The thermal properties of the cryogenic medium have a significant influence on the tribological performances of the composites.

Due to the lower frictional heat at low sliding speed, the effect of low temperatures on the tribological behaviour of these composites was more clearly detected in this case, with a change in wear mechanism from mainly adhesive to more abrasive.

Experiments in LN<sub>2</sub> give the best friction and wear performance at low as well as at high sliding speed. The behaviour of these composites in LHe does not benefit from the low temperature properties of polymers due to the low heat of evaporation of LHe.

The influence of hydrogen was particularly seen after the tribological experiments performed in LH<sub>2</sub> on the surface of the disc. The reduction effect of hydrogen may have an influence on the tribochemical reactions which appear during sliding, enhancing the formation of iron fluorides, but no influence of the metal fluorides on the tribological performance could be determined in this study.



## Zusammenfassung

Viele neue Technologien nutzen Anwendungen bei extremen Bedingungen, wie etwa bei tiefen Temperaturen oder in Wasserstoffumgebung. Dies stellt neue Forderungen an die Werkstoffe, insbesondere an ihre Funktionsfähigkeit und Zuverlässigkeit. Um dem gerecht zu werden, wurde das tribologische Verhalten von kohlefaserverstärkten PTFE- und PEEK-Verbundwerkstoffen bei tiefen Temperaturen und in Wasserstoff mit Hilfe von Oberflächenanalysen untersucht.

Für ein besseres Verständnis des tribologischen Verhaltens und wegen der temperaturabhängigen Eigenschaften der Polymere wurden zuerst thermische und mechanische Untersuchungen bei tiefen Temperaturen durchgeführt. Temperatur-Wechselbeanspruchungen sowie Kryo- und Wasserstoffbehandlungen wurden durchgeführt. Unterschiedliche Wärmeausdehnungskoeffizienten innerhalb der Materialien verursachen Trennungen von Partikeln besonders bei PTFE-Verbundwerkstoffen.

Experimente zur Bestimmung der Zugfestigkeit zeigen an, dass der E-Modul bei  $T = 77$  K im Vergleich zur Raumtemperatur zunimmt. Diese Verbesserung ist jedoch für PEEK-Material nicht sehr ausgeprägt, da es sich bei Raumtemperatur bereits unter seinem Glasübergang befindet.

In der Hauptuntersuchung wurden tribologische Experimente zuerst bei  $T = 77$  K durchgeführt, um den Einfluss der Matrix, der Füllstoffe und der Fasern auf das Materialverhalten im Vergleich zur Raumtemperatur zu beobachten. Der Reibwert- und die Verschleißabnahme bei  $T = 77$  K ist mit den Tieftemperatur-Eigenschaften der Polymer-Materialien zu erklären, insbesondere wegen des höheren E-Moduls bei  $T = 77$  K. Während Reibung und Verschleiß bei Raumtemperatur stark von dem CF-Gehalt abhängig sind, hat die Menge der Füllstoffe und der Fasern wenigen Effekt auf das tribologische Verhalten bei tiefen Temperaturen.

Bei 77 K ist das tribologische Verhalten von PTFE und PEEK hauptsächlich durch die Matrix bestimmt. PEEK-Komposite haben ein besseres tribologisches Verhalten als PTFE, insbesondere im Hinblick auf den Verschleißwiderstand.

Außerdem wurde der Einfluss des Kältemittels mit tribologischen Experimenten untersucht, die in  $\text{LN}_2$  ( $T = 77$  K),  $\text{LH}_2$  ( $T = 20$  K) und  $\text{LHe}$  ( $T = 4,2$  K), sowie in Helium bei  $T = 77$  K und Wasserstoff bei Raumtemperatur durchgeführt wurden. Die thermischen Eigenschaften des Kältemittels haben einen bedeutenden Einfluss auf die tribologischen Eigenschaften.

Wegen der niedrigeren Reibungswärme bei geringerer Gleitgeschwindigkeit wurde die Wirkung der Tieftemperaturen auf das tribologische Verhalten dieser Verbundwerkstoffe in diesem Fall besonders deutlich. Dabei ist der Wechsel des Verschleißmechanismus von vorwiegend adhäsiv zu vorwiegend abrasiv zu beobachten.

Ergebnisse in  $\text{LN}_2$  zeigen die niedrigsten Reibungszahlen und Verschleißwerte, sowohl bei niedriger als auch bei hoher Gleitgeschwindigkeit. Das Verhalten dieser Verbundwerkstoffe in  $\text{LHe}$  profitiert aufgrund dessen geringer Verdampfungswärme nicht von den Tieftemperatur-Eigenschaften der Polymere.

## Zusammenfassung

Der Einfluss des Wasserstoffs wurde besonders bei den Oberflächenanalysen der Scheibe nach den tribologischen Experimenten in  $\text{LH}_2$  beobachtet. Die reduzierende Eigenschaft des Wasserstoffs könnte einen Einfluss auf die tribochemischen Reaktionen und darüber hinaus eine fördernde Wirkung auf die Bildung der Metallfluoride haben. Ein Einfluss dieser Metallfluoride auf das tribologische Verhalten konnte in dieser Arbeit nicht beobachtet werden.



# Contents

<b>Acknowledgement</b>	<b>III</b>
<b>Abstract</b>	<b>V</b>
<b>Zusammenfassung</b>	<b>VII</b>
<b>Contents</b>	<b>IX</b>
<b>Nomenclature</b>	<b>XIII</b>
<b>1 Introduction and Aim of the Study</b>	<b>1</b>
1.1 Introduction	1
1.2 Applications: tribosystems in cryotechnics	3
1.3 Problems in cryogenic applications	4
1.4 Aim and structure of the study	4
<b>2 State of the Art</b>	<b>7</b>
2.1 Basics of tribology	7
2.1.1 Definitions	7
2.1.2 Surfaces in contact	7
2.1.2.1 Real area of contact	7
2.1.2.2 Surface temperature	9
2.1.3 Friction	9
2.1.3.1 Mechanisms of friction	10
2.1.3.2 The adhesion component of friction	10
2.1.3.3 The deformation component of friction	11
2.1.4 Wear	12
2.1.4.1 Mechanisms of wear	12
2.1.4.2 Wear measurements	14
2.1.5 Tribological system	15
2.2 Properties of polymer composites	16
2.2.1 Polymer composites in tribology	16
2.2.2 Low temperature properties	18
2.2.2.1 Specific heat	18
2.2.2.2 Thermal expansion	19
2.2.2.3 Thermal conductivity	20
2.2.2.4 Mechanical deformation behaviour	21
2.2.3 Properties in liquid hydrogen	22
2.3 Cryotribology	23

## Contents

<b>3</b>	<b>Experiments</b>	<b>25</b>
3.1	Materials	25
3.1.1	Polymer composites	25
3.1.1.1	Matrix	25
3.1.1.2	Reinforcing fibres	26
3.1.1.3	Fillers	27
3.1.1.4	Compositions	27
3.1.1.5	Processing	30
3.1.2	Steel counterface	30
3.2	Cryogenic environments	30
3.3	Test procedures	32
3.3.1	Thermophysical testings	32
3.3.2	Thermal and environmental testings	32
3.3.3	Mechanical testings	33
3.3.4	Tribological tests	34
3.3.5	Surface analyses	36
<b>4</b>	<b>Results</b>	<b>37</b>
4.1	Material properties	37
4.1.1	Thermophysical testings	37
4.1.1.1	Specific heat	37
4.1.1.2	Thermal expansion	37
4.1.1.3	Thermal conductivity	41
4.1.2	Thermal and environmental treatments	41
4.1.2.1	Thermal shock cycle experiments	41
4.1.2.2	Cryo-treatment	45
4.1.2.3	Thermal ageing in hydrogen	46
4.1.3	Mechanical testings	46
4.2	Tribological experiments	49
4.2.1	Selection of test parameters	49
4.2.1.1	Load and surface preparation	49
4.2.1.2	Sliding distance and velocity	50
4.2.1.3	Wear measurement	51
4.2.1.4	Test parameters	51
4.2.2	Influence of the thermal treatment on friction at RT	51

4.2.3	Influence of the material composition at RT and at $T = 77\text{K}$	54
4.2.3.1	Friction and wear measurements	54
4.2.3.2	Surface analyses of the pins	59
4.2.3.3	Surface analyses of the discs	65
4.2.4	Influence of the cryogenic environment	70
4.2.4.1	Friction measurements	70
4.2.4.2	Wear measurements	75
4.2.4.3	Surface analyses	76
<b>5</b>	<b>Discussion</b>	<b>89</b>
5.1	Material properties	89
5.1.1	Thermophysical testings	89
5.1.2	Thermal and environmental testings	89
5.1.2.1	Thermal shock cycles	89
5.1.2.2	Cryo-treatment	90
5.1.2.3	Thermal ageing in hydrogen	90
5.1.3	Mechanical testings	91
5.1.4	Consequences for tribological applications	92
5.2	Tribological experiments	92
5.2.1	Influence of the thermal treatments on friction at RT	92
5.2.2	Influence of the material composition at RT and at $T = 77\text{ K}$	93
5.2.2.1	PTFE and PEEK content	93
5.2.2.2	Carbon fibre content	95
5.2.2.3	Fillers in PTFE and transfer film formation	95
5.2.3	Influence of the cryogenic environment	97
5.2.3.1	Friction	97
5.2.3.2	Wear	101
5.2.3.3	Chemical analyses of the transfer film	102
<b>6</b>	<b>Conclusion</b>	<b>105</b>
	<b>References</b>	<b>109</b>



## Nomenclature

As commonly used in cryogenic studies, temperatures are given in Kelvin. However, some important polymer properties are indicated as well in Celsius, which is generally found in the literature.

AFM	Atomic Force Microscopy
CF	Carbon fibres
DIN	Deutsches Institut für Normung
DSC	Differential Scanning Calorimetry
EDX	Energy Dispersive X-ray spectroscopy
GF	Glass fibres
He	Helium
LH <sub>2</sub>	Liquid hydrogen
LHe	Liquid helium
LN <sub>2</sub>	Liquid nitrogen
PEEK	Poly(etheretherketone)
PTFE	Poly(tetrafluoroethylene)
RT	Room temperature
SEM	Scanning Electron Microscopy
XPS	X-Ray Photo Electron Spectroscopy

$\alpha_e$	coefficient of thermal expansion	1
$\alpha_\tau, \alpha_0$	pressure coefficient of $\tau$	1
$\beta$	roughness coefficient	1
$\varepsilon$	deformation	1
$\gamma_a$	surface energy of body a	J/m <sup>2</sup>
$\gamma_{ab}$	boundary surface energy	J/m <sup>2</sup>
$\gamma_b$	surface energy of body b	J/m <sup>2</sup>
$\gamma_g$	GRUENEISEN parameter	1
$\tan \delta$	mechanical loss factor	1
$\phi$	relative contact area	1

## Nomenclature

$\kappa$	thermal diffusivity	m <sup>2</sup> /s
$\lambda$	thermal conductivity	W/(m K)
$\lambda_a$	thermal conductivity for amorphous polymer	W/(m K)
$\lambda_{semi}$	thermal conductivity for semicrystalline polymer	W/(m K)
$\mu$	coefficient of friction	1
$\mu_a$	adhesion component of the coefficient of friction	1
$\mu_d$	deformation component of the coefficient of friction	1
$\eta_0$	viscosity of the viscoplastic state	MPa s
$\eta_r$	viscosity of the relaxed state	MPa s
$\rho$	density	kg/m <sup>3</sup>
$\sigma_0$	unidirectional stress	MPa
$\sigma_y$	yield strength	MPa
$\sigma_{dF}$	compression yield point	MPa
$\tau$	time of relaxation	s
$\tau_s$	shear strength	MPa
$\xi$	parameter depending on the surface	1
$A_i^j$	area of individual contact spots	m <sup>2</sup>
$A$	area	m <sup>2</sup>
$A_0$	nominal area of contact	m <sup>2</sup>
$A_r$	real area of contact	m <sup>2</sup>
$c$	proportionality factor	1
$c_{com}$	specific heat of the composite	kJ/(kg K)
$c_f$	specific heat of the fillers	kJ/(kg K)
$c_m$	specific heat of the matrix	kJ/(kg K)
$c_p$	specific heat	kJ/(kg K)
$E$	YOUNG's modulus	MPa
$E_r$	relaxation modulus	MPa
$F_a$	adhesion component of the friction force	N
$F_d$	deformation component of the friction force	N

$F_f$	friction force	N
$F_N$	normal load	N
$h$	depth of penetration	$\mu\text{m}$
$h_e$	depth of elastic penetration	$\mu\text{m}$
$h_{\text{max}}$	maximal roughness	$\mu\text{m}$
$h_p$	depth of plastic penetration	$\mu\text{m}$
$k$	wear factor	$\text{mm}^3/\text{Nm}$
$K$	compression modulus	MPa
$\Delta l$	length change	m
$n, n_1, n_2$	exponential factor	1
$p$	normal pressure	MPa
$p_y$	yield pressure	MPa
$\dot{Q}$	heat power	W
$q$	heat flux density	$\text{W}/\text{cm}^2$
$q_c$	critical heat flux density	$\text{W}/\text{cm}^2$
$q_r$	calculated heat flux density	$\text{W}/\text{cm}^2$
$s$	sliding distance	m
$T$	temperature	K
$t$	time	s
$T_b$	boiling temperature	K
$T_{\text{bulk}}$	bulk temperature	K
$T_c$	critical temperature	K
$T_{\text{flash}}$	flash temperature	K
$T_g$	glass transition	K
$T_i$	instantaneous temperature	K
$v$	sliding velocity	m/s
$V_f$	filler content by volume	1
$W_{\text{ab}}$	least energy needed to separate contacting surfaces	$\text{J}/\text{m}^2$
$W_h$	linear wear	m
$W_v$	wear volume	$\text{m}^3$





# 1 Introduction and Aim of the Study

## 1.1 Introduction

Up to now, low temperature technology has been mainly restricted to space applications and in superconductivity. To a minor extend, cryogenic engineering is involved in cryogenic treatment of materials and medical diagnostic.

However, new applications of cryotechnology are ready to take off in the near future.

After the rocket technology showed the large potential of using liquid hydrogen (LH<sub>2</sub>) for efficient and even pollution free power supply systems, the use of liquid hydrogen as an environmentally friendly energy supply and transportation system receives more and more interest [Spin98]. Recent publications [DWV04] reported many applications of hydrogen for aviation and automobile: Munich airport is equipped with hydrogen buses, BMW produced cars with hydrogen combustion and the Deutsche Aerospace Airbus (DASA) is currently developing the prototype of an aircraft with a hydrogen engine.

These applications involve new requirements of material properties, in particular regarding operability and reliability. Materials developed in the past cannot be transferred directly to new areas of cryogenic applications without more intense investigations. Requirements can differ considerably from those already established in cryotechnical systems. One example, described in [Hüb98], is the hydrogen technology.

- Liquid hydrogen-fuelled propulsion units for space flights are constructed for a few minutes lifetime. Propulsions units for aircraft have to work more than 40,000 hours. The long term behaviour of materials and components is yet unknown.
- In the space shuttle, the main engines are powered by LH<sub>2</sub> and LOx, which are pressurized by turbopumps with rotational speeds up to 50 000 min<sup>-1</sup> with working temperatures ranging from  $T = 20$  K to  $T = 900$  K.
- For civilian applications, the safety of the equipment should be the prime requirement, since the technology is used by many people.

Undetected leaks which can develop during operation can cause uncontrolled escape of gas with the consequence that ignitable gas mixtures may occur, and in the case of hydrogen, this can cause violent fire. Special attention must be paid to permeation, sealing and insulation.

Systematic investigations of materials at low temperatures are mainly focussed on thermal and mechanical characteristics [Kase75, Hart97a, Ahlb89, Ahlb91, Reed83].

Stainless steels are well qualified for cryogenic applications because of the properties of their austenitic structure which enables high strength and sufficient ductility even at low temperatures. However, due to their high density, they tend to be replaced in many applications by polymer and polymer composites. Furthermore, in LH<sub>2</sub>, the formation of martensite structure can lead to losses of ductility and changes in magnetic properties [Hüb01].

## 1 Introduction and Aim of the Study

At low temperatures, the YOUNG's modulus and the hardness of polymers are much higher compared to room temperature, whereas the already low heat conductivity continues to decrease [Hart94]. Polymers are particularly suitable for cryogenic applications because of their low thermal and electrical conductivity as well as their permeation characteristics for applications in superconductivity [Sana97]. Fibre reinforced epoxy resins have been well investigated [Suzu97, Taka97] and used in aerospace. In particular, the outstanding features of fibre composites favour their application in low temperature technology. The high specific strength and stiffness, the high fatigue life and the low density are some of the advantages in their use in cryogenic system as alternative to metals. Some of the main areas of applications of fibre composites at low temperatures are presented in *Table 1.1*.

In hydrogen technology, fibre reinforced polymer composites are prime candidates and are used in lightweight pressure vessels for storage and transportation of liquefied gases [Hart98].

Components of cryotechnical machines and plants with interacting surfaces in relative motion such as bearings, seals or valves, tribosystems in general, are critical parts. Such tribosystems are characterized not only by low temperatures but also by special media. Environments are gaseous helium, cryogenic liquids or vacuum. Thus, materials of such systems have to be resistant to extreme conditions of simultaneous influences of low temperatures, mechanical deformation at the surface, special environments and the mutual interactions of these influences. In the case of tribological applications in hydrogen, possible chemical reactions due to mechanical activation are also to be expected [Hein84].

Conventional lubricants cannot be used at very low-temperatures. Similar technical solutions must be found to the conditions in vacuum, which are based on materials with good tribological characteristics. Polymers and polymer composites are widely used as dry sliding materials in friction assemblies, where external supply of lubricants is impossible or not recommended. Poly(tetrafluoroethylene) (PTFE) and Poly(etheretherketone) (PEEK) materials are good candidates due to their favourable characteristics at ambient and high temperature. In particular, PTFE and PTFE filled composites have been successfully used in rocket applications [Glae74, Fusa90].

Tribological experimental data of materials at low temperatures and in hydrogen environment are hardly available due to cost and safety reasons. Therefore, it is necessary to fill the lack of information since conventional materials cannot automatically be employed.

## 1.2 Applications: tribosystems in cryotechnics

As mentioned above, the mains areas of applications of tribosystems in cryotechnics are:

- storage and distribution of refrigerants: pumps, valves, bearing, seals
- aero- und space technology
- superconductivity: fusion technology, cryogenic electronic, magnet systems

One of the specific area of interest is the hydrogen technology, which is considered to be the new generation of clean and renewable energy source instead of gasoline in the transportation industry. During refuelling, servicing and maintenance processes, safety has to be guaranteed. Insulation and sealing of components as well as permeation through the materials are of increased importance.

In superconductivity, with the controlled nuclear fusion, large scale superconducting magnets are necessary for plasma confinement. For example, the Tokamak reactor employs a variety of superconducting magnets which are operated at cryogenic temperatures. In these types of applications, support elements which link cryogenic devices to RT environment require a high mechanical strength and a particularly high thermal insulating power.

*Table 1.1: Some of the main areas of applications of fibre composites at low temperatures [Hart98]*

Application	Examples
Superconducting magnets	fusion technology, accelerators, energy storage, magnetic levitation, cryoelectronics
Support elements for cryogenic devices	in tension or compression
Compensating support elements	support elements with a strong negative thermal expansion coefficient for compensating unwanted expansion
Non-metallic cryostats	for superconducting quantum interference device (SQUID) detectors or liquefied gases, hydrogen technology
Cryogenic vessels	storage and transportation of liquefied gases, hydrogen technology
Space technology	cooling of equipment, cryogenic wind tunnels, space antennas without thermal expansion

### 1.3 Problems in cryogenic applications

In order to satisfy the demand for new cryotechnologies further material investigations need to be performed taking into account the following material requirements:

Tribological performances of polymers depend significantly on the temperature at the friction contact. That applies also to very low temperature tribosystems, especially for polymers with low heat conductivity. This can be a problem due to bad evacuation of frictional heat at the contact area. The heat dissipation at the contact area is therefore an important factor to consider. In applications of superconduction, the frictional heat produced by electromagnetically induced movements is not desired [Nish97, Suzu97]. The frictional heat is sufficient for local rise in temperature over the critical temperature  $T_C$ . This can lead to the evaporation of the refrigerant, which can damage the magnet of the superconductor [Kens81].

Another problem for most designs of cryogenic support structures comes from the thermal expansion, especially if different materials are involved. In composite materials, different thermal coefficients of expansion between matrix and fibres can lead to mechanical stresses in the boundary surfaces of the components. Such damage mechanisms were examined mainly for long fibres reinforced polymers [Ahlb89, Hart98, Hart97b].

The structure of the polymers can be relevant at low temperatures. The respective molecular structure is also to be considered in composites. With decreasing temperature, material properties do not change in the same way but depend on the chemical compositions [Hüb98]. Therefore, the tribological properties of a friction couple can differ at low temperatures, as well as the wear process.

Experiments in hydrogen need to be carried out in order to consider the influence of its chemical reactivity on the performance of the materials.

Finally, another specific cryogenic problem is due to the brittleness of some polymeric materials like epoxy resin at low temperatures. Precautions should be taken for the choice of the materials. Some polymers like PTFE and PEEK possess however a relative ductility at low temperatures [Hart98].

### 1.4 Aim and structure of the study

It is the aim of this study to investigate the tribological behaviour of PTFE- and PEEK-matrix composites with different filling and reinforcement materials at low temperatures and in hydrogen environment.

Firstly, because of the temperature-dependent characteristics of polymer materials and for a better understanding of the tribological behaviour, it is necessary to investigate the thermal and mechanical characteristics of these composites at low temperatures. Particular attention is given to the thermal effect in composites with regards to the compatibility of the components and the different thermal coefficients of expansion between matrix and fillers.

Secondly, the good tribological behaviour of PTFE and PEEK materials observed at room temperature (RT) should be verified at low temperatures. The influence of the matrix, fillers

and fibres on the tribological performance as well as the mutual influence of the components at low temperatures are investigated.

Thirdly, due to the frictional heat produced at the contact, experiments are performed in different cryogenic environments. Special attention is given to the influence of hydrogen on the tribological performances of these composites.

Suggestions are made regarding the composites and the conditions in which these materials can be used in cryotribosystems.

This work is based on a joined project supported by the German Science Foundation (DFG), between the Federal Institute for Materials Research and Testing, BAM, Berlin, and the Institute for Composite Materials, IVW, Kaiserslautern.



## 2 State of the Art

### 2.1 Basics of tribology

#### 2.1.1 Definitions

The main definitions concerning tribology are summarised in [Czic86] and [Czic92] as followed:

**Tribology:** The term tribology is derived from the Greek word *tribos*, which means rubbing. It is defined as the science and technology of interacting surfaces in relative motion and of related subjects and practices [Lub66]. Tribology embraces the scientific investigation of all types of friction, lubrication and wear and also the technical application of tribological knowledge.

**Friction:** Resistance against the lateral reciprocal motion of two surfaces relative to each other. The friction force is the resisting force tangential to the common boundary between two bodies when, under the action of an external force, one body moves, or tends to move, relative to the surface of the other.

**Wear:** The progressive loss of material from the surface of a solid body due to mechanical action, i.e. the contact and relative motion against a solid, liquid or gaseous counterface.

Friction and wear are not intrinsic material properties but are characteristics of the engineering system (so-called Tribosystem). Friction and wear are respectively serious causes of energy dissipation and material dissipation.

#### 2.1.2 Surfaces in contact

##### 2.1.2.1 Real area of contact

The surfaces of tribological contacts are covered with asperities of a certain height distribution which deform elastically or plastically under a given load [Czic86]. The summation of individual contact spots gives the real area of contact which is generally much smaller than the apparent nominal geometrical contact area  $A_0 = a b$  (fig. 2.1).

The real area of contact is given by

$$A_r = \sum_{i=1}^n A_r^i , \quad (1)$$

where  $A_r$  is the real area of contact and  $A_r^i$  the area of individual contact spots.

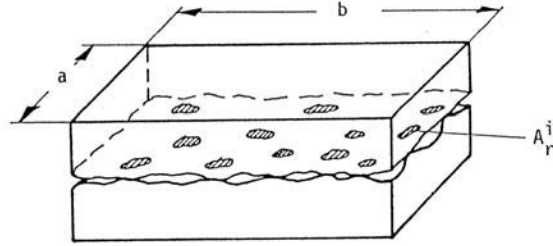


Figure 2.1: Real area of contact [Czic92]

For an elastic contact the real contact area  $A_r$ , is approximately proportional to the normal load force  $F_N$ , and inversely proportional to the YOUNG's modulus  $E$  [Czic86]

$$A_r = c \left( \frac{F_N}{E} \right)^n, \text{ where } \frac{2}{3} \leq n \leq 1. \quad (2)$$

The relative contact area  $\phi$  which is the quotient of the real contact area  $A_r$  and the nominal geometric contact area  $A_0$  can also be expressed by the following equation [Song93]

$$\phi = \frac{A_r}{A_0} = 1 - e^{-\frac{\beta p}{E}}, \quad (3)$$

where  $E$  is the YOUNG's modulus,  $\beta$  the roughness coefficient and  $p$  the normal pressure.

For a plastic contact, the real contact area  $A_r$  can be expressed by

$$A_r = c \left( \frac{F_N}{p_y} \right) \approx \frac{F_N}{H}, \quad (4)$$

where  $H$  is the hardness and  $p_y$  the yield pressure [Czic86].

For polymeric materials in contact, viscoelastic and viscoplastic effects and relaxation phenomena must be taken into consideration. These influences lead to a time-dependence of the contact area and to hysteresis losses in loading/unloading cycles.

The deformation characteristics can be described by the Burger-Model (equation 5, [Czic92]) which consists of a combination of spring and damping elements

$$\varepsilon = \left( \frac{1}{E} + \frac{t}{\eta_o} + \frac{1}{E_r} \left( 1 - e^{-\frac{t}{\tau}} \right) \right) \sigma_o \text{ with } \tau = \frac{\eta_r}{E_r}, \quad (5)$$

where  $\varepsilon$  is the deformation,  $E_r$  the relaxation modulus,  $\eta_r$  the viscosity of the relaxed state,  $\eta_o$  the viscosity of the viscoplastic state,  $\tau$  the time of relaxation and  $\sigma_o$  the unidirectional stress.



### 2.1.2.2 Surface temperature

Most of the energy expended for deformation of the surfaces in contact is dissipated as heat, and causes an increase in surface temperature. It is very important to estimate temperatures in the contact area since they influence the mechanical and microstructural properties of solids. Thermally activated processes such as recrystallisation, transformation, precipitation or chemical reaction can change contact conditions and hence friction and wear.

The temperature distribution in the surface in contact depends on surface pressure, velocity, geometry of contact, surface roughness, thermal conductivity. In the contact of individual asperities, energy is being dissipated so quickly that there is no time for substantial heat flow into regions outside the contact zone. Hence very high temperatures, the so-called flash temperatures are induced locally, particularly for polymers which have a low thermal conductivity. The instantaneous temperature of surface asperities in contact can be expressed as followed

$$T_i = T_{\text{bulk}} + \Delta T_{\text{flash}} , \quad (6)$$

where  $T_{\text{bulk}}$  is the bulk temperature and  $T_{\text{flash}}$  the flash temperature.

Furthermore, in cryogenic applications, it is essential to consider the thermal properties of the environment since heat transfer to the environmental medium can have an important effect on the surface temperature.

### 2.1.3 Friction

If two bodies are placed in contact under a normal load  $F_N$ , a finite force is required to initiate or maintain sliding; this force is the friction force  $F_f$ .

Friction between sliding surfaces results in complex molecular-mechanical interactions, e.g. the deformation of the roughness, ploughing by debris and roughness of the harder counterpart, and the adhesion between the contact surfaces.

According to Tabor [Tabo81], three basic phenomena are involved in friction:

- the real area of contact between the sliding surface,
- the type and strength of the bond that is formed at the interface where contact occurs,
- and the way in which the material in and around the contacting regions is sheared and ruptured during sliding.

## 2 State of the Art

### 2.1.3.1 Mechanisms of friction

Friction is essentially an energy dissipation process which can be characterized by two different models [Bris86a]:

- the adhesion model of friction, which occurs at the interfacial zone and corresponds to high rates of energy dissipation,
- the deformation model of friction, which involves deformation and ploughing within a larger volume of material and hence lower rates of energy dissipation.

The friction force  $F_f$  can then be separated into an adhesive ( $F_a$ ) and a deformation ( $F_d$ ) component [Song93]

$$F_f = F_a + F_d . \quad (7)$$

The friction coefficient can be described analogously by

$$\mu = \mu_a + \mu_d . \quad (8)$$

The value of each component depends on the conditions of the sliding surfaces, which can be influenced by the characteristics of the materials involved, the topography of the surfaces and the environmental conditions.

### 2.1.3.2 The adhesion component of friction

Adhesion is defined as the intermolecular interaction between solid-state bodies [Song93]. In order to separate contacting surfaces, the minimum energy  $W_{ab}$  needed is

$$W_{ab} = \gamma_a + \gamma_b - \gamma_{ab} , \quad (9)$$

where  $\gamma_a$  and  $\gamma_b$  are the surface energies of the separated surfaces, and  $\gamma_{ab}$  is the boundary surface energy of the two contacting surfaces.

The relevant influencing properties such as the interfacial shear strength or the surface energy, are characteristics related to the given pair of materials rather than to the single components involved.

The adhesion component of friction ( $F_a$ ) is produced by the formation and rupture of interfacial adhesion bonds [Bris90]. The attractive interaction forces are due to primary chemical bonds, i.e. metallic, covalent and ionic, as well as secondary VAN DER WAALS bonds. VAN DER WAALS forces act in the adhesion between polymeric solids.

$F_a$  introduces strain due to the interfacial stresses generated by the adhesive forces operating between the two solids. It can be expressed as

$$F_a = \tau_s A_r , \quad (10)$$

where  $\tau_s$  is the shear strength of the contacts, and  $A_r$  is the real contact surface.

Analogously, the adhesive friction coefficient can be expressed as

$$\mu_a = \frac{\tau_s A_t}{F_N} . \quad (11)$$

The determining factors for the adhesive friction coefficient are the adhesive interaction and the real contact surface.

Since  $F_N = \rho A_0$ , the adhesive component of friction can be derived from eqs. (3) and (11) [Song93]

$$\mu_a = \frac{\tau_s A_t}{F_N} = \frac{\tau_s A_t}{\rho A_0} = \frac{\tau_s}{\rho} \left( 1 - e^{-\frac{\beta p}{E}} \right) . \quad (12)$$

The adhesive component of the friction coefficient can be reduced by increasing the YOUNG's modulus and by decreasing the shear strength of the contacts.

### 2.1.3.3 The deformation component of friction

When a surface in a sliding tribo-contact is harder than the other, the harder asperities may penetrate into the softer surface. In tangential motion, a certain force results because of ploughing resistance. This may contribute to the friction resistance.

Because of the deformation during sliding contact, mechanical energy may be dissipated through plastic deformation effects [Song93].

The work input into the material is a function of the modulus and/or the flow stress, depending on the deformation mode (viscoelastic, plastic, tearing or brittle) and the contact conditions.

For elastic deformation, the depth  $h_e$  of penetration is proportional to the normal pressure  $p$  and inversely proportional to the YOUNG's modulus  $E$

$$h_e = c h_{\max}^{n_1} \left( \frac{p}{E} \right)^{n_2} . \quad (13)$$

For plastic deformation, the depth  $h_p$  of penetration is given by the equation

$$h_p = c h_{\max} \left( \frac{p}{\sigma_{dF}} \right)^{n_2} , \quad (14)$$

where  $\sigma_{dF}$  is the compression yield point.

## 2 State of the Art

Since the deformation resistance is proportional to the depth of penetration, and since the friction represents a kind of dissipation of mechanical energy, which is proportional to the mechanical loss factor  $\tan \delta$ , Song has suggested the following relationship for the deformation component of friction

$$\mu_d = \xi \frac{p}{E} \tan \delta, \quad (15)$$

where the constant  $\xi$  depends on the characteristics of the surface.

### 2.1.4 Wear

Damage occurring when two bodies are in contact and in relative motion, produces debris. Wear is produced when this debris is removed from the contact [Bris90]. The rate of expulsion of the debris depends on the contact geometry. Confined or conforming contact will not allow debris to displace. The wear particles may act as weak layers which reduce friction, i.e. as lubricants. They have a much more complex effect such as making the counterpart smoother. The contact zone is seen as having changing morphology, structure, chemistry, particle size and aspect ratio. It will be stretched, compacted and rolled by the repeated deformations in the contact.

#### 2.1.4.1 Mechanisms of wear

According to the former DIN 50320, wear mechanisms are divided into four basic categories under the headings of adhesion, abrasion, surface fatigue and tribochemical reactions. These are presented in *table 2.1*.

##### 2.1.4.1.1 Adhesive wear mechanisms

The adhesive wear processes are initiated by the interfacial adhesive junctions which form if solid materials are in contact [Czic86]. Different adhesive junctions may result depending on the nature of the solids in contact.

*Table 2.1: Wear mechanisms according to former DIN 50320.*

Wear mechanism	
Adhesion	Formation and breaking of interfacial adhesive bonds
Abrasion	Removal of material due to scratching
Surface fatigue	Fatigue and formation of cracks in surface regions due to tribological stress cycles that result in the separation of material
Tribochemical reactions	Formation of chemical reaction products as a result of chemical interactions between the elements of a tribosystem initiated by tribological action

The properties of the contacting solids influence the adhesive wear mechanisms. Since both adhesion and fracture are influenced by surface contaminants and the effect of the environment, it is quite difficult to relate adhesive wear processes with elementary bulk properties of materials. The tendency to form adhesion junction depends on physical and chemical properties of the materials in contact, the mode and value of loading and properties of the contacting surfaces such as contamination or roughness.

The main contributions to adhesion that may be expected are:

- for metals: primary bonds, metallic and covalent, and secondary bonds such as VAN DER WAALS;
- for polymers: VAN DER WAALS bonds, electrostatic bonds due to electrically charged double-layers, and hydrogen bonding by polar molecules.

Many theories of adhesion have been proposed in the literature. KINLOCH presented five main groups of mechanisms of adhesion (see *table 2.2*).

#### 2.1.4.1.2 Abrasive wear mechanisms

The effect of abrasion occurs in contact situation, in which direct physical contact between two surfaces is given, where one of the surfaces is considerably harder than the other one [Czic86]. The harder surface asperities penetrate into the softer surface with plastic flow of the softer surface occurring around the asperities of the harder surface. When a tangential motion is imposed, the harder surface removes the softer material by combined effects of micro-ploughing, micro-cutting and micro-cracking.

Abrasion is the wear by displacement of materials from surfaces in relative motion caused by the presence of hard protuberances or by the presence of hard particles either between the surfaces or embedded in one of them [Lee85].

*Table 2.2: Mechanisms of adhesion [Kin87]*

Adhesion theories	
Mechanical interlocking	Adhesion due to interlocking surface irregularities
Diffusion	Atoms or molecules diffuse across the interface between the two contacting bodies.
Electrons	Electron transfer across the interface of contacting bodies with different electronic band structures. A metal in contact with a polymer acts as donor of electrons.
Chemical	Chemical adsorption occurs at the interface of contacting bodies. Strong chemical bonds, i.e metallic, ionic and covalent type established at the interface, can cause metal transfer to the polymer after desintegration of the compound.
Adsorption	Adhesion between surfaces in intimate intermolecular contact to forces due to secondary bonds, such as VAN DER WAALS forces

## 2 State of the Art

### 2.1.4.1.3 Surface fatigue and delamination wear mechanisms

Wear by surface fatigue can be characterized by crack formation and flaking of material caused by repeated alternating loading of solid surface. Localised fatigue may occur on a microscopic scale due to repeated sliding contact of asperities on the surfaces of solids in relative motion.

Under repeated tribological loading, surface fatigue phenomena may occur leading finally to the generation of wear particles. These effects are mainly based on the action of stresses in or below the surfaces without needing a direct physical solid contact of the surfaces under consideration.

A delamination of wear [Suh73] has been described in which the generation of sheet-like wear particles is explained on the basis of the chain of events.

### 2.1.4.1.4 Tribochemical wear mechanisms

Whereas the mechanisms of surface fatigue and abrasion can be described mainly in terms of stress interactions and deformation properties, tribochemical wear has a third partner, the environment [Czic86]. The wear process proceeds by continual removal and new formation of layers on the contacting surfaces. In the presence of oxygen, worn debris consists largely of oxides which have been formed upon the surfaces and have been removed by rubbing.

The dynamic interaction between the material components and the environment determine the wear processes. These interactions may be expressed as cyclic stepwise processes.

First, the material surface reacts with the environment. In this process, reaction products are formed on the surfaces. Secondly, the reaction products wear away as a result of crack formation and abrasion in the contact process interactions of the materials. When this occurs fresh i.e. reactive surface parts of the materials are formed and step 1 continues [Czic86].

### 2.1.4.2 Wear measurements

The former DIN 50321 described several wear measurements depending on the direct or indirect method of measurements. Basically, the wear can be estimated by measuring either the thickness or volume of the material loss or by weighting the sample.

The linear wear  $W_h$  describes the thickness of the material loss during the experiment.

The wear can be expressed by the wear factor  $k$ , also called specific wear rate, which is defined as

$$k = \frac{W_v}{s F_N} , \quad (16)$$

where  $W_v$  is the volume of the worn material,  $s$  is the sliding distance and  $F_N$  is the normal load.

Measuring the weight of the worn material is not very suitable for polymeric materials since the worn polymeric material is not always separated from the specimens. This is especially true for tough polymeric materials [Song93].

### 2.1.5 Tribological system

Friction and wear are not intrinsic material properties but depend on so many influencing factors that, in any given situation, the whole tribological system must be considered. Thus, measured quantities of friction and wear, e.g. friction coefficient or wear rate, depend on the following basic groups of parameters [Czic86]:

- the structure of the tribological system, i.e. the material components of the system and the relevant tribological properties of the system's components,
- the operating variables, including load (or stress), kinematics, temperature, operating duration, etc,
- and the tribological interactions between the system components.

Figure 2.2 illustrates the basic parameter groups of tribological systems according to CZICHOS.

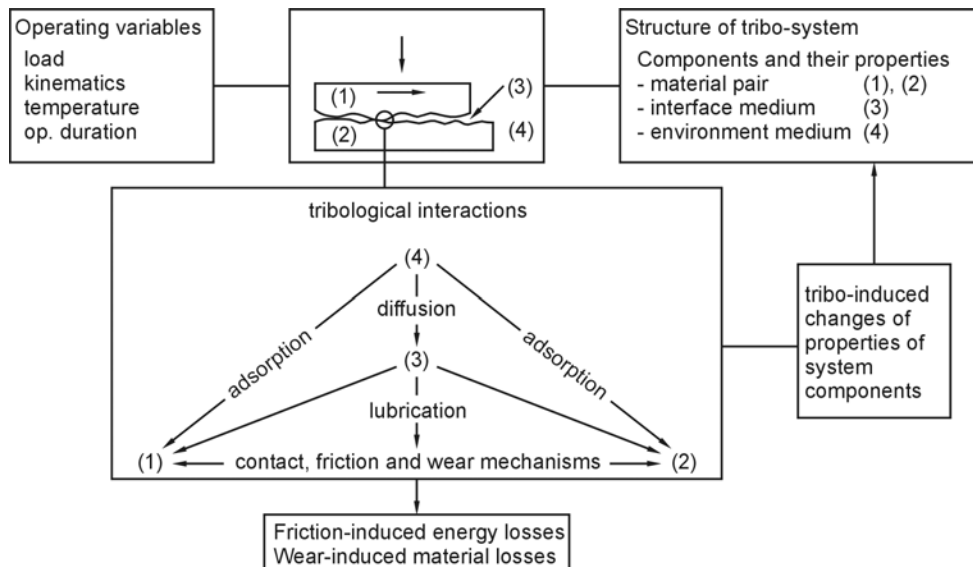


Figure 2.2: Basic parameter groups of tribological systems [Czic86]

## 2.2 Properties of polymer composites

Polymers and polymer composites are widely used as dry sliding materials in friction assemblies, where external supply of lubricants is impossible or not recommended. The field of application of self-lubricating materials in tribological systems is considerably extending to the detriment of metal components. This includes parts such as piston rings, seals, brakes, joints, gears and dry bearings.

There is a large number of advantages of using polymeric materials in particular due to the following properties: lower density, relatively cheap and easy to fabricate complex shapes, resistance to chemical attack, low friction coefficient, no scuffing or seizure.

However, the physical and mechanical properties of polymers can give some limitations compared to metal, notably due to their viscoelastic properties, lower moduli, higher thermal expansion which introduces dimensional stability problems, and lower thermal conductivity which leads to poor dissipation of frictional heat at low temperatures. Therefore, the most important material properties relevant to tribology are [Evan79]:

- ultimate strength (compressive and tensile),
- elastic modulus,
- creep resistance,
- thermal conductivity/expansion,
- and environment stability.

Additives are frequently introduced into polymers to modify one or more of these properties (section 2.2.1). At room temperature, these material properties are easily available, which is not always the case in extreme environmental conditions like in cryogenic applications. Section 2.2.2 presents some of the low temperature properties of polymer composites.

### 2.2.1 Polymer composites in tribology

There are several types of fillers which can be incorporated to polymers to improve their tribological properties.

As reinforcements, particulates and especially fibres can be added to increase the load-carrying capacity of polymers. Short fibres are also used to increase the creep resistance and the compressive strength of the polymer matrix. Metals and inorganic compounds improve the wear resistance. Polymers can also be used to reinforce high wear polymers like PTFE.

A second type of components are lubricating additives such as PTFE and graphite which decrease the friction coefficient. One of the mechanisms responsible for the reduction of friction is the formation of a transfer film on the surface of the counterpart.

Another type of additives are components that improve the thermal conductivity of composites like bronze particles. The materials commonly used in tribological applications are given in *table 2.3*.



Over the years, many studies with PTFE and PEEK materials were accomplished. Particular attention was given to the friction and wear mechanisms of PTFE that has a unique tribological behaviour due to its band structure [Tana73] and its ability to form a thin transfer film at the surface of the counterpart. PTFE compounds filled with fibres and/or particulates were characterized in detail by many workers [Tana73, Bris86a, Baha92] regarding their tribological behaviour at ambient temperature.

More recent investigations deal with the tribological characterization of high strength and high temperature thermoplastic PEEK as well as its compounds [Frie95].

BRISCOE [Bris86b] investigated a number of PEEK/PTFE composites over a wide composition range. He found that the inclusion of PTFE reduces the friction of PEEK with only a small loss in wear resistance. The inclusion of PTFE also reduces the magnitude of certain mechanical properties such as the hardness. The optimal PTFE amount was found to be 10%.

Lu [Lu95] examined different PEEK/PTFE compounds as a function of the mixing proportion at ambient temperature. The results of these investigations showed an optimal range for the PEEK/PTFE composites with 15% to 20% PTFE at ambient temperature.

HAEGER [Haeg97] investigated PEEK for the use in sliding bearings and sliding elements regarding mechanical and thermal characterization of the materials. In a further study [Flöc99] PEEK/CF materials were examined regarding their friction and wear characteristics as a function of the fibre volume content. The influence of the carbon fibres, PAN-CF (Polyacrylonitril-based) or pitch-CF (pitch-based), was also investigated regarding friction and wear characteristics. It was found that the pitch-based carbon fibres improved the friction behaviour due to higher graphitisation compared with the more rigid PAN-based carbon fibres. However, both fibre types showed the same behaviour in wear experiments. The optimal fibre volume content of PEEK/CF was found between 10% to 15%.

Table 2.3: *Polymers and additives used for tribological applications*

Materials	Examples
Polymers	polyethylene, polyacetal, polyamides, polyphenylene sulphides (PPS), PTFE, PEEK, phenolics, epoxies, silicones, polyimides (PI)
Reinforcements	fibres (glass, carbon, aramides...), metals (Fe, Sn ...), inorganic compounds (SiO <sub>2</sub> , TiO <sub>2</sub> ...), polymers (PEEK, PI, PPS)
Solid lubricants	graphite, molybdenum disulphide, PTFE
Thermal conductivity additives	bronze, graphite, silver

## 2 State of the Art

### 2.2.2 Low temperature properties

Most polymers possess molecular relaxations, i.e. at certain temperatures various molecular segments are freed up, which gives the capacity of movement [Hart94].

The glass transition is the temperature above which the movement of the main chain in the polymer obtains its greatest degree of freedom and thus the polymer obtains a great deal of plasticity above this temperature. Molecular chains become viscoelastic, and deformations are controlled mainly by intrachain forces. Thermal properties are dominated by short-wave vibrations, which propagate along the chains only (intrachain vibrations). Below the glass transition, other relaxations can occur, which are related to movements of molecular segments and side chains. At low temperatures, polymeric chains get frozen, and thermal vibrations and deformations are controlled mainly by the weak interchain binding forces (VAN DER WAALS). Thermal low-temperature properties are dominated by long-wave vibrations, which are able to propagate between chains (interchain vibrations). Elastic properties are determined mainly by the interchain force constant given by the VAN DER WAALS forces. These restrictions of movements can seriously affect the properties of a polymer and thereby the tribological behaviour, for example by hindering the formation of thin shear layer.

Some of the main low temperature properties of polymer materials are summarised in this section.

#### 2.2.2.1 Specific heat

Specific heat of polymers as a function of temperature has been investigated by HARTWIG who observed that  $c_p$  decreases drastically at low temperatures. This is explained by a quantum-mechanical theory [Hart94]. The thermal vibrations which are the carriers of heat, can be described by phonons. The quantization of the phonon energy causes a temperature dependence of the internal energy quite different from the classical theory. This change is especially strong at low temperatures at which phonon energy is small, and only few phonons are activated.

At elevated temperature  $c_p$  is proportional to the temperature  $T$ , which is specific for linear polymers.

At low temperatures and especially for composites with small coefficients of expansion, there is nearly no difference of the specific heat at constant pressure or volume. Furthermore, the temperature dependence of the specific heat is different for amorphous polymers and crystalline polymers below  $T = 60$  K (*table 2.4*).

For composite materials, the specific heat  $c_{com}$  can be calculated from the specific heat  $c_m$  of the matrix and  $c_f$  of the fillers by a linear mixing rule

$$c_{com} = V_f c_f + (1 - V_f) c_m , \quad (17)$$

where  $V_f$  is the volume content of the fillers.

## 2.2.2.2 Thermal expansion

The linear thermal expansion coefficient  $\alpha_e$  is defined by the relative length change per temperature variation

$$\alpha_e = \frac{1}{l} \frac{dl}{dT} . \quad (18)$$

The integral thermal expansion is defined by the coefficient of thermal expansion  $\alpha_e$  and the temperature difference relative to room temperature

$$\frac{\Delta l}{l_0} = \frac{l(T) - l(293\text{ K})}{l(293\text{ K})} = \int_T^{293\text{ K}} \alpha_e(T) dT . \quad (19)$$

For most materials  $\alpha_e$  is positive and  $\Delta l/l_0$  becomes negative on cooling. Thermal expansion of polymers originates from different modes of vibrations and is strongly influenced by the degree of crystallisation and by glass transitions.

The coefficient of thermal expansion  $\alpha_e$  is related to the specific heat  $c_p$  by the GRUENEISEN relation

$$\alpha_e = \frac{1}{3} \frac{\rho}{K} \gamma_g c_p . \quad (20)$$

where  $\rho$  is the density,  $K$  the compression modulus and  $\gamma_g$  the GRUENEISEN parameter.

In composite materials, thermal expansion depends on the direction of the reinforcement and on the volume fraction. The thermal expansion along the reinforcing fibre tends to be dominated by the fibre, while transverse to the reinforcement the thermal expansion is dominated by the matrix [Clar83].

One particularity of carbon fibres (and Kevlar) is that they are anisotropic. They show a small negative thermal expansion coefficient  $\alpha_e$  in the fibre direction, but a very large positive one in the transverse direction. Experiments indicated that in carbon fibre filled PEEK composites the transverse expansion of unidirectional composites is  $\Delta l/l_0 = -0.6\%$  to  $-0.8\%$  between RT and  $T = 4.2\text{ K}$ , whereas the thermal expansion in parallel direction is slightly positive (table 2.5).

Table 2.4: Temperature dependence of the specific heat of polymers at low temperatures [Hart94]

Temperature range	Crystalline polymers	Amorphous polymers
> 100 K	$c_p \propto T$	$c_p \propto T$
~ 10 K - 60 K	$c_p \propto T^3$	$c_p \propto T^2$
~ 1 K - 10 K	$c_p \propto T^3$	$c_p \propto T^{3.5}$
> 1 K	$c_p \propto T^3$	$c_p \propto T$

## 2 State of the Art

Table 2.5: Thermal expansion of 60% CF filled PEEK composite [Hart98]

Fibre direction	Thermal expansion $\Delta l / l_0$ (293 K $\rightarrow$ 4.2 K)
//	+0.004
$\perp$	-0.6

Table 2.6: Thermal expansion according to \*[Hart94], \*\*[Clar83], \*\*\*[Frey81]

Material	Thermal expansion $\Delta l / l_0$ (%)	
	293 K $\rightarrow$ 4.2 K	293 K $\rightarrow$ 77 K
PTFE *	-1.8	-1.7
PEEK *	-1.0	-0.9
Copper **	-0.32	-0.30
Carbon fibre in Epoxy matrix ***(//)		+ 0.01

Problems arise for most designs of cryogenic support structures from the thermal expansion, especially if different materials are involved. In composite materials, different thermal coefficients of expansion between matrix and fibres can lead to mechanical stresses at the interface of components. Table 2.6 summarizes some data on thermal expansion of different materials from the literature.

### 2.2.2.3 Thermal conductivity

Thermal conductivity occurs when a thermal excitation gives rise to transport of energy with permanent local thermalization. The resulting temperature gradient drives the flux of energy carriers which are phonons in the case of insulators [Hart94]. The relationship between the heat power  $\dot{Q}$  per area  $A$  and the temperature gradient is given by the thermal conductivity  $\lambda$

$$\frac{\dot{Q}}{A} = -\lambda \text{ grad } T \quad . \quad (21)$$

Thermal conductivity is proportional to the specific heat

$$\lambda = \kappa c_p \rho \quad , \quad (22)$$

where  $\kappa$  is the thermal diffusivity.

The temperature dependence of thermal conductivity is summarised in table 2.7.

Table 2.7: Temperature dependence of the thermal conductivity [Hart94]

Temperature range	Temperature dependence
Amorphous polymers	
$T < 1 \text{ K}$	$\lambda_a \propto T^2$
$T \sim 4 \text{ K} - 10 \text{ K}$	$\lambda_a \propto \text{constant}$
$T > 30 \text{ K}$	$\lambda_a \propto T^{0.3} \text{ to } T^{0.5}$
Semicrystalline polymers	
$T < 20 \text{ K}$	$\lambda_{\text{semi}} \propto T^2$
$T > 30 \text{ K}$	$\lambda_{\text{semi}}$ is determined mainly by $\lambda_a$

The thermal conductivity of polymers at cryogenic temperatures depends little on the composition. For semi-crystalline polymers, it depends mainly on the crystalline content and on the crystallite size [Hart94].

Carbon fibre composites have a strong temperature dependence. They exhibit a very low thermal conductivity at very low temperatures.

#### 2.2.2.4 Mechanical deformation behaviour

The correlation between applied mechanical load and resulting deformation is described by viscoelastic moduli. The basic component of viscoelastic moduli is controlled by binding forces, originating from deformations of the electron configurations. The load acts against the binding forces. This component reacts nearly immediately and is responsible for the elastic behaviour. External forces cause deformations of molecular segments and of electron orbital in polymers. The deformation can be elastic, viscoelastic or viscous. At very low temperatures and not too high stress levels the deformation behaviour is determined by VAN DER WAALS binding potential. Time-dependent viscoelastic effects are negligible and most polymers behave elastically [Hart94].

Experiments reveal that the chemical compositions of polymers have a rather small influence on the low-temperature deformation behaviour. Also, below  $T = 100 \text{ K}$ , no large differences exist between the modulus of amorphous and crystalline polymers (*table 2.8*). In the vicinity of secondary and tertiary glass transitions, however, viscoelastic processes decrease the modulus of the amorphous domains.

*Table 2.9* indicates Brinell hardness values for materials tested at RT and at  $T = 77 \text{ K}$ .

## 2 State of the Art

Table 2.8: *E*-modulus at low temperatures [Hart94].

Polymer	<i>E</i> -modulus
Semicrystalline and cross-linked	$E = 7\text{-}9$ Gpa (below 100 K)
Amorphous	$E = 5\text{-}8$ Gpa

Table 2.9: 10 s Brinell hardness values for materials tested at  $T = 293$  K and  $T = 77$  K [Mich91]

Material	Hardness (MPa)	
	293 K	77 K
PTFE	33	450
Copper	550	800
Stainless steel	1760	3120

### 2.2.3 Properties in liquid hydrogen

The hydrogen atom is far away the smallest chemical element which combines spontaneously with a second atom to form  $H_2$  molecule:  $2H \rightarrow H_2 + 437.6$  kJ. Due to its small size and its lightness (14 times lighter as air), hydrogen gas diffuses in most engineering materials. Problems occur when H atoms recombine with themselves or combine with carbon to form methane gas. This builds up an enormous pressure and can initiate cracks and degrade the mechanical properties of metals. Therefore, embrittlement is the most severe technological problem encountered in the containment of gaseous hydrogen [Moul83].

This is why polymer composites are good candidates for hydrogen vessels. However, only few studies reported on the effect of liquid hydrogen on the mechanical properties of reinforced polymers. CANFER and EVANS summarized some of them [Canf98]. They reported that epoxy reinforced with glass fabric showed an increase in flexural strength with decreasing temperature down to  $T = 77$  K. However, the flexural strength at  $T = 20$  K in liquid hydrogen was found to be lower than that at  $T = 77$  K, up to 20% for a specific epoxy resin (fig. 2.3). The flexural modulus at  $T = 20$  K in liquid hydrogen was also lower than that at  $T = 77$  K in liquid nitrogen. Since material performance usually increases with decreasing temperature, this reduction in performance in  $LH_2$  may be an evidence of the effect of liquid hydrogen on polymers.

Other studies mentioned in [Canf98] indicated also a drop in certain properties of composites tested in liquid hydrogen ( $T = 20$  K) compared to those in liquid nitrogen ( $T = 77$  K) temperatures. Stress at failure was lower at  $T = 20$  K than at  $T = 77$  K. CANFER and EVANS concluded from their experiment that  $LH_2$  has a long-term effect on the mechanical properties of certain reinforced polymers, over and above that expected from a purely temperature effect.

GEISS also investigated the influence of low temperature and hydrogen on glass fibre composites [Geis00]. He found a positive effect of hydrogen on unidirectional glass fibre reinforced epoxy in fatigue tests.

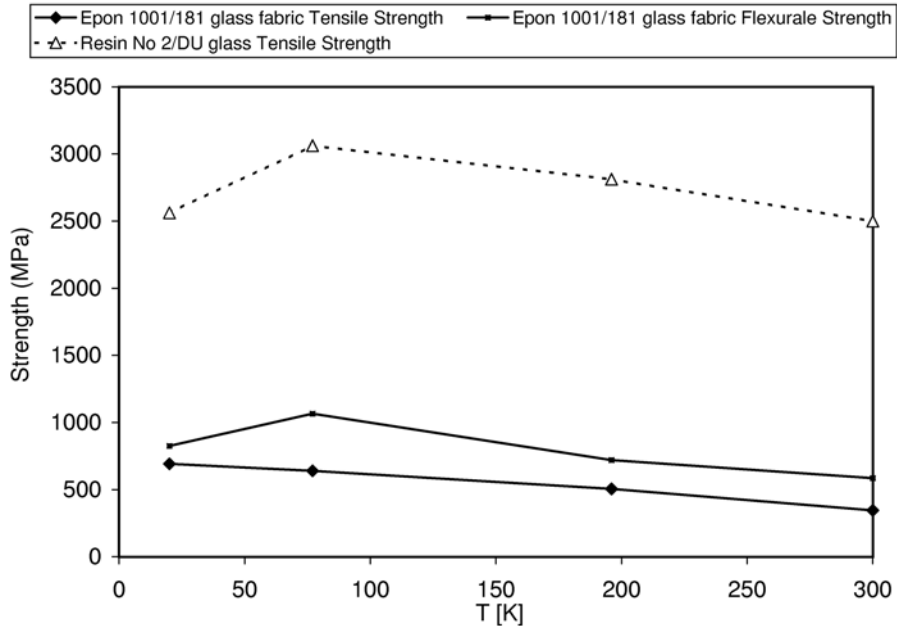


Figure 2.3: Effect of test environment on tensile strength of different epoxy resins [Canf98]

After three months of storage of samples in gaseous hydrogen at  $T = 353 \text{ K}$  ( $80^\circ\text{C}$ ), the subsequent vibration test at  $T = 77 \text{ K}$  showed a 30% increase of fatigue strength compared to samples not stored in this way. He suggested that hydrogen could break the double bonds in the resin.

### 2.3 Cryotribology

The first major works on cryogenic self-lubricating composites were accomplished by NASA Lewis Research Center tribologists during the early 1960s [Wiss59, Brew66]. They investigated steel bearings which operated in liquid hydrogen and liquid oxygen pumps in rocket engines. Various types of reinforced PTFE self-lubricating ball bearings were investigated. Other investigations for cryogenic friction and wear have been carried out for metal/insular parts in superconducting magnet windings. Most of the tribological studies for space applications were carried out in  $\text{LN}_2$ , which is a good compromise between  $\text{LOx}$  and  $\text{LH}_2$ . Tribological experiments in  $\text{LHe}$  are rare.

Different theories exist concerning the tribological behaviour of polymers at low temperatures. According to GARDOS [Gard86], friction should increase at low temperatures. However, most of the other works found a better performance of polymer composites at low temperatures, even if the wear mechanism is still being discussed.

## 2 State of the Art

WISANDER [Wiss59] investigated the friction and wear of PTFE composites in LN<sub>2</sub> for seals and bearings for missile power plants. He found good tribological properties for carbon filled PTFE materials at low temperatures.

GLAESER [Glae74] studied the wear mechanisms of polymers at cryogenic temperatures. It was concluded from the surface analyses of the wear tracks that the wear process in pure PTFE at  $T = 77$  K in LN<sub>2</sub> is totally different from that at room temperature. Wear at RT is a combination of gross plastic deformation or creep and shearing by prow formation. Wear at  $T = 77$  K is closer to an abrasive wear mechanism producing fine powder debris.

Other work carried out by MICHAEL [Mich91] indicated that the wear mechanism remains constant from RT to low temperature and that the wear rate decreases at low temperatures due to a much larger hardness. He concluded that adhesive wear is the dominant polymer wear mechanism not only at room temperature, but also at cryogenic temperatures. The correlation between friction and wear was generally much better at the cryogenic temperatures, where the deformation mode of the polymers is primarily plastic, than at room temperature, where their deformation is predominantly viscoelastic-plastic.

In a further work, MICHAEL [Mich94] studied the influence of the sliding velocities at cryogenic temperatures. According to his low temperature experiments, below the glass transition, the friction coefficients become essentially independent of the velocity.

BOZET [Boze93] studied in detail the tribological behaviour of polyimide in LN<sub>2</sub>. The reduction of friction coefficient in LN<sub>2</sub> compared to RT is caused by a sizeable reduction of deformation of the composite. According to him, adhesion should increase at low temperatures, and he concluded that adhesion phenomena are more important than deformation phenomena at cryogenic temperatures.

HÜBNER and GRADT [Hüb98] have investigated a wide range of materials at low temperatures. The behaviour of the materials indicated a significant influence of the temperatures as well as of the cryogenic environments. Experiments with different polymer materials indicated that the friction does not decrease homogeneously with temperature, instead a rise at  $T = 4.2$  K in liquid helium was observed as compared to LN<sub>2</sub>. It was also concluded that the molecular structure of the materials must be considered.



## 3 Experiments

### 3.1 Materials

#### 3.1.1 Polymer composites

Despite its poor mechanical properties and high wear rate, PTFE is one of the most used polymers in tribological applications due to its low friction coefficient. It has also a good behaviour at low temperatures as reported in section 2.3. On the other hand, PEEK has very good mechanical properties, but a higher friction coefficient. Since safety requirements are essential in hydrogen technology, only composites with optimal performances should be employed in this condition. This is why in the current work, PTFE- and PEEK-matrix composites filled with different amounts of fillers and fibres were chosen to be investigated for tribological applications at low temperatures and in hydrogen environment.

PTFE-matrix composites were filled with either bronze, aromatic polyester, or PEEK, and PEEK-matrix composites were filled with PTFE. In addition, all the materials were reinforced with short carbon fibres.

##### 3.1.1.1 Matrix

#### **Poly(tetrafluoroethylene) (PTFE)**

PTFE exhibits a very low coefficient of friction and retains useful mechanical properties at temperatures from  $T = 13 \text{ K}$  ( $-260^\circ\text{C}$ ) to  $T = 533 \text{ K}$  ( $260^\circ\text{C}$ ) for continuous use [Tana86]. The crystalline melting point is  $T = 600 \text{ K}$  ( $327^\circ\text{C}$ ), much higher than that of most other semi-crystalline polymers. Several transitions have been observed over the temperature range from  $T = 4 \text{ K}$  to  $T = 600 \text{ K}$  [Bryd72].

At  $T = 176 \text{ K}$  ( $-97^\circ\text{C}$ ), the transition is associated with behaviour in the amorphous regions, and is the most dominant in dynamic mechanical and in electrical tests. It is assumed to be due to fairly short segment mobility. At  $T = 292 \text{ K}$  ( $19^\circ\text{C}$ ) and  $T = 303 \text{ K}$  ( $30^\circ\text{C}$ ), transitions are associated with first order crystalline changes. At about  $T = 400 \text{ K}$  ( $127^\circ\text{C}$ ), an amorphous transition is observed, which corresponds to a motion of a chain segment of 50-100 backbone atoms.

PTFE is nearly inert chemically and does not absorb water, leading to excellent dimensional stability. These characteristics of PTFE are very useful in the matrix of polymer-based composites which are used in sliding applications. The unique tribological properties of PTFE are due to its peculiar molecular and morphological structures [Tana86]. On the other hand, PTFE is subjected to marked cold flow under stress and reveals the highest wear amongst the semi-crystalline polymers. This disadvantage is much improved by incorporating a filler into the PTFE.

### 3 Experiments

#### Poly(ether-ether-ketone) (PEEK)

PEEK is a tough aromatic thermoplastic polymer with properties which make it very attractive for use as high-quality engineering thermoplastic. It is a semi-crystalline polymer with a crystalline melting point around  $T = 613 \text{ K}$  ( $340^\circ\text{C}$ ) and a glass transition at around  $T = 416 \text{ K}$  ( $143^\circ\text{C}$ ). Its relative stiff backbone gives excellent high-temperature stability. It has a high continuous service temperature with the advantages of easy processability by injection molding and other techniques common to thermoplastic polymers.

Some of the mechanical properties of PTFE and PEEK at RT are shown in *table 3.1*.

*Table 3.1: Mechanical properties of PTFE and PEEK at RT*

Properties at RT	PTFE (Dyneon TF1750)	PEEK (Vitrex 450)
Density	2.16	1.3
Tensile strength [Mpa]	42	103
Tensile modulus [Gpa]	0.6	3.6
Poisson's ratio	0.46	0.4

#### 3.1.1.2 Reinforcing fibres

##### Short carbon fibres

Carbon fibres (CF) are produced from organic fibres (rayon, acrylic) or from residues of petroleum or tar distillation. The first ones are called PAN-CF, the others, pitch-CF. Some of the mechanical properties are shown in *table 3.2*.

For tribological applications, the addition of CF usually reduces the friction coefficient and increases the wear resistance. Their influence depends on the degree of graphitisation. High modulus CF with high graphitisation are used in tribological applications rather than high strength CF. FRIEDRICH [Frie92] showed that pitch-based fibres have a better wear reduction property than PAN-based fibres. The optimum CF content was found to be 20%. Another advantage of CF compared to glass fibres (GF) is that they are not so abrasive as GF, so that the wear due to abrasion is reduced.

In this investigation, pitch-CF have a diameter of about  $20 \mu\text{m}$ , whereas PAN-CF have a diameter of about  $6\text{-}8 \mu\text{m}$ .

*Table 3.2: Mechanical properties of carbon fibres [CF03]*

Characteristics	Fibres from PAN	Fibres from pitch
Tenacity (GPa)	1.8 - 7.0	1.4 - 3.0
Modulus (GPa)	230 - 540	140 - 820
Elongation at break (%)	0.4 - 2.4	0.2 - 1.3
Density ( $\text{g}/\text{cm}^3$ )	1.75 - 1.95	2.0 - 2.2

## 3.1.1.3 Fillers

**Aromatic polyester**

Ekonol<sup>®</sup> polyester is a linear aromatic thermoplastic. The absence of aliphatic hydrogen contributes to its excellent thermal stability. It is a highly crystalline polymer. Flow and creep are virtually non-existent below  $T = 588 \text{ K}$  ( $315^\circ\text{C}$ ) [Ekon03]. When combined with PTFE, it produces a composite material that has excellent temperature and wear resistance. The Ekonol<sup>®</sup> polyester PTFE blend has also a high thermal conductivity, long-term thermal resistance, low thermal expansion and low moisture absorbance.

**PEEK**

PEEK as filler has been investigated in PTFE-matrix notably by BRISCOE and FRIEDRICH [Bris86b, Frie95]. It reduces wear and increases strength.

**PTFE**

PTFE as filler is one of the most used solid lubricants. It reduces friction coefficient and stick/slip behaviour of pure PEEK [Bris86b].

**Bronze**

Bronze is well known for its wear reduction properties and improves thermal conductivity.

The chemical composition of the polymers used in this study is represented in *figure 3.1*.

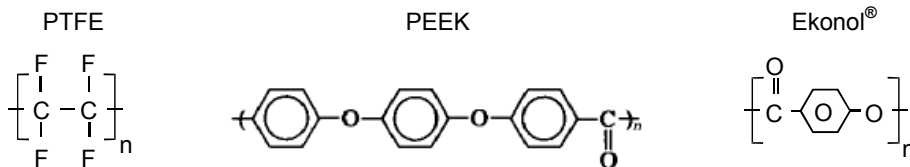


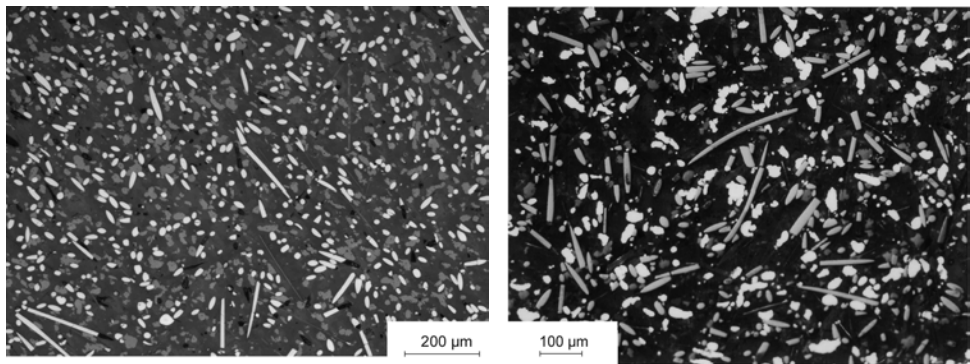
*Figure 3.1: Chemical composition of PTFE, PEEK and Ekonol<sup>®</sup> polymers*

## 3.1.1.4 Compositions

To get an overview of the tribological characteristics of PTFE- and PEEK-matrix materials at cryogenic temperatures, several composites have been selected from the RT experiments carried out at IVW, Kaiserslautern. *Tables 3.3 to 3.5* give the compositions of the PTFE-matrix materials. *Table 3.6* gives the compositions of the PEEK-matrix materials. Room temperature properties of these composites are described in detail in [Klei05].

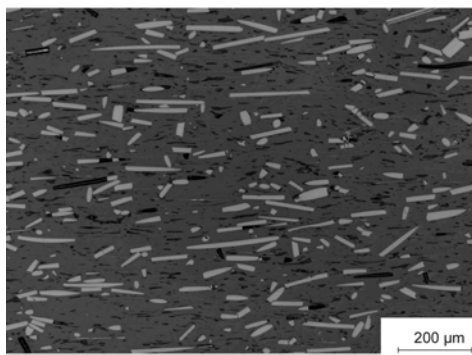
Optical microscopy images of three of these composites are shown in *figure 3.2*.

### 3 Experiments



a) PTFE filled with 15% CF and 9% PEEK

b) PTFE filled with 10% CF and 30% bronze



c) PEEK filled with 15% CF and 15% PTFE

Figure 3.2: Optical microscopy images of three polymer composites

Table 3.3: PTFE composites filled with bronze and CF

PTFE-matrix	Bronze	CF
Dyneon TF1750	N.A	Pitch-CF
wt%	wt%	wt%
60	30	10

Table 3.4: PTFE composites filled with Ekonol® and CF

PTFE-matrix	Aromatic polyester	CF
	Ekonol® T103, St Gobain	PAN-CF, Fortafil 383
wt%	wt%	wt%
75	10	15
75	20	5
65	20	15
60	20	20

Table 3.5: PTFE composites filled with PEEK and CF

PTFE-matrix	PEEK	CF
Standard Dyneon	Victrex 150XF	Pitch-CF, Kureha M 201 S
wt%	wt%	wt%
76	9	15
71	14	15
66	19	15
60	25	15

Table 3.6: PEEK composites filled with PTFE and CF

PEEK-matrix	PTFE	CF
Victrex 450G	Dyneon 9207	Pitch-CF, Kureha M-2007
wt%	wt%	wt%
100	0	0
80	5	15
70	15	15
65	20	15
75	10	15
65	15	20
55	15	30

## 3 Experiments

### 3.1.1.5 Processing

The PTFE compounds were processed via a sinter process at temperatures between  $T = 633 \text{ K}$  ( $360^\circ\text{C}$ ) and  $T = 653 \text{ K}$  ( $380^\circ\text{C}$ ). Materials were delivered as compression moulded discs by Dyneon. The mixing of the PEEK composites was achieved by a twin-screw-extruder at about  $T = 673 \text{ K}$  ( $400^\circ\text{C}$ ) with standard screw configuration. Materials were prepared as injection-moulded plates by IVW.

Samples were then cut into pins, discs or bars for the tribological, thermal or mechanical tests.

### 3.1.2 Steel counterface

For the tribological experiments, 100 Cr 6 steel discs (AISI 52 100) were used. It is the most frequently used steel for bearing applications. It exhibits numerous advantages: high purity and tenacity, suitability for hardening without carburising, flexibility in the heat treatment. Chemical composition and some of its mechanical properties are indicated in *table 3.7*.

*Table 3.7: Composition and mechanical properties of the steel discs [SNR]*

100 Cr 6 (AISI 52100)			
Chemical composition		Mechanical property	
C	0.98-1.10 %	Coefficient of thermal expansion	$\alpha_e = 12 \cdot 10^{-6} \text{ mm/mm.K}$
Si	0.20-0.35 %	E-modulus	$E = 205\,000 \text{ N/mm}^2$
Mn	0.25-0.45 %	Poisson ratio	0.3
Cr	1.3-1.6 %	Rockwell hardness	~ HRC 62

## 3.2 Cryogenic environments

The tribological experiments were carried out in air, nitrogen, helium and hydrogen environments as indicated in *table 3.8*. Nitrogen is often used as cryogenic medium since it is a cheap and inert coolant, which allows to carry out many low temperature experiments at  $T = 77 \text{ K}$ . Due to the higher price of helium (*table 3.9*), fewer tests were performed at  $T = 4.2 \text{ K}$ . Experiments in hydrogen were carried out only with selected composites for safety and cost reasons (*table 3.9*).

*Table 3.10* gives some of the important thermal properties of the cryogenic liquids at boiling point  $T_b$ , and the properties of air at  $T = 293 \text{ K}$  for comparison.

Table 3.8: Experimental environments

Environment	Temperature	
Air	293 K (RT)	20°C
Nitrogen	77 K	-196°C
Helium	77 K	-196°C
	30 K	-243°C
	4.2 K	-268.8°C
Hydrogen	293 K (RT)	20°C
	20 K	-253°C

Table 3.9: Price of tribological tests in LHe and LH<sub>2</sub>

Cryogenic liquid	Raw price	Average price for a 2.5 hour test
LHe	5.5 €/l	1650 €
LH <sub>2</sub>	1.25 €/l	500 €

Table 3.10: Some properties of the cryogens and of air for comparison [Frey81]

Property		LHe	LH <sub>2</sub>	LN <sub>2</sub>	Air
Boiling temperature $T_b$ , 1 bar	K	4.2	20.4	77.3	80
Heat of evaporation at $T_b$	kJ/kg	20.9	446	199.1	205.2
Density					
at $T_b$	Kg/m <sup>3</sup>	124.8	70.8	804.2	
at $T = 273$ K, 1 bar	Kg/m <sup>3</sup>				1.29
Specific heat					
at $T_b$	kJ/kgK	4.4	9.3	2	
at $T = 273$ K, 1 bar	kJ/kgK				1.0
Thermal conductivity					
at $T_b$	10 <sup>-3</sup> W/mK	27.2	119	139.8	
at $T = 273$ K, 1 bar	10 <sup>-3</sup> W/mK				24.1
Viscosity					
at $T_b$	10 <sup>-7</sup> kg/ms	35	133	1650	
at $T = 273$ K, 1 bar	10 <sup>-7</sup> kg/ms				24.1

### 3.3 Test procedures

For a better understanding of the tribological properties, physical and mechanical tests were performed on selected composites.

#### 3.3.1 Thermophysical testings

Thermophysical tests were carried out at the Aerospace Materials Technology Testhouse (AMTT) of the Austrian Research Centers Seibersdorf (ARCS).

Differential Scanning Calorimetry measurements were performed with a DSC 404C Netzsch equipment. The specific heat  $c_p$  was measured from  $T = 173$  K to  $T = 423$  K in helium atmosphere. The disc samples were 5 mm in diameter and 1 mm thick.

Integral and coefficient of thermal expansion were measured with a push rod dilatometer DIL 402C from Netzsch over the temperature range from  $T = 113$  K to  $T = 433$  K. Sample dimensions were  $4 \times 4$  mm<sup>2</sup> and 12 mm length.

Thermal conductivity measurements were carried out on a guarded heat flow meter Holometrix. The experiments were performed from  $T = 223$  K to  $T = 373$  K. The specimens were discs with 50 mm in diameter and 20 mm thick.

#### 3.3.2 Thermal and environmental testings

Thermal shock experiments were performed in two cryogenes: LN<sub>2</sub> and LHe. Two processes were conducted (*table 3.11*) and repeated 50 times. Sample dimensions were  $4 \times 4$  mm<sup>2</sup> and 12 mm length.

Cryo-treatments were performed with PTFE and PEEK composites similarly to [Indu99] which showed an improvement of the abrasion resistance of some polymers after treatment in LN<sub>2</sub>. In this work, the samples were cooled down stepwise at a rate of 30 K/h from RT down to  $T = 77$  K using a copper heating system placed in a LN<sub>2</sub> tank. After 40 hours immersed in the cryogenic liquid, samples were heated up at the same rate. Sample dimensions were  $4 \times 4$  mm<sup>2</sup> and 12 mm length.

Table 3.11: Thermal cycle processes

Process 1		Process 2	
cooling in LN <sub>2</sub> or LHe	(30 s)	cooling in LN <sub>2</sub> or LHe	(30 s)
heating up in water ( $T \approx 273$ K)	(30 s)	drying in warm air ( $T \approx 323$ K)	(10 s)
drying in warm air ( $T \approx 323$ K)	(10 s)		



Thermal ageing in hydrogen at ambient or cryogenic temperatures for a long time was not possible during this study. Since thermal ageing at higher temperature is often used to detect the influence of the medium and since frictional heat can induce hot spots at the contact area, heat treatment experiments were carried out in hydrogen. Polymer composites were heated at 5 K/min from RT to  $T = 473$  K, kept at  $T = 473$  K for three hours and then cooled down to RT at 5 K/min. Sample dimensions were  $4 \times 4$  mm<sup>2</sup> and 12 mm length.

The samples were examined before and after each thermal testing with Atomic Force Microscopy (AFM) at BAM Berlin, in order to determine the effects on the topography of the composites. AFM analyses were performed with a Topometrix equipment (Explorer<sup>®</sup>). The localisation of the cantilever tip relative to the surface was precisely recorded with a camera to be able to analyse the same position before and after the thermal experiments.

Furthermore, friction tests were performed after the thermal shock and the cryo-treatment experiments to determine the influence of the thermal experiments on the tribological behaviour of the composites.

### 3.3.3 Mechanical testings

Tests were carried out on a Shimadzu Universal testing machine AG-10TC at AMTT. Tensile tests were performed using a reversing cage at room temperature and at  $T = 77$  K in a bath of liquid nitrogen. For the experiments at  $T = 77$  K, an isolated tank was used (*figures 3.3 and 3.4*). The specimen dimensions were  $10 \times 2$  mm<sup>2</sup> and 80 mm length. *Table 3.12* gives the elongation rates. Tensile strength and elongation at break were recorded. An extensometer was used to calculate accurately the YOUNG's modulus.

Samples were investigated after the experiments by means of Scanning Electron Microscopy (SEM).

### 3 Experiments

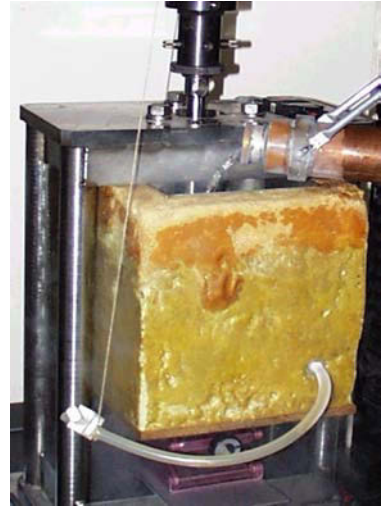


Figure 3.3: Universal testing with reversing cage at AMTT    Figure 3.4: LN<sub>2</sub> bath at AMTT

Table 3.12: Elongation rates for tensile testing

Material	Temperature	Elongation rate
PTFE composite	300 K	4 mm/min
PTFE composite	77 K	1 mm/min
PEEK composite	300 K	1 mm/min
PEEK composite	77 K	1 mm/min

#### 3.3.4 Tribological tests

Tribological tests were carried out at BAM in the tribometers CT2 and CT3 represented in *figures 3.5 and 3.6* and described in detail in [Grad01a]. Both cryotribometers are thermally insulated by vacuum superinsulation and cooled directly by a bath of liquid cryogen (CT2) or by a heat exchanger (CT3). For experiments at RT in air, in LN<sub>2</sub>, and in LHe the tribometer CT2 was used. The investigations in helium gas (He-gas) and hydrogen were carried out in CT3. Each experiment was repeated two or three times.

The pin-on-disc configuration (*fig. 3.7*) consists of a fixed 2-pins holder continuously sliding against a rotating disc. The rotation is transmitted via a rotary vacuum feedthrough to a shaft with the sample disc at the lower end. Loading is established by pressurized He-gas acting on a piston which presses a lever with the sample holder upwards against the lower face of the rotating disc.

During the tribological tests, normal and friction forces are measured by strain gauges. Wear was planned to be measured by weight loss, in order to compare the results with the RT experiments performed at IVW.

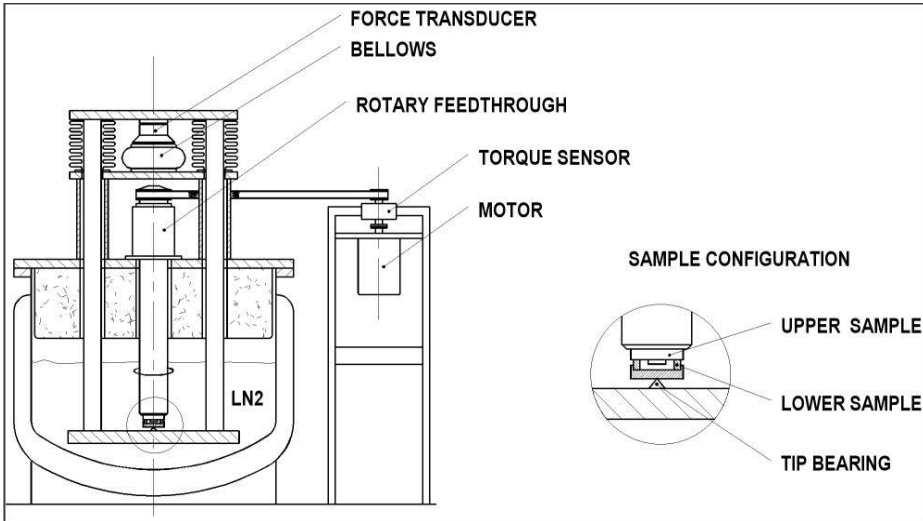


Figure 3.5: CT2 Cryotribometer [Grad01a]

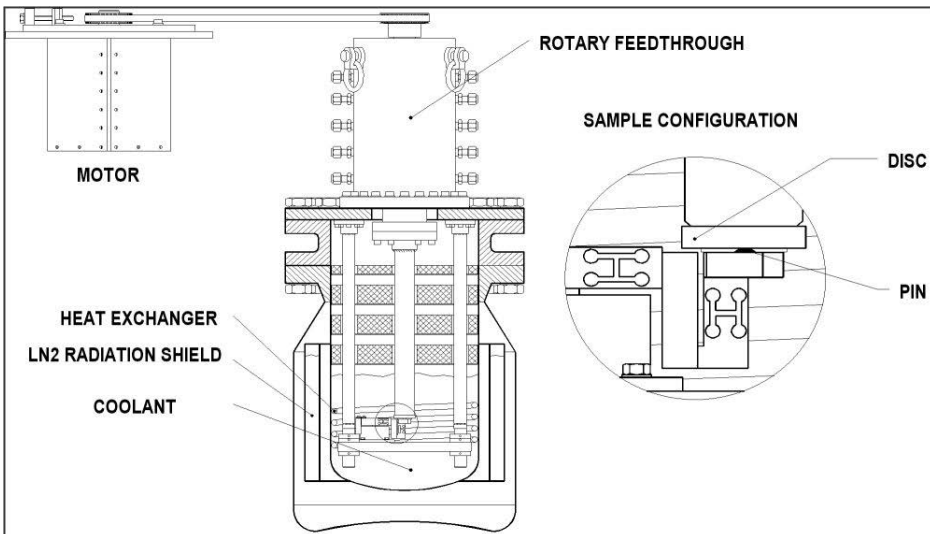


Figure 3.6: CT3 Cryotribometer [Grad01a]

### 3 Experiments

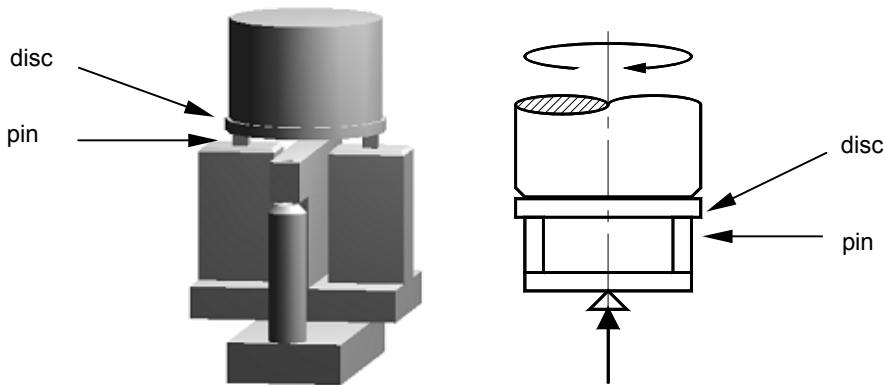


Figure 3.7: Pin-on-disc configuration

Polymer composites were cut into pins (4x4x12 mm<sup>3</sup>). In order to reduce the time of the running-in period, specimens were pre-worn with grinding paper (Grid 800) against the disc counterpart and then carefully cleaned with ethanol. With this method, the roughness of the specimens before testing was always the same, and so was the apparent area of contact with the steel disc due to a better parallelism between the two mating surfaces.

Steel discs with an inside diameter of 25 mm and an outside diameter of 42 mm were cleaned with ethanol before used.

#### 3.3.5 Surface analyses

After the tribological experiments the transfer film on the disc and the surface of the pins were examined with optical microscopy, SEM (Cambridge Stereoscan 180) as well as with AFM (Explorer<sup>®</sup>). Before SEM analyses, polymer pins as well as the transfer film on the steel discs were sputter coated with gold (and exceptionally nickel for two samples) to increase the conductivity and preserve the polymer from damage by the electron beam.

Profilometry measurements of the surface of the discs were carried out using a Hommelwerke at BAM and a 3D-laser profilometry system from UBM at IVW.

Energy Dispersive X-ray analyses (EDX) were performed with a Si-Drift detector X-flash from Rontec to examine the composition of the worn surface. Prior to analyses samples were sputter coated with carbon.

X-ray Photo Electron Spectroscopy (XPS) was conducted on the surface of the discs with a SSX-100 from Surface Science Instruments/VG Scientific, to detect chemical reactions between the PTFE-matrix material and the steel counterface. XPS analyses were planned and performed conscientiously directly at the end of each tribological test and samples were transported in a desiccator in order to minimize the contamination of the surface.

## 4 Results

Before presenting the tribological performance of PTFE- and PEEK-matrix composites at low temperatures and in hydrogen, some of the material properties relevant for tribological applications are given in the following chapter.

### 4.1 Material properties

#### 4.1.1 Thermophysical testings

##### 4.1.1.1 Specific heat

*Figures 4.1 and 4.2* show the specific heat  $c_p$  measured at constant pressure from  $T = 173$  K to  $T = 423$  K of one PTFE- and one PEEK-matrix composites respectively. As expected,  $c_p$  decreases with decreasing temperature. A noticeable peak at about  $T = 300$  K indicates a PTFE transition associated with crystalline changes.

##### 4.1.1.2 Thermal expansion

*Figures 4.3 and 4.4* show the integral and the coefficient of thermal expansion for PTFE-matrix composite filled with 15% CF and 9% PEEK respectively. Both properties decrease with temperature. The PTFE transition at about  $T = 300$  K is detected in both graphs, but particularly in *figure 4.4* by a large peak. The curves in *figure 4.4* present two further slight deflections at  $T = 170$  K and  $T = 410$  K, which could be associated with the second glass transition of PTFE and the glass transition of PEEK respectively.

*Figures 4.5 and 4.6* show the integral and the coefficient of thermal expansion for a PEEK-matrix composite filled with 15% PTFE and 15% CF respectively. Similar curves are observed as in the case of the PTFE composite. However, the variation of expansion is smaller for the PEEK composite over the temperature range of the experiment. The transition detected at about  $T = 300$  K corresponds to the glass transition of the PTFE filler (*fig. 4.6*).

## 4 Results

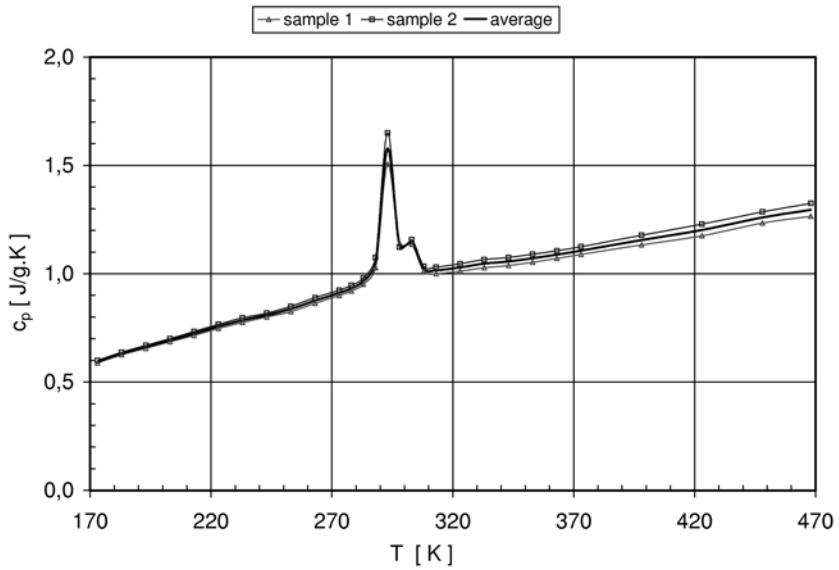


Figure 4.1: Specific heat of PTFE composite filled with 15% CF and 9% PEEK

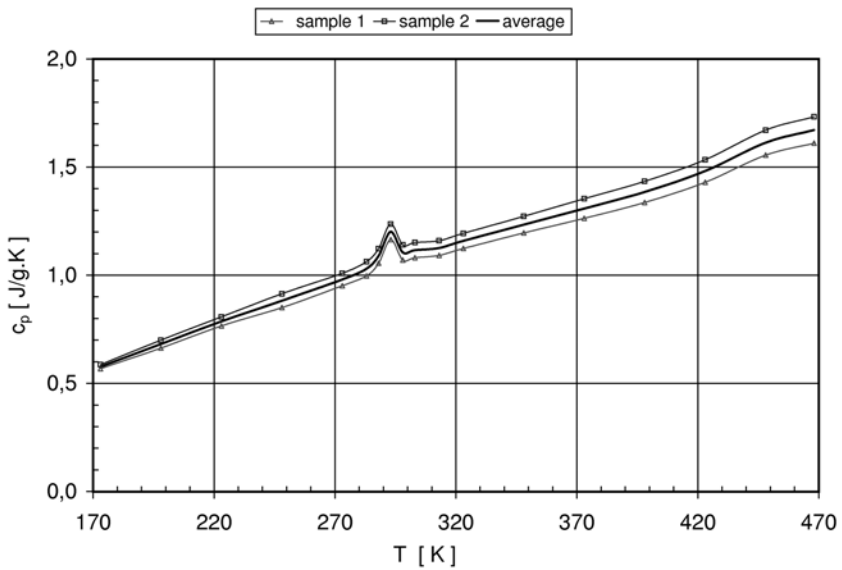


Figure 4.2: Specific heat of PEEK composite filled with 15% CF and 15% PTFE

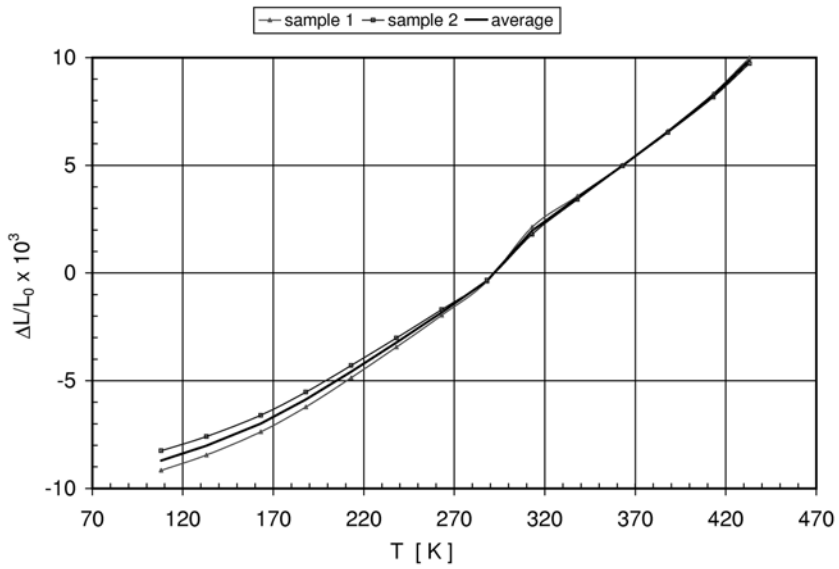


Figure 4.3: Integral thermal expansion of PTFE composite filled with 15% CF and 9% PEEK

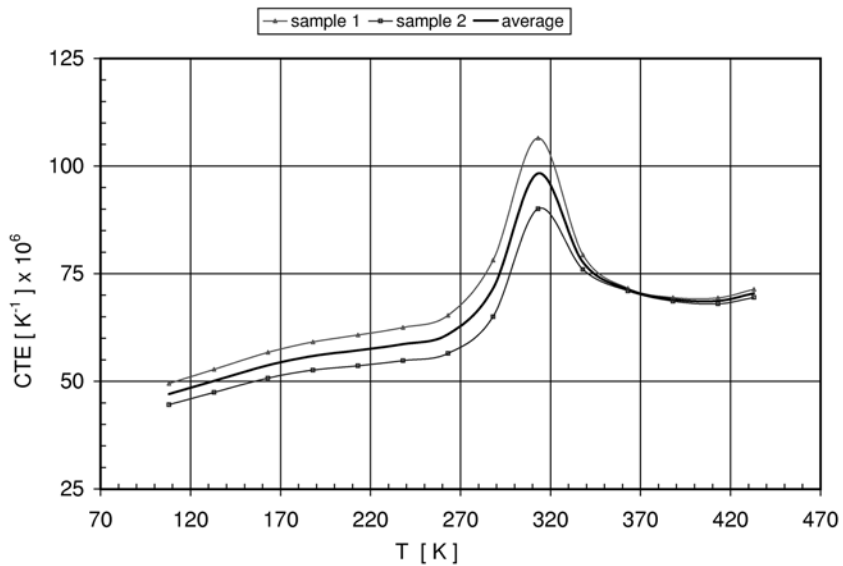


Figure 4.4: Coefficient of thermal expansion of PTFE composite filled with 15% CF and 9% PEEK

## 4 Results

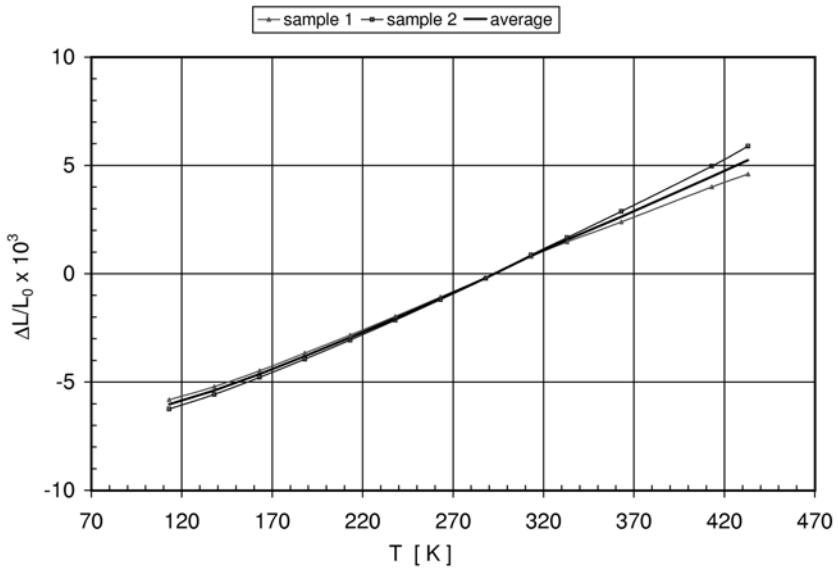


Figure 4.5: Integral thermal expansion of PEEK composite filled with 15% CF and 15% PTFE

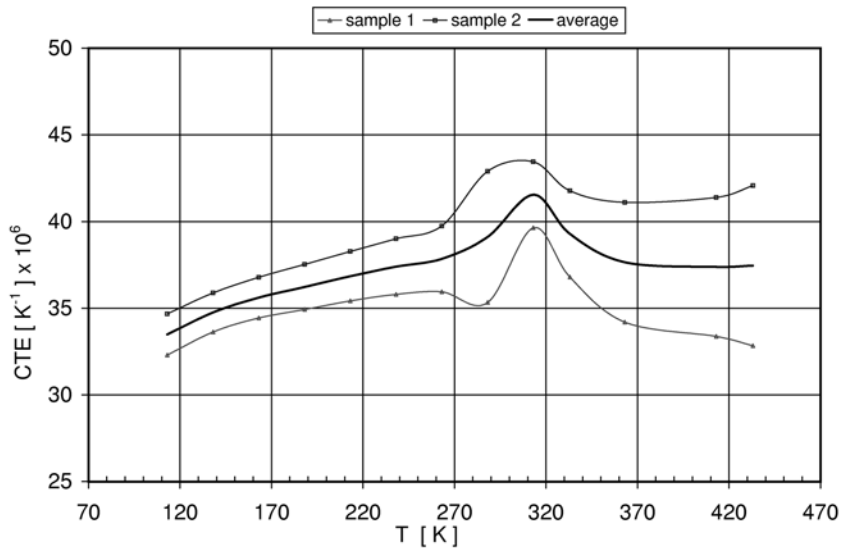


Figure 4.6: Coefficient of thermal expansion of PEEK composite filled with 15% CF and 15% PTFE



#### 4.1.1.3 Thermal conductivity

Thermal conductivity experiments were carried out from  $T = 223$  K to  $T = 373$  K. The graph (fig. 4.7) indicates that the thermal conductivity decreases slightly with temperature and that the PTFE composite has a higher conductivity than the PEEK composite.

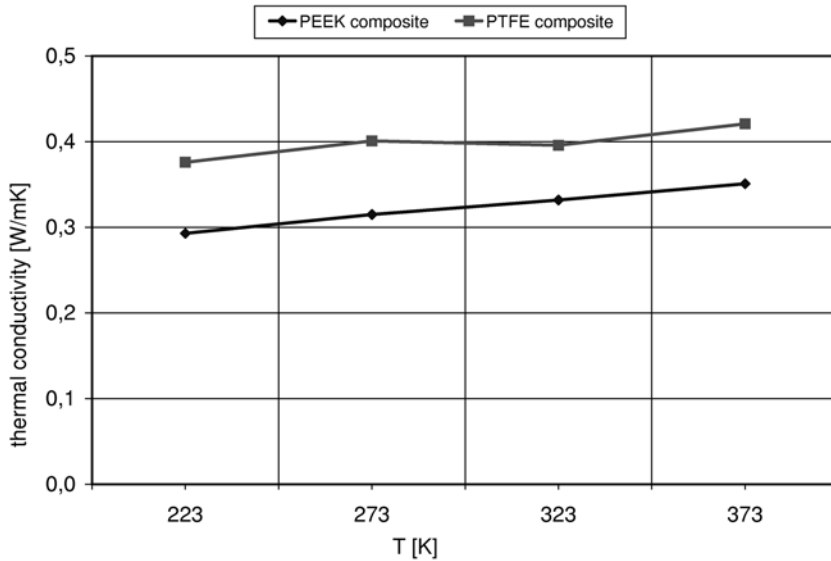


Figure 4.7: Thermal conductivity of PTFE composite filled with 15% CF and 9% PEEK and PEEK composite filled with 15% CF and 15% PTFE

#### 4.1.2 Thermal and environmental treatments

##### 4.1.2.1 Thermal shock cycle experiments

Firstly, thermal shock experiments were performed with bronze/CF filled PTFE composite in  $\text{LN}_2$  with the process 1 as described in section 3.3.2, i.e. heating up with warm water. AFM images before and after the thermal cycles indicate some changes on the surface of the composite. Before the experiment, the CF is well embedded in the matrix. After 50 thermal cycles, the short fibre is separated from the matrix with a significant gap at the interface (fig. 4.8). This can lead to a separation of the fibre from the matrix, as illustrated in figure 4.9 by the linescan of the surface of the composite before and after the thermal cycle experiment.

Moreover, deformations are observed on the surface of the matrix. This shows that the thermal shock cycles carried out between room temperature and  $\text{LN}_2$  damage the PTFE-matrix composite. However, despite the expansion of PTFE, no cracks were observed within the matrix.

## 4 Results

Secondly, thermal shock cycles were performed in LHe with the process 1. Experiments were conducted with bronze/CF filled PTFE and with PEEK/CF filled PTFE composites. The AFM images taken after the experiments show similar effects to the one observed in LN<sub>2</sub> for these two PTFE composites. The interface between the bronze particle and the matrix is stressed after the thermal cycles. Analyses of the PEEK/CF filled PTFE indicate not only a change at the interface between matrix and particle (*fig. 4.10*) but also a change in the matrix, whose deformation is well emphasized after the thermal shock (*fig. 4.11*).

Thirdly, thermal shock cycles were performed in LHe with the process 2 as described in section 3.3.2, i.e. heating up without water and only with warm air. AFM analyses of the polymer composites show fewer damage of the surface than the one observed after the experiment with the process 1.

Finally, a PEEK composite filled with 15% PTFE and 15% CF was investigated in LN<sub>2</sub> with the process 1, which produced the most surface damages in the case of PTFE-matrix composites. The AFM analyses did not indicate any significant debonding between the matrix and the fibres, as showed in *figure 4.12*. This material is more temperature resistance than PTFE-matrix composites.

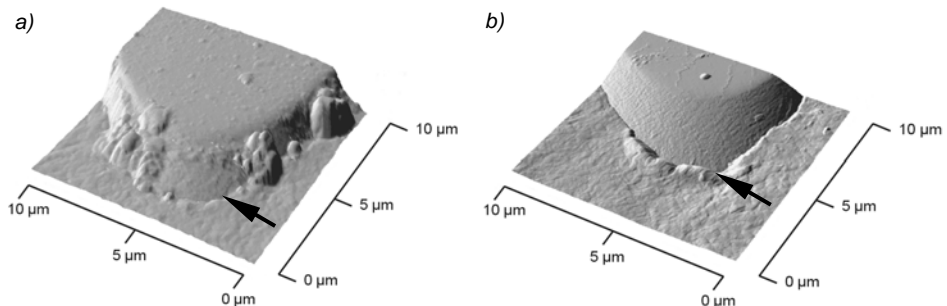


Figure 4.8: AFM images of CF in PTFE composite  
a) before and b) after thermal cycles in LN<sub>2</sub>

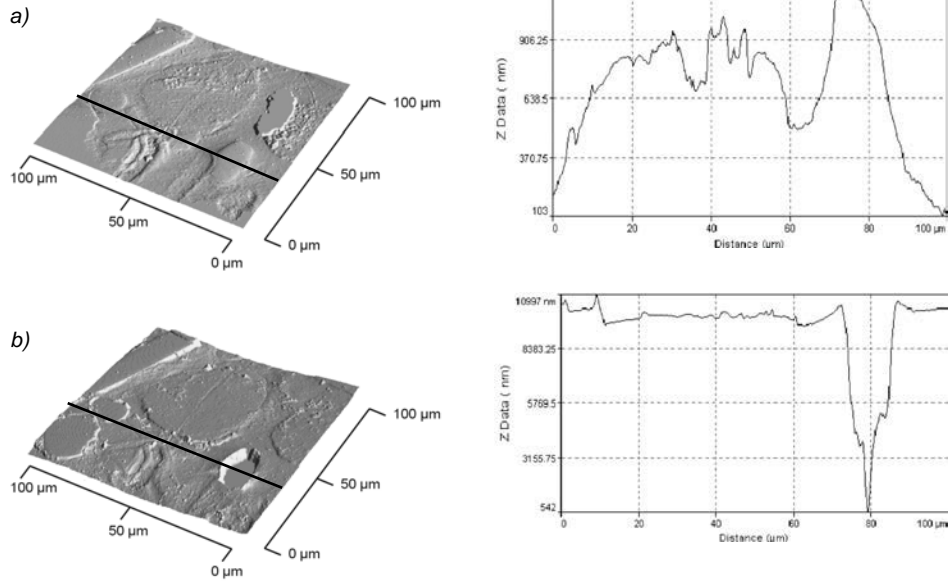


Figure 4.9: AFM images and linescans of bronze/CF filled PTFE composite  
a) before and b) after thermal cycles in LN<sub>2</sub>

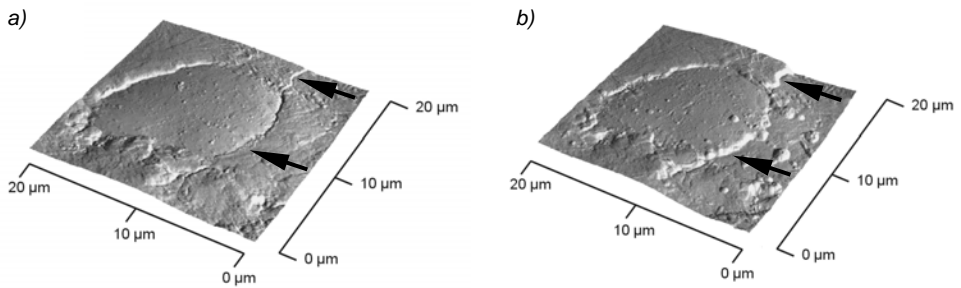
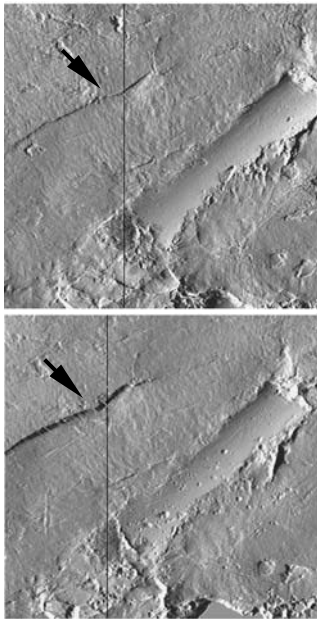
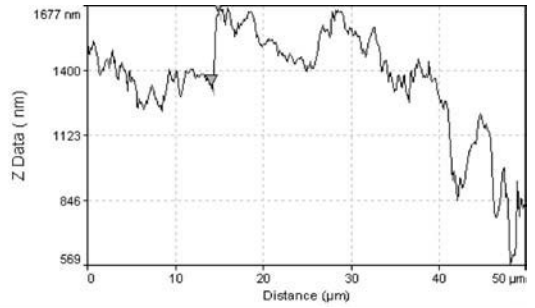


Figure 4.10: AFM images of CF in PTFE composite  
a) before and b) after thermal cycles in LHe

## 4 Results



a)



b)

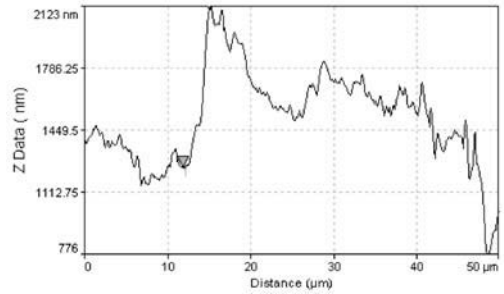
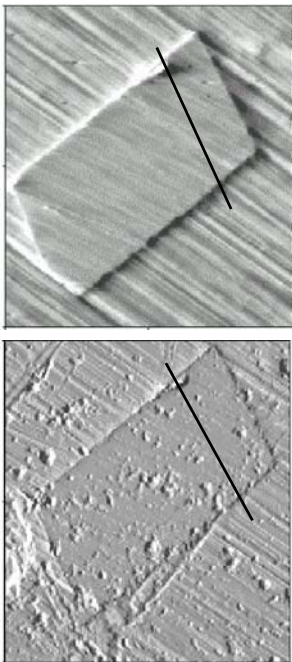
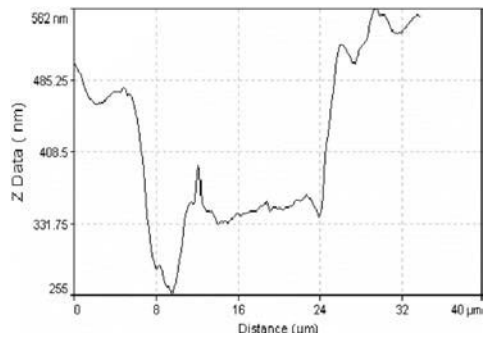


Figure 4.11: AFM images of PEEK/CF filled PTFE composite  
a) before and b) after thermal cycles in LHe



a)



b)

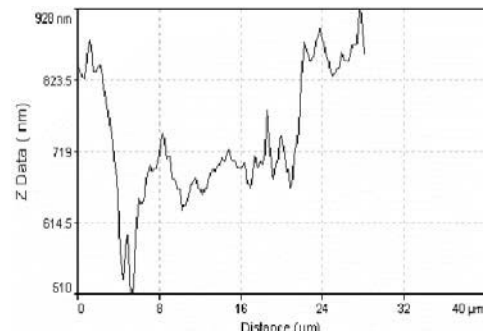


Figure 4.12: AFM images of PTFE/CF filled PEEK composite  
a) before and b) after thermal cycles in LN<sub>2</sub>

## 4.1.2.2 Cryo-treatment

AFM images indicate some changes of the surface of the composite after the cryo-treatment (*fig. 4.13*). Before the experiment, the particle is embedded in the matrix whereas after the experiment, it has been pulled out of the surface and a significant gap can be observed at the interface between matrix and particle. Linescan images confirm the elevation of the particle (*fig. 4.14*).

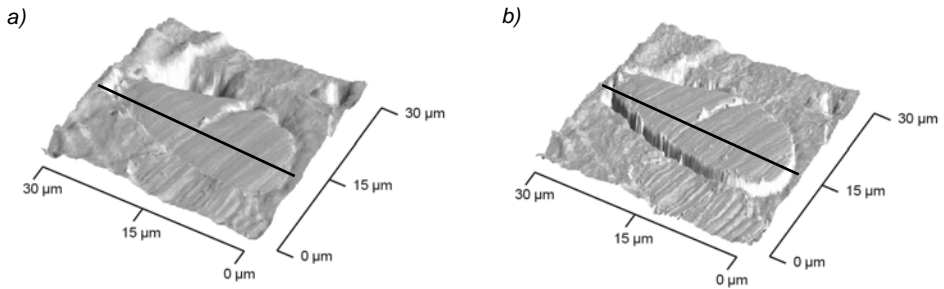


Figure 4.13: AFM images of bronze/CF filled PTFE composite  
a) before and b) after the cryo-treatment 40 hours in  $LN_2$

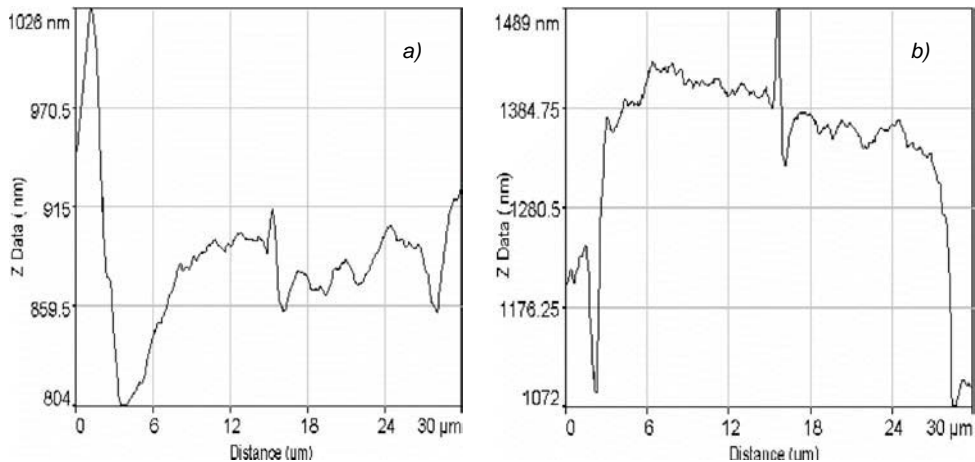


Figure 4.14: AFM linescans of bronze/CF filled PTFE composite  
a) before and b) after the cryo-treatment 40 hours in  $LN_2$

## 4 Results

### 4.1.2.3 Thermal ageing in hydrogen

Four samples were weighted before and after the experiment in order to detect any reaction with hydrogen (*table 4.1*). Taking into account the sensibility of the equipment ( $10^{-4}$  g), the change in weight of each sample was not significant.

Surface analyses using AFM were performed before and after the experiment, to estimate the influence of the temperature on the composite surface (*fig. 4.15*).

The changes at the surface are especially observed with the PTFE-matrix composite at the interface between matrix and CF.

### 4.1.3 Mechanical testings

The results of the tensile tests are summarised in *table 4.2*.

*Figure 4.16* shows that the YOUNG's modulus of each material increases at low temperatures from 1.4 GPa to 6.3 GPa for the PTFE composite filled with 15% CF and 9% PEEK and from 5.5 GPa to 7.4 GPa for the PEEK composite filled with 15% CF and 15% PTFE.

The elongation at break reduced significantly for the PTFE-matrix composite from 140% at RT down to 3% at  $T = 77$  K (*fig. 4.17*). Tensile strength increases from 10 N/mm<sup>2</sup> at RT to 35 N/mm<sup>2</sup> at  $T = 77$  K for this material. The improvement of the PEEK composite properties at low temperatures is relatively smaller (*fig. 4.18*). However, the tensile strength still increases from 60 N/mm<sup>2</sup> at RT to almost 100 N/mm<sup>2</sup> at  $T = 77$  K.

*Figure 4.19* summarizes the results obtained in LN<sub>2</sub>. It indicates that the elongation at break depends little on the composition of the composite since both materials have similar values (~3%). The stress, however, is significantly higher for the PEEK composite than for the PTFE material.

*Table 4.1: Weight before and after the thermal ageing experiment.*

Sample N.	Material	Weight before (g)	Weight after (g)
1	PTFE + 15% CF + 9% PEEK	0.3080	0.3076
2	PTFE + 15% CF + 9% PEEK	0.4237	0.4231
3	PEEK + 15% CF + 15% PTFE	0.2683	0.2674
4	PEEK + 15% CF + 15% PTFE	0.2725	0.2714

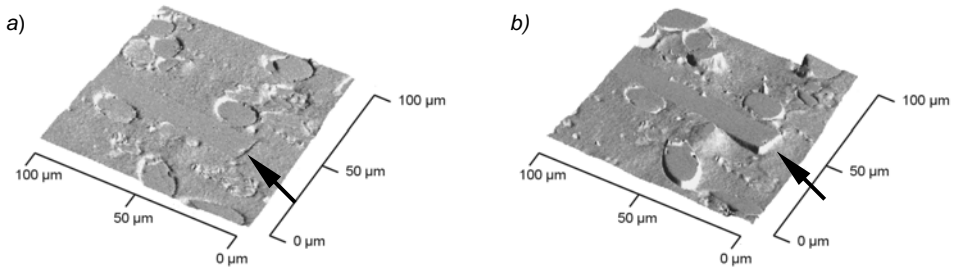


Figure 4.15: AFM images of PTFE composite filled with 15% CF and 9% PEEK  
a) before and b) after the hydrogen treatment at  $T = 473\text{ K}$

Table 4.2: Average values of the tensile test results

Composite	T	E-Modulus (GPa)	Tensile strength $R_m$ (N/mm <sup>2</sup> )	Elongation at break (%)	Number of samples
PTFE	RT	1.4	9.7	146.3	3
PTFE	77 K	6.3	35	1.4	3
PEEK	RT	5.5	58	0.6	3
PEEK	77 K	7.4	96.2	0.6	4

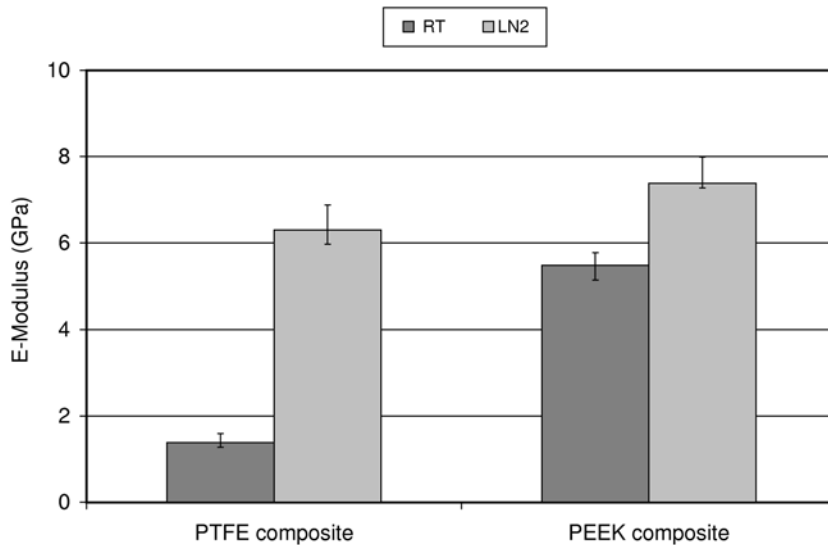


Figure 4.16: YOUNG's modulus of PTFE- and PEEK-matrix composites at RT and at  $T = 77\text{ K}$

## 4 Results

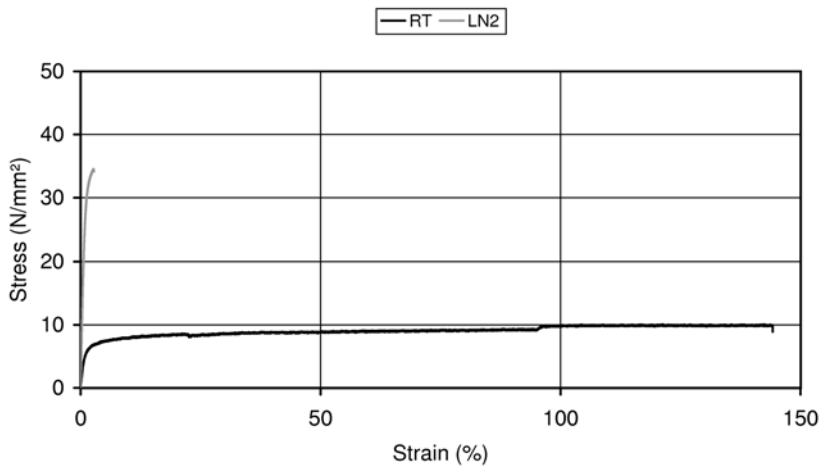


Figure 4.17: Stress-Strain curves of PTFE composite filled with 15% CF and 9% PEEK at RT and at  $T = 77\text{ K}$

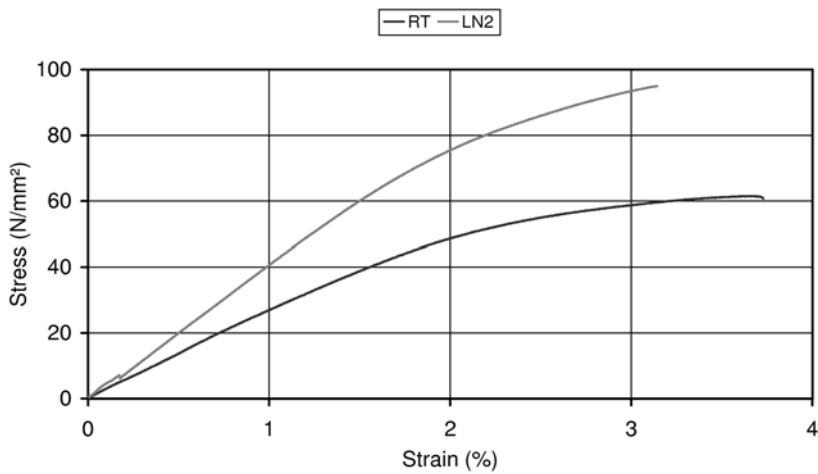


Figure 4.18: Stress-Strain curves of PEEK composite filled with 15% CF and 15% PTFE at RT and at  $T = 77\text{ K}$



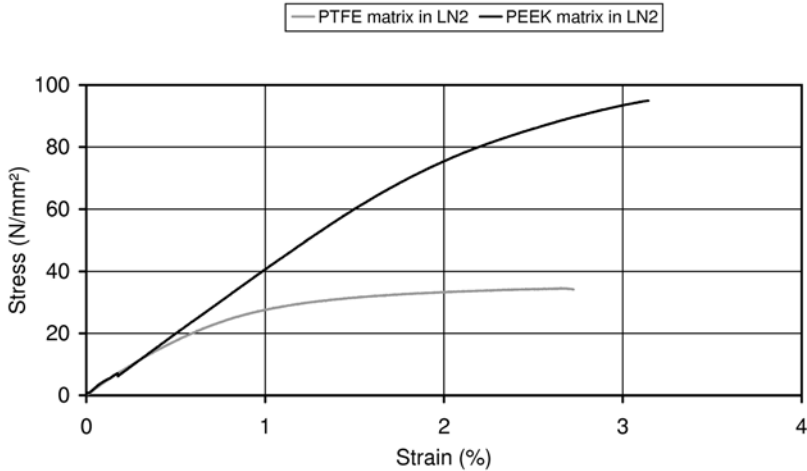


Figure 4.19: Comparison of PTFE and PEEK composites at  $T = 77\text{ K}$

## 4.2 Tribological experiments

This chapter presents the tribological experiments performed in this study, starting with the screening tests needed to select the test parameters. Then, RT friction measurements on thermally treated composites are presented before going into detail in the third part with the tribological performance of PTFE- and PEEK-matrix composites filled with different amount of fillers and fibres at RT and at  $T = 77\text{ K}$  in  $\text{LN}_2$ . Finally with selected composites, the fourth part describes the influence of the cryogenic medium with experiments performed in nitrogen, helium and hydrogen environments.

### 4.2.1 Selection of test parameters

#### 4.2.1.1 Load and surface preparation

Firstly, tribological tests were performed with a load of 16 N and unpolished discs ( $R_a = 0.145\ \mu\text{m}$ ) were used in order to compare the results with the RT experiments carried out at IVW. In these conditions, it was very difficult to observe the material transferred onto the disc after the experiments in  $\text{LN}_2$ . Surface analysis images showed mainly scratches caused by the surface preparation of the disc.

Since the aim of this study was to investigate the tribological behaviour of polymer composites at low temperatures, it was important to be able to look at the surfaces properly and to analyze the polymer transfer. The first step was to increase the load of 50 N in  $\text{LN}_2$ , but still no material transfer could be observed at the surface of the disc. It was then decided to use polished discs ( $R_a = 0.01\ \mu\text{m}$ ). Under these conditions, material transfer could be analyzed at the surface of the disc.

## 4 Results

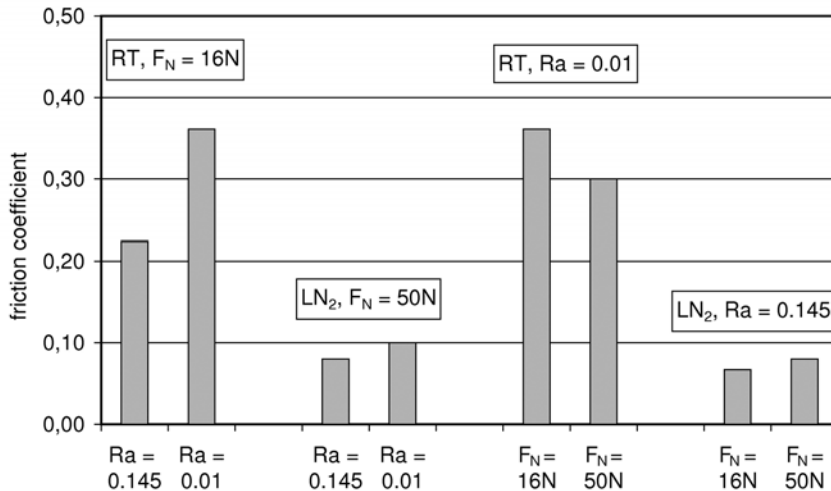


Figure 4.20: Influence of the disc roughness  $Ra$  [ $\mu\text{m}$ ] and the load  $F_N$  on the friction coefficient of PTFE composite filled with 30% bronze and 10% CF tested at RT in air and in  $\text{LN}_2$

Figure 4.20 shows the influence of the disc roughness and the load on the friction coefficient of a PTFE composite at RT and in  $\text{LN}_2$ . The friction coefficient at RT changed considerably with increasing load as well as when using a polished disc. Results at  $\text{LN}_2$  indicated only a slight influence of these parameters.

Taking into account these results, the study was carried on only with polished discs and a load of 50 N.

### 4.2.1.2 Sliding distance and velocity

For uncoated materials, friction usually stabilises after a running-in period which depends on the materials and the test conditions. However, for wear measurement, it is important to perform tests as long as possible. Since materials were investigated in cryogenic environments, the cost was also an important factor to be considered in order to establish the time of the test. The longer the test the more cryogenic liquid is needed. Therefore, it was decided to test the materials over a 2000 m sliding distance, and over 1500 m in the case of very slow sliding speeds, which is above the critical running-in time.

The sliding velocity remained a variable parameter in this study.

#### 4.2.1.3 Wear measurement

In this experiment, the weight loss of the flat pin could not be measured since the wear was too small at low temperatures. An attempt was made to estimate the linear wear of the composite after the relatively short sliding period (2000 m) by measuring the displacement of the pin, using an inductive sensor in CT2. Measurements were carried out before and after the tests with a load of 50 N, when the temperature of the system has returned to RT. Since linear wear was still very small at low temperatures, and since the inductive sensor could not be used in LH<sub>2</sub> environment, a second method was then applied using spherical pins. The wear scar was measured after the experiments and the wear volume calculated.

To take into account the measurement of the creep behaviour of the composite at room temperature, a static experiment was carried out with the same load applied and for the same period of time. The displacement obtained was then deduced from the total displacement measured after the RT wear test. Creep behaviour is not present at low temperatures due to a much harder behaviour of the polymers [Hart94].

Despite of all the precautions undertaken, wear results obtained in this experiment should be taken only as relative values in order to estimate and compare the behaviour of the composites in different cryogenic media.

#### 4.2.1.4 Test parameters

According to the screening tests described above, the following test parameters were chosen (*table 4.3*):

*Table 4.3: Test parameters*

Parameter	Friction measurement and linear wear (flat pins)	Wear measurement (spherical pins)
Normal load	50 N	16 N
Sliding speed	1 m/s, 0.2 m/s, 0.06 m/s	0.2 m/s
Sliding distance	2000 m, 1500 m	2000 m

#### 4.2.2 Influence of the thermal treatment on friction at RT

Friction measurements at RT were carried out after thermal shock cycles, cryo-treatment in LN<sub>2</sub> and after thermal ageing in hydrogen. The results are respectively presented in the *figures 4.21 to 4.23*.

Tribological tests at RT were performed before and after thermal shock treatments on PEEK/CF filled PTFE-matrix and PTFE/CF filled PEEK-matrix composites with the parameters  $F_N = 50$  N and  $v = 0.2$  m/s (*fig. 4.21*). The friction behaviour of the PTFE composite slightly improves after the thermal shock treatments, whereas no significant changes are recorded for the PEEK composite.

## 4 Results

After the cryo-treatment, no changes in friction behaviour were detected for the PTFE composite (fig. 4.22). A slight increase of the friction coefficient was observed for the PEEK composite. However, a significant influence of the cryo-treatment on the tribological behaviour of PTFE and PEEK composites, as suggested in other work regarding abrasive wear measurements [Indu99], cannot be clearly deduced from these results.

Similar tribological experiments were carried out with a PTFE- and a PEEK-matrix composites before and after the treatment in hydrogen. The results in figure 4.23 indicate no significant changes. Friction tends to decrease for PTFE composite and to increase for PEEK composite after the treatment.

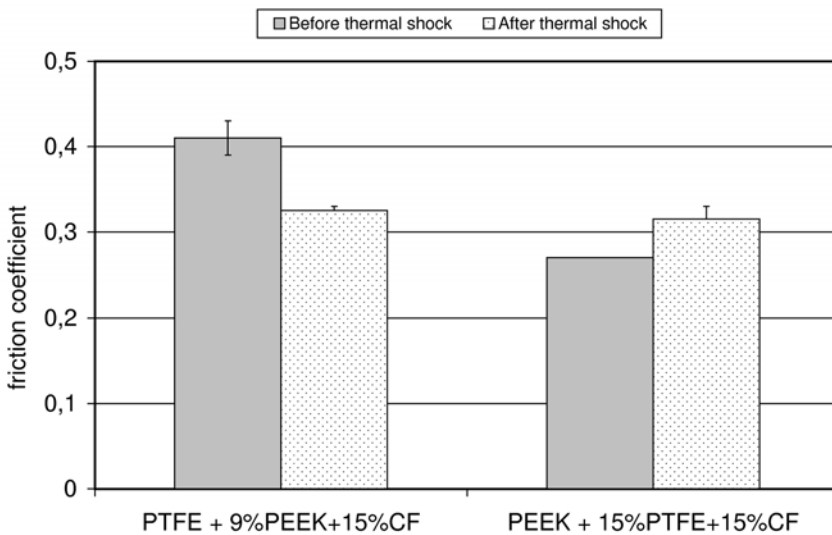


Figure 4.21: Friction coefficient of PTFE and PEEK composites before and after thermal shock cycles experiments in  $LN_2$  ( $T = RT$ ;  $v = 0.2$  m/s)

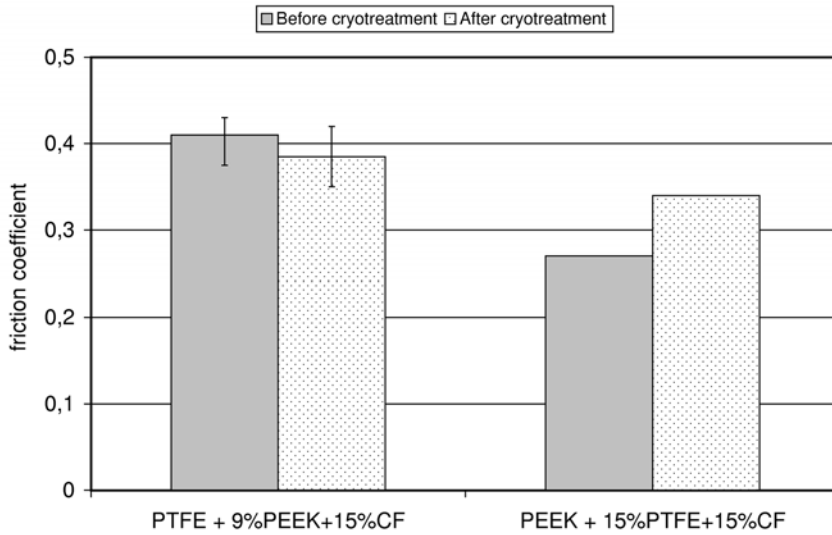


Figure 4.22: Friction coefficient of PTFE and PEEK composites before and after cryo-treatment in  $LN_2$  ( $T = RT$ ;  $v = 0.2$  m/s)

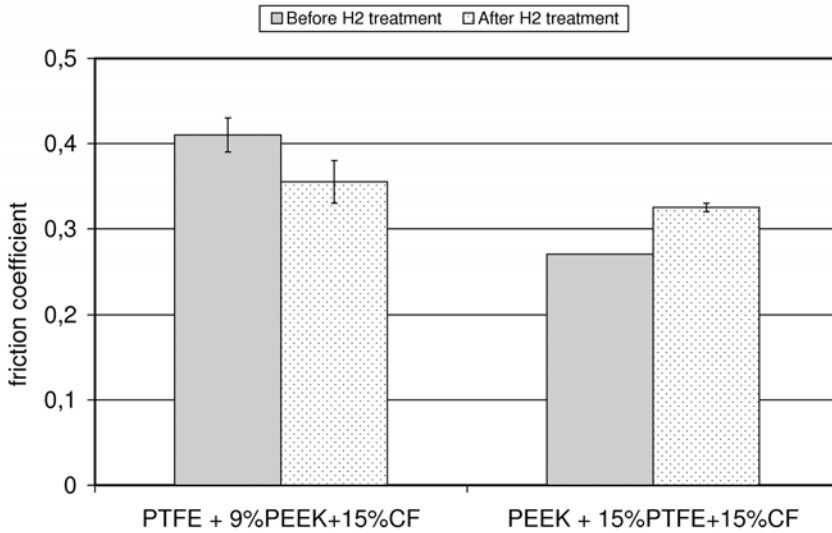


Figure 4.23: Friction coefficient of PTFE and PEEK composites before and after thermal treatment in hydrogen ( $T = RT$ ;  $v = 0.2$  m/s)

## 4 Results

### 4.2.3 Influence of the material composition at RT and at $T = 77\text{K}$

#### 4.2.3.1 Friction and wear measurements

##### 4.2.3.1.1 Influence of PTFE and PEEK content

Figure 4.24 shows the coefficient of friction for PTFE and PEEK composites filled with 15% CF at RT in air and at  $T = 77\text{K}$  in  $\text{LN}_2$ . The graph illustrates clearly the better performance of the composites at low temperatures, since at  $T = 77\text{K}$  the friction coefficient is much smaller than at RT. Whereas the composition of the materials plays an important role at RT, the percentage of the fillers does not influence the friction coefficient in  $\text{LN}_2$  as much.

The linear wear of the PEEK composites is presented in figure 4.25. At RT the wear increases when the PTFE content is higher than 15%. At  $T = 77\text{K}$  in  $\text{LN}_2$ , the amount of PTFE has no influence on the wear of these polymer composites. Furthermore, the wear is much smaller after the experiments in  $\text{LN}_2$  than after the ones at RT. The negative data may be due to some wear debris at the surface of the pin. It is obvious that the sensor could not detect any significant wear after the experiments in  $\text{LN}_2$ . This is why further tests were conducted with spherical pins (fig. 4.26).

According to figure 4.26, the wear volume of the PEEK composite is generally much smaller than that of PTFE composite. For both materials, the wear volume after the experiments in  $\text{LN}_2$  is much lower than after RT tests.

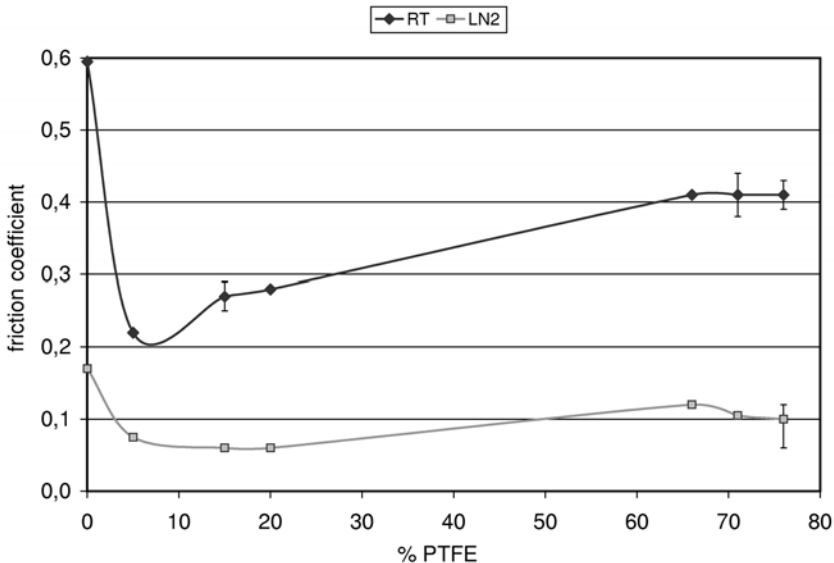


Figure 4.24: Friction coefficient of PTFE and PEEK composites filled with 15% CF at RT and in  $\text{LN}_2$  ( $v = 0.2\text{ m/s}$ ; pure PEEK without CF)

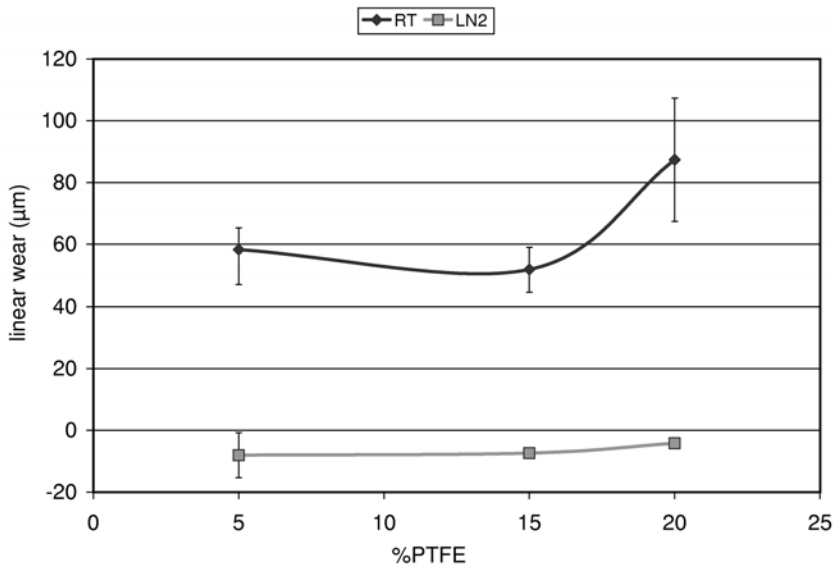


Figure 4.25: Linear wear of PEEK composites filled with 15% CF at RT and in LN<sub>2</sub> ( $v = 0.2$  m/s)

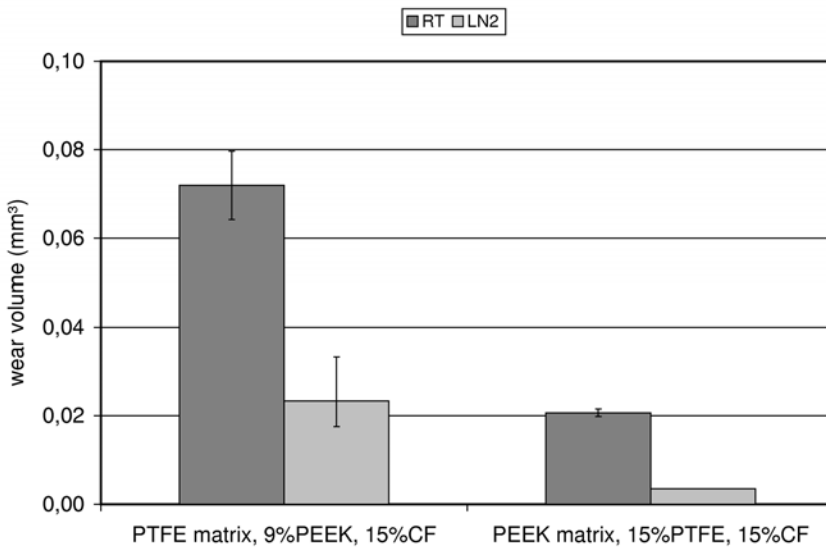


Figure 4.26: Wear volume of PTFE and PEEK composites at RT and in LN<sub>2</sub> ( $v = 0.2$  m/s)

## 4 Results

### 4.2.3.1.2 Influence of CF content

Figure 4.27 presents the friction coefficient of three PTFE composites filled with CF and 20% Ekonol<sup>®</sup>. Similar to the results shown in figure 4.24, it is also noticeable here that the friction decreases clearly in LN<sub>2</sub> compared to RT. Furthermore, increasing the CF content has a much more significant influence on the friction coefficient at RT than in LN<sub>2</sub>. By varying the CF content in PEEK materials, a similar behaviour is observed (fig. 4.28). However, the influence of the CF is not as significant at RT as for the PTFE composites.

The linear wear of the Ekonol<sup>®</sup> filled PTFE composites is given in figure 4.29. The graph indicates lower wear values in LN<sub>2</sub> than at RT. At RT, a significant increase in wear is seen above 15% CF content. This increase is almost negligible in LN<sub>2</sub>.

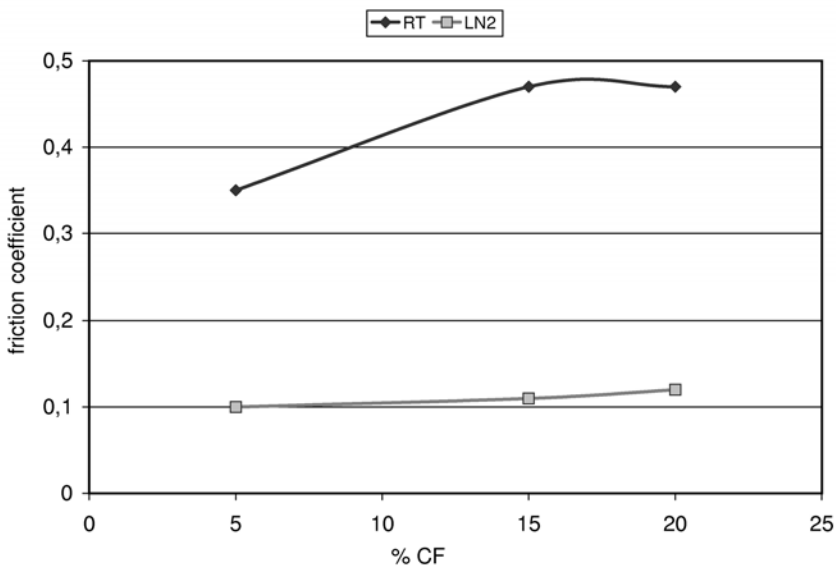


Figure 4.27: Friction coefficient of PTFE composites filled with 20% Ekonol<sup>®</sup> at RT and in LN<sub>2</sub> ( $v = 0.2 \text{ m/s}$ )



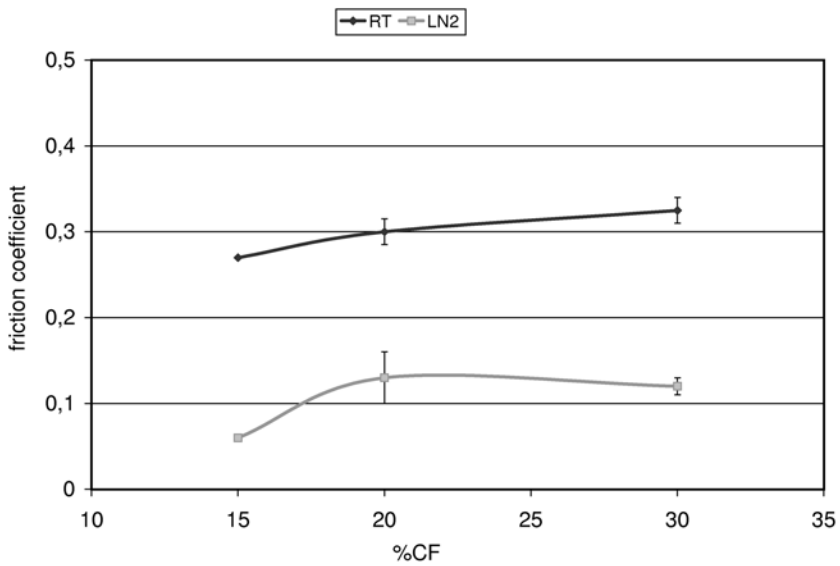


Figure 4.28: Friction coefficient of PEEK composites filled with 15% PTFE at RT and in LN<sub>2</sub> ( $v = 0.2$  m/s)

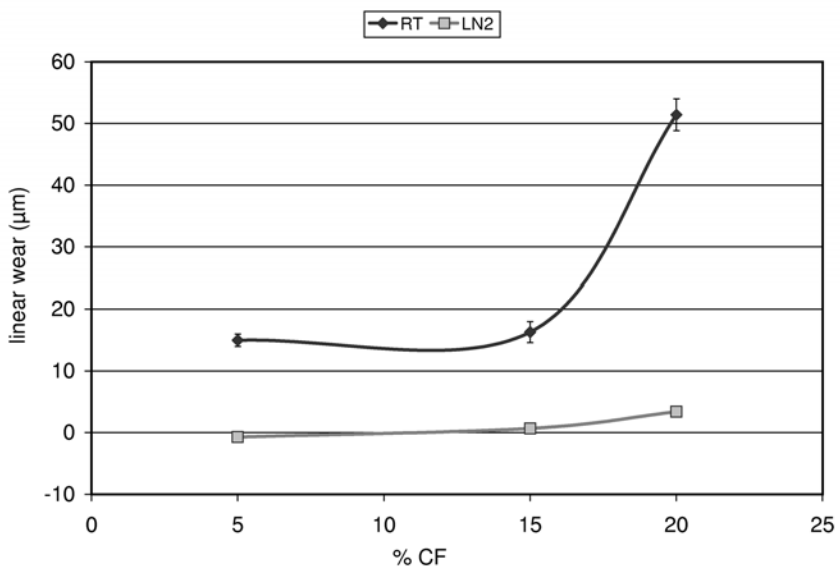


Figure 4.29: Linear wear of PTFE composites filled with 20% Ekonol<sup>®</sup> at RT and in LN<sub>2</sub> ( $v = 0.2$  m/s)

## 4 Results

### 4.2.3.1.3 Influence of the fillers in PTFE composites

Figure 4.30 represents the friction coefficient of three PTFE composites at RT in air and in LN<sub>2</sub>. It is obvious that the type of fillers does not influence the friction behaviour of PTFE composites.

Regarding the wear behaviour, figure 4.31 indicates a much better performance of the composite filled with bronze compared to the composites filled with Ekonol<sup>®</sup> and PEEK especially at RT.

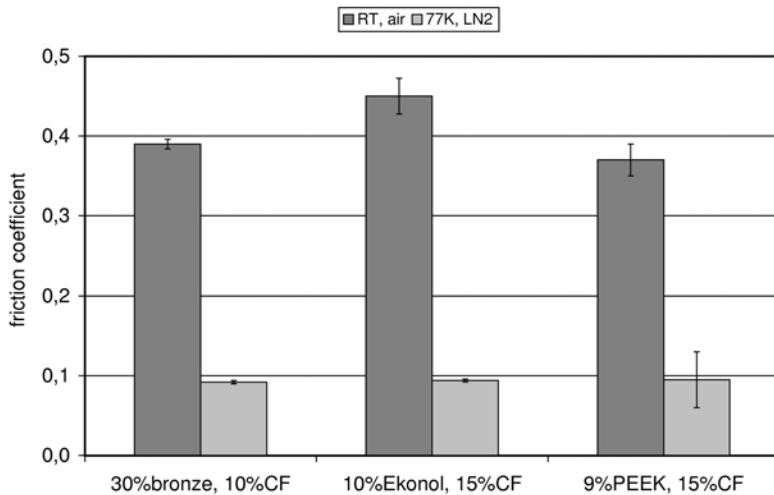


Figure 4.30: Friction coefficient of PTFE composites filled with different types of fillers ( $v = 0.2$  m/s)

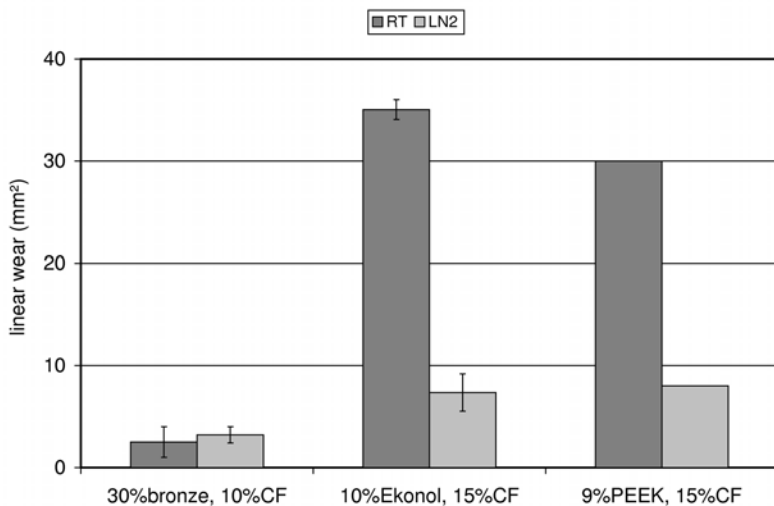


Figure 4.31: Linear wear of PTFE composites filled with different types of fillers ( $v = 0.2$  m/s)

## 4.2.3.2 Surface analyses of the pins

## 4.2.3.2.1 PTFE and PEEK matrices

At RT, the surface of PTFE filled with 9% PEEK and 15% CF (*fig. 4.32a*) and PEEK filled with 15% PTFE and 15% CF (*fig. 4.32b*) composites are characterized by some grooves and wear debris. CF are uncovered especially in the PTFE-matrix composite, which suggests that this matrix wears more away than the PEEK-matrix.

After tests in LN<sub>2</sub>, the surface of the composite presents some cracks, in perpendicular direction of the sliding motion (*fig. 4.33*). CF are well embedded in the matrix, which is an indication that the wear process has been hindered.

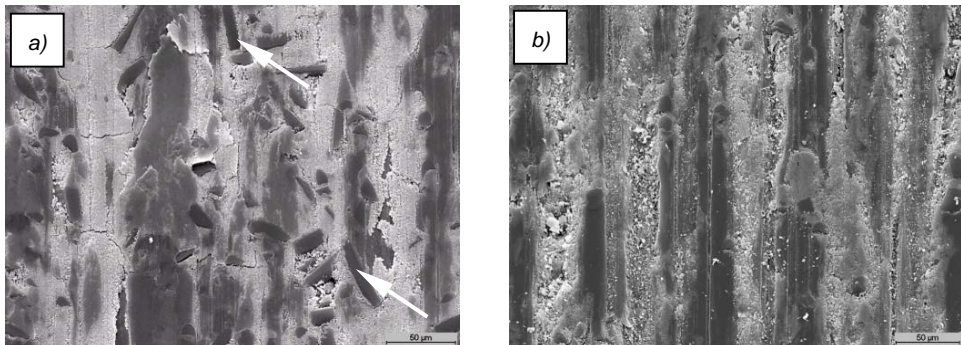


Figure 4.32: SEM images of a) PTFE filled with 9% PEEK and 15% CF and b) PEEK filled with 15% PTFE and 15% CF, after tests at RT

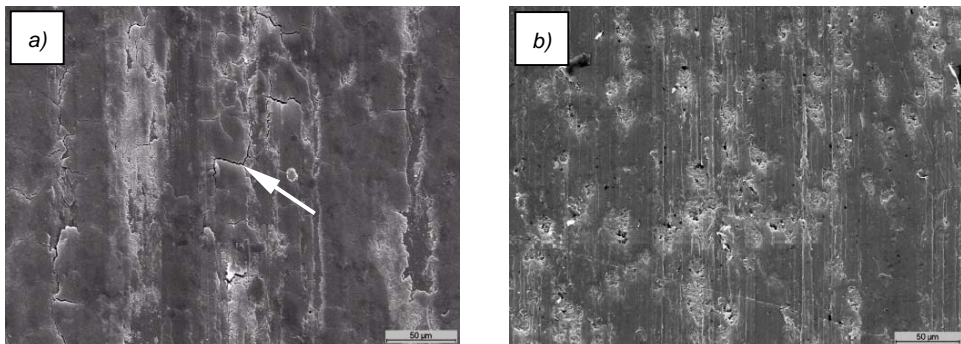


Figure 4.33: SEM images of a) PTFE filled with 9% PEEK and 15% CF and b) PEEK filled with 15% PTFE and 15% CF, after tests in LN<sub>2</sub>

## 4 Results

### 4.2.3.2.2 Influence of PTFE content in PEEK composites

The SEM images indicate that more CF are present on the surface of the PEEK-matrix composite with 20% PTFE (*fig. 4.34b*) compared to the surface of the composite with only 5% PTFE (*fig. 4.34a*) at RT. The composite with a higher PTFE content wears more than the composite with a lower PEEK content.

After the experiments in LN<sub>2</sub>, both surfaces present fewer damages, the CF are still covered by the matrix (*fig. 4.35*).

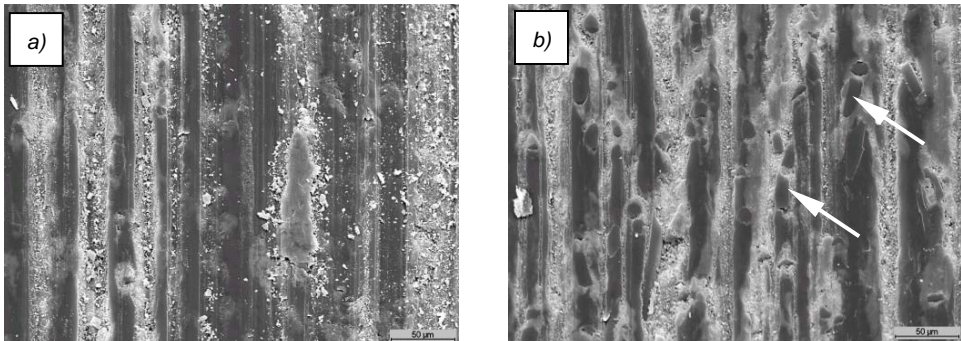


Figure 4.34: SEM images of PEEK-matrix composites filled with 15% CF and a) 5% PTFE or b) 20% PTFE, after tests at RT

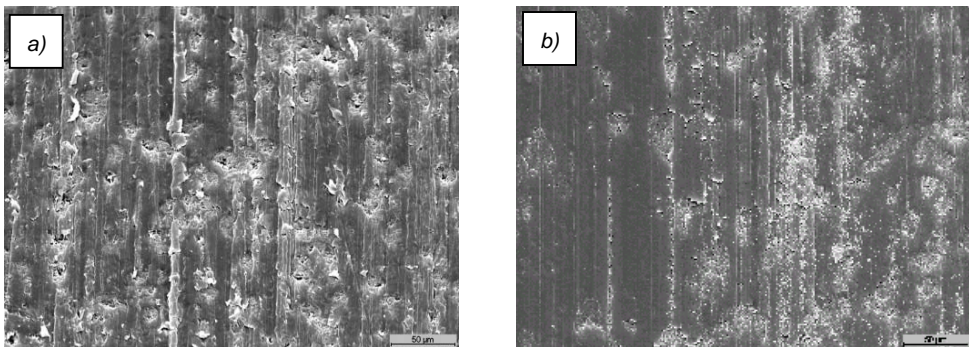
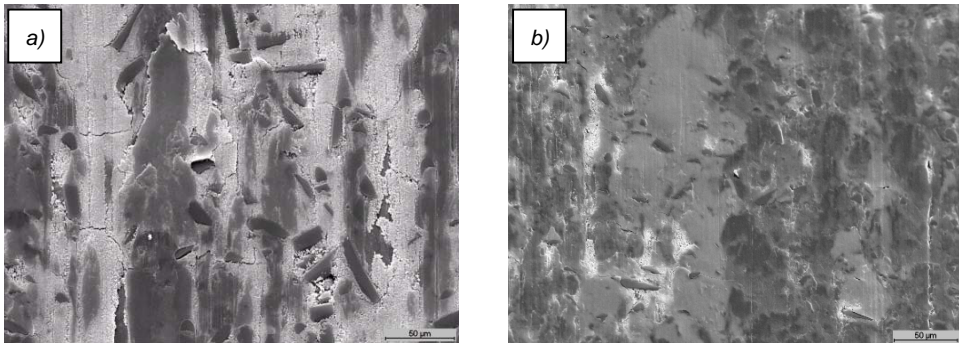


Figure 4.35: SEM images of PEEK-matrix composites filled with 15% CF and a) 5% PTFE or b) 20% PTFE, after tests in LN<sub>2</sub>

## 4.2.3.2.3 Influence of PEEK content in PTFE composites

Similar observations are seen at the surface of the PTFE composites (*figs. 4.36* and *4.37*, which compare the material represented in *figs. 4.32a* and *4.33a* with another composite). At RT, the composite with a higher PEEK content (*fig. 4.36b*) wears less than the other one (*fig. 4.36a*), whereas after the experiments in LN<sub>2</sub>, both surfaces are similar (*fig. 4.37*).



*Figure 4.36* SEM images of PTFE composites filled with 15 %CF and a) 9% PEEK or b) 25% PEEK, after tests at RT

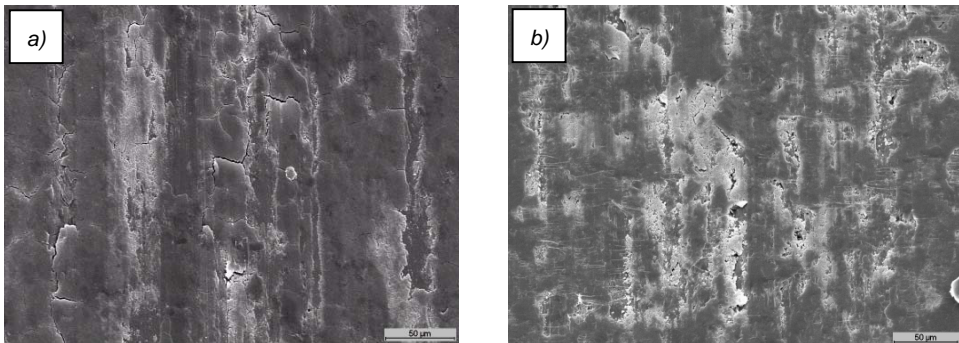


*Figure 4.37* SEM images of PTFE composites filled with 15% CF and a) 9% PEEK or b) 25% PEEK, after tests in LN<sub>2</sub>



## 4 Results

### 4.2.3.2.4 Influence of CF in PTFE composites

Figures 4.38 and 4.39 show the surfaces of two PTFE composites with different amount of CF, after experiments at RT and in LN<sub>2</sub>. CF are present on the surface of both composites at RT. They are well embedded in the matrix of the composite with 5% CF (fig. 4.38a), but some detachments of the fibres are seen at the surface of the composite with 20% CF (fig. 4.38b). After the experiments in LN<sub>2</sub>, the CF are totally detached for the material with 20% CF (fig. 4.39).

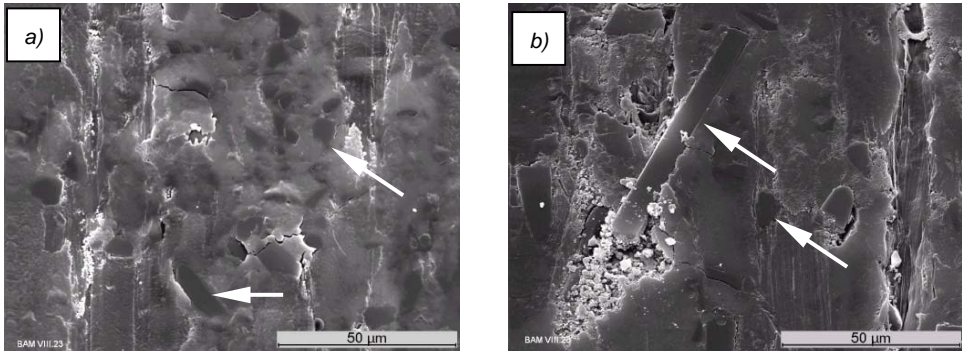


Figure 4.38: SEM images of PTFE composites filled with 20% Ekonol® and a) 5% CF or b) 20% CF, after tests at RT

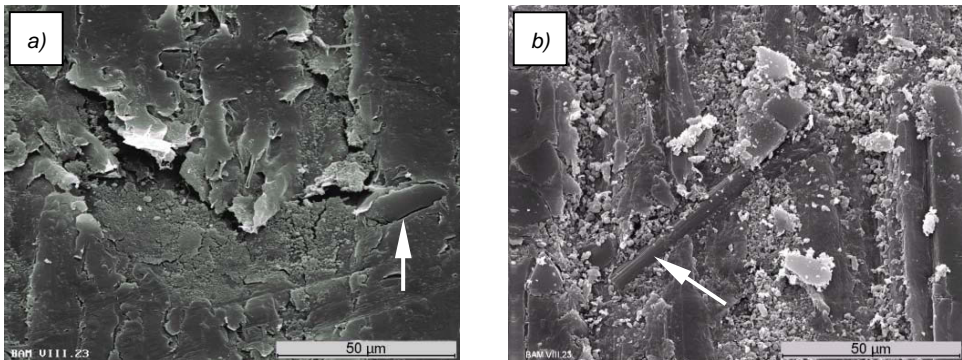


Figure 4.39: SEM images of PTFE composites filled with 20% Ekonol® and a) 5% CF or b) 20% CF, after tests in LN<sub>2</sub>

## 4.2.3.2.5 Influence of CF in PEEK composites

Figures 4.40 and 4.41 present SEM images of two PEEK composites filled with 15% (a) and 30% CF (b) respectively, after tests at RT and in LN<sub>2</sub>. The CF content does not have a significant influence on the surface of the worn PEEK materials. This is in accordance with the friction results shown in figure 4.28.

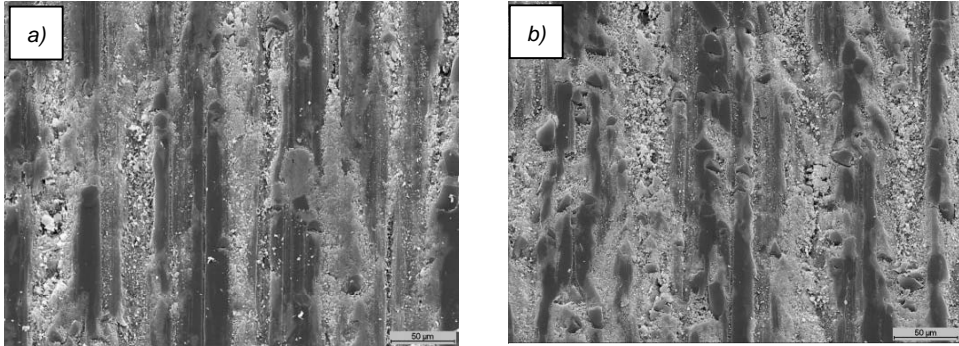


Figure 4.40: SEM images of PEEK composites filled with 15% PTFE and a) 15% CF or b) 30% CF, after tests at RT

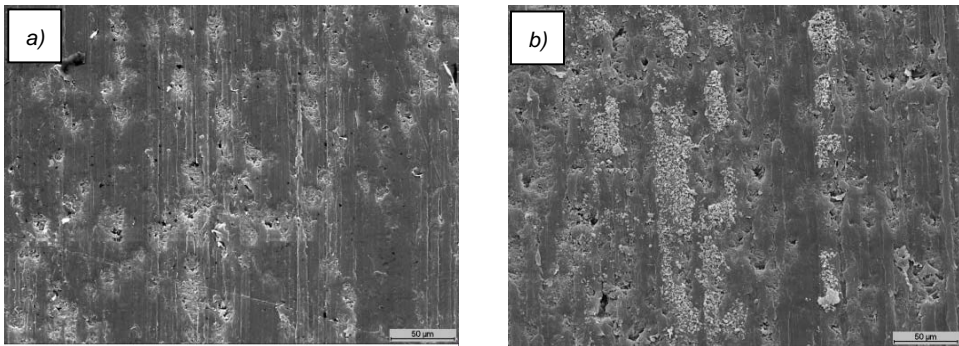


Figure 4.41: SEM images of PEEK composites filled with 15% PTFE and a) 15% CF or b) 30% CF, after tests in LN<sub>2</sub>

## 4 Results

### 4.2.3.2.6 Influence of the fillers in PTFE composites

SEM images of the surface of two PTFE composites filled with CF and Ekonol<sup>®</sup> (a), and CF and bronze (b) are represented in figures 4.42 and 4.43. After the tests at RT, the surface of both composites are similar, CF as well as Ekonol<sup>®</sup> and bronze particles are uncovered and thus clearly visible (fig. 4.42). This is due to the fact that the PTFE-matrix wears out producing a flat surface.

After the experiments in LN<sub>2</sub> (fig. 4.43), the SEM image of PTFE-matrix composite filled with CF and Ekonol<sup>®</sup> shows some cracks, which are not detected for the bronze filled composite under the same test conditions.

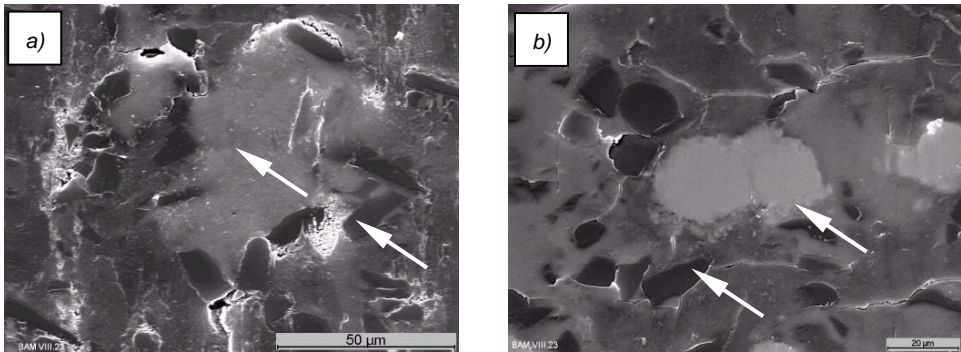


Figure 4.42: SEM images of PTFE-matrix composites filled with CF and a) Ekonol<sup>®</sup> or b) bronze after tests at RT

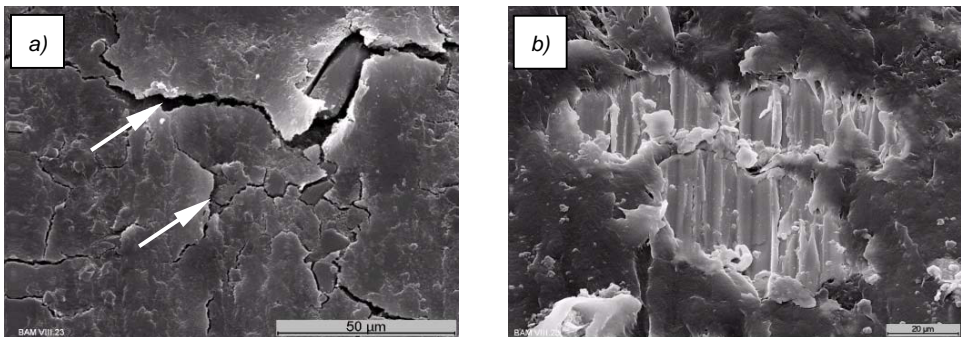


Figure 4.43: SEM images of PTFE-matrix composites filled with CF and a) Ekonol<sup>®</sup> or b) bronze after tests in LN<sub>2</sub>



#### 4.2.3.3 Surface analyses of the discs

##### 4.2.3.3.1 Tests against PTFE filled with bronze and CF

The optical microscopy images of the surface of the disc after the experiments against bronze/CF filled PTFE point out the difference between the material transferred by the experiments at RT (*fig. 4.44*), and the material transferred by the LN<sub>2</sub> tests (*fig. 4.45*). After the RT experiments, the film is homogenous, whereas in LN<sub>2</sub>, the transfer consists of fine polymer particles.

Profilometry measurements (*figs. 4.46* and *4.47*) indicate that the transfer film is much thinner at low temperatures than at RT.

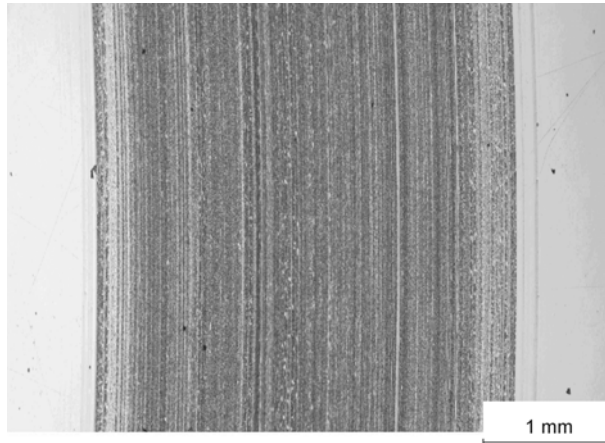


*Figure 4.44: Surface of the disc after experiment at RT against PTFE filled with 10% CF and 30% bronze*

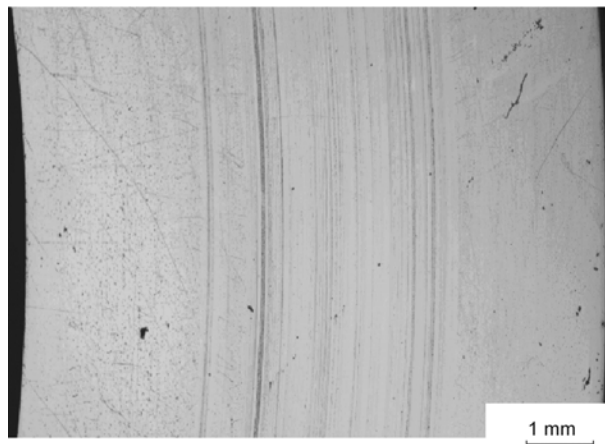


*Figure 4.45: Surface of the disc after experiment in LN<sub>2</sub> against PTFE filled with 10% CF and 30% bronze*

## 4 Results

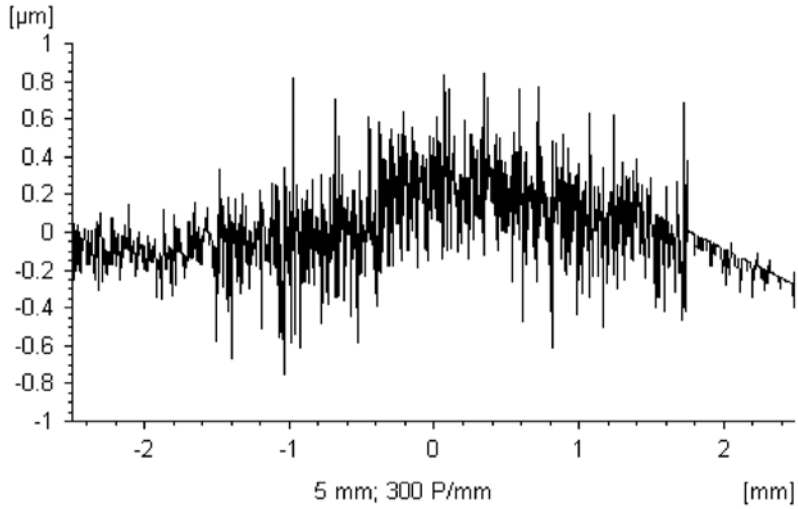


Figure 4.46: Profile of transfer film on the disc after experiment at RT against PTFE filled with 10% CF and 30% bronze

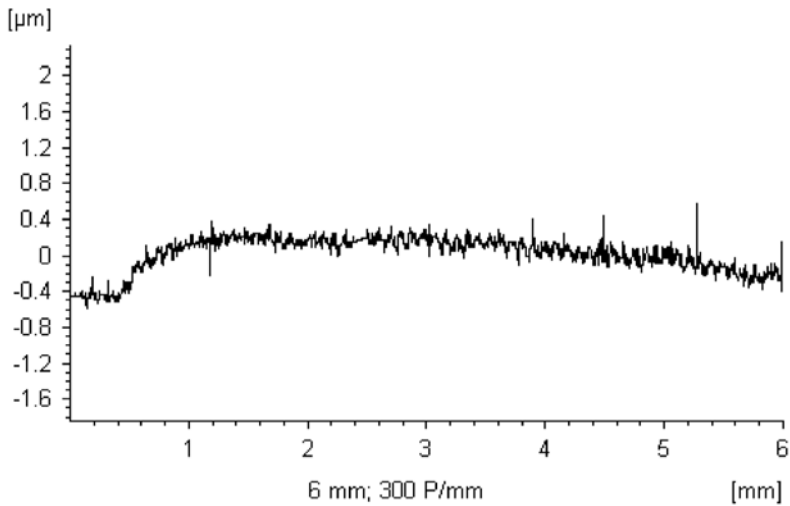
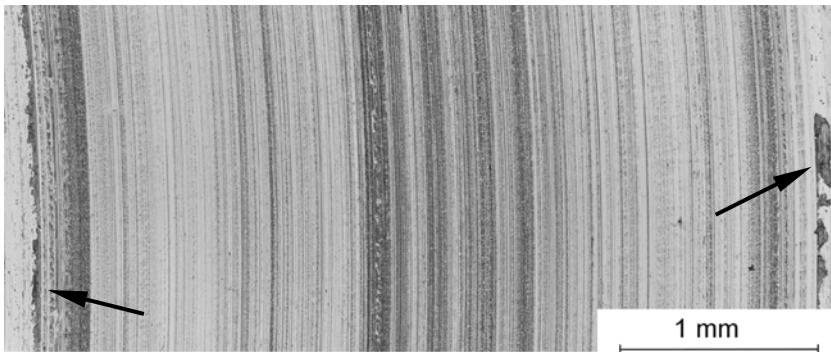


Figure 4.47: Profile of the transfer film on the disc after experiment in  $\text{LN}_2$  against PTFE filled with 10% CF and 30% bronze

#### 4.2.3.3.2 Tests against PTFE filled with PEEK and CF

After the tests at RT, the surface of the disc is covered with PTFE transfer. Wear debris are visible at the edges of the sliding area (*fig. 4.48*). After the experiments in LN<sub>2</sub>, the transfer film is smaller and consists of polymer bands (*fig. 4.49*).

SEM images indicate that after the tests at RT, the transfer is rather homogeneous (*fig. 4.50*), whereas after the LN<sub>2</sub> experiments, the transfer is substantially smaller and consists of scattered polymer particles (*fig. 4.51*).



*Figure 4.48: Surface of the disc after experiment at RT against PTFE filled with 15% CF and 9% PEEK*

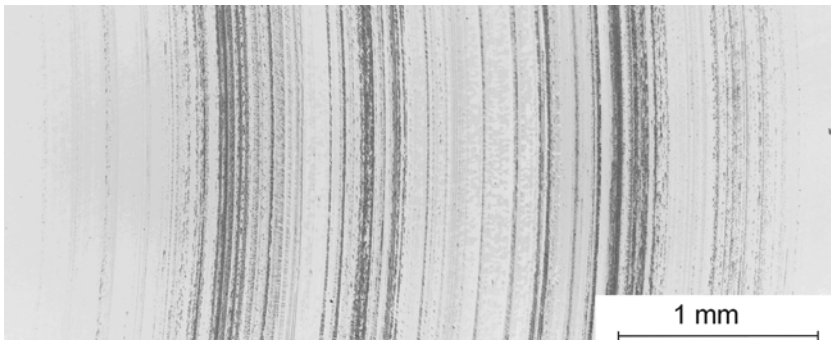


*Figure 4.49: Surface of the disc after experiment in LN<sub>2</sub> against PTFE filled with 15% CF and 9% PEEK*

## 4 Results

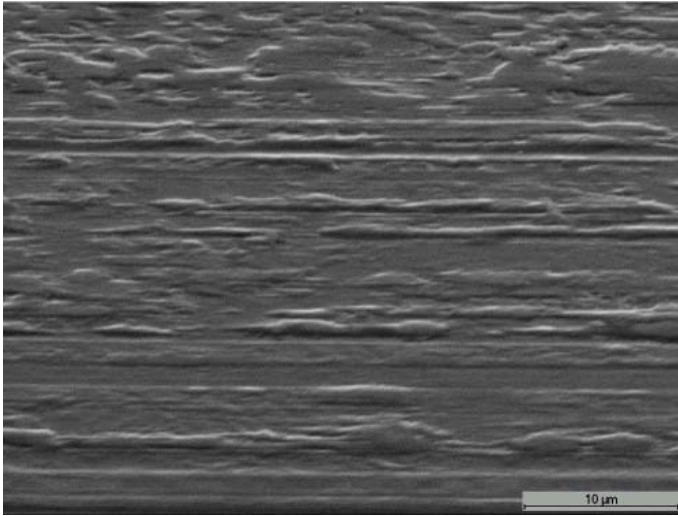


Figure 4.50: SEM image of the disc tested against PTFE filled with 15% CF and 9% PEEK after test at RT

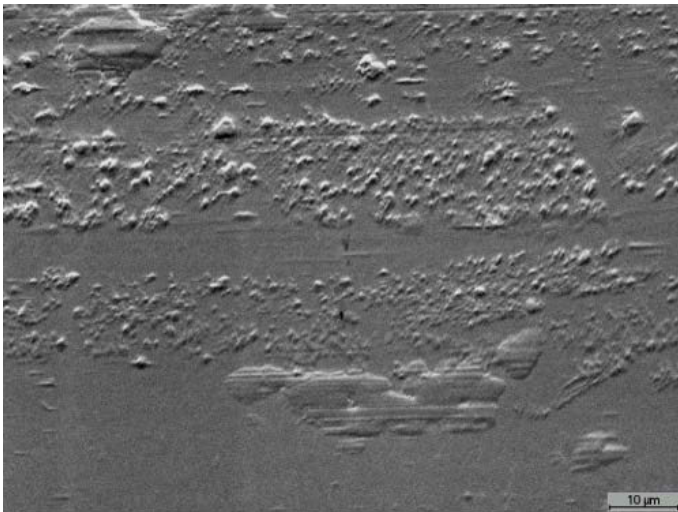


Figure 4.51: SEM image of the disc tested against PTFE filled with 15% CF and 9% PEEK after test in LN<sub>2</sub>

## 4.2.3.3.3 Tests against PEEK filled with PTFE and CF

Similar observations are seen after the experiments with a PEEK composite (figs. 4.52 and 4.53). The material transferred after the tests in LN<sub>2</sub> is even thinner than the one produced with PTFE material.

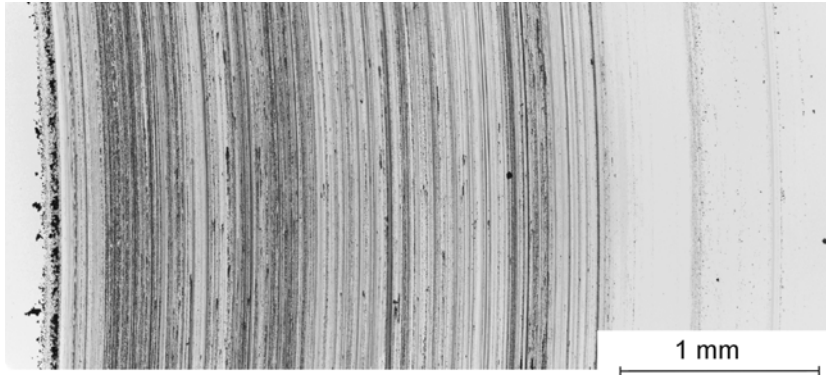


Figure 4.52: Surface of the disc after experiment at RT against PEEK filled with 15% CF and 15% PTFE

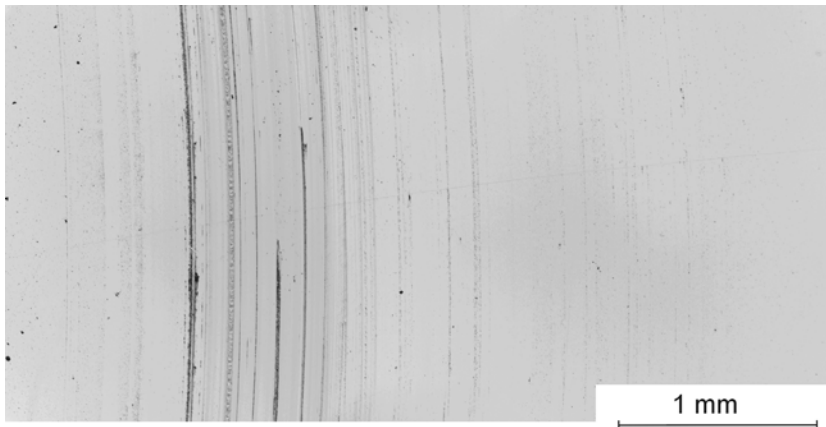


Figure 4.53: Surface of the disc after experiment at RT against PEEK filled with 15% CF and 15% PTFE

## 4 Results

### 4.2.4 Influence of the cryogenic environment

Cryogenic applications are not restricted to  $T = 77\text{ K}$  in  $\text{LN}_2$ , but most of them are conducted in helium and hydrogen environments at different temperatures, which can influence the behaviour of the material. This is why this chapter presents the tribological performance of some selected PTFE and PEEK composites according to the following factors:

- Different temperatures in the same environment (helium),
- different environments at a constant temperature ( $T = 77\text{ K}$ ),
- influence of the cryogenic liquids ( $\text{LN}_2$ ,  $\text{LHe}$  and  $\text{LH}_2$ ), and
- influence of the hydrogen environment.

#### 4.2.4.1 Friction measurements

##### 4.2.4.1.1 Influence of the temperature in helium environment

*Figure 4.54* represents the friction coefficient of bronze/CF filled PTFE in helium environment at  $T = 77\text{ K}$ ,  $T = 30\text{ K}$  and  $T = 4.2\text{ K}$ . It can be noticed that at high speed ( $v = 1\text{ m/s}$ ), the friction is the same whatever the temperature. At a lower speed ( $v = 0.2\text{ m/s}$ ), the coefficient of friction decreases with the temperature. These results point out the importance of the sliding speed on the frictional behaviour of this material at cryogenic temperatures.

##### 4.2.4.1.2 Influence of the environment at $T = 77\text{ K}$

*Figure 4.55* represents the friction coefficient of bronze/CF filled PTFE at  $T = 77\text{ K}$  in He-gas and in  $\text{LN}_2$  for the two sliding speeds  $v = 1\text{ m/s}$  and  $v = 0.2\text{ m/s}$ . The importance of the cryogenic medium is clearly shown: the friction coefficient in  $\text{LN}_2$  is smaller than the one in helium at the same temperature for the two sliding speeds.

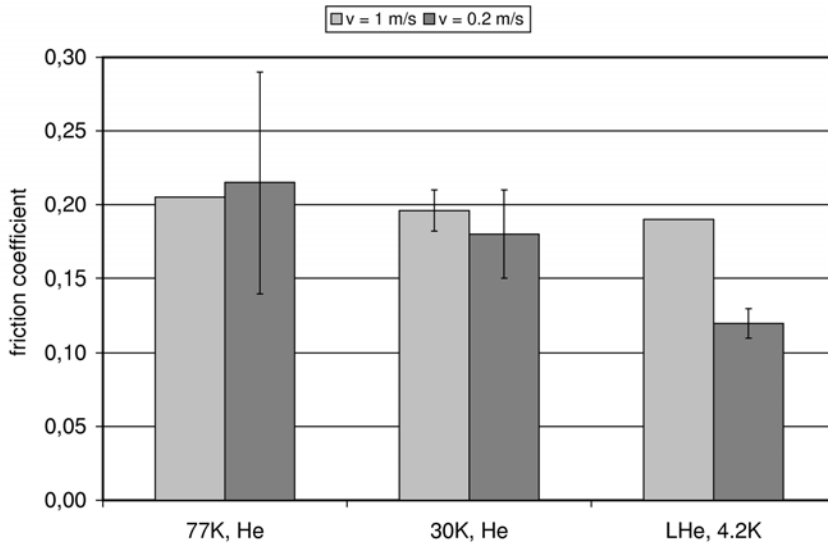


Figure 4.54: Friction coefficient of PTFE filled with 30% bronze and 10% CF in He-gas at  $T = 77 \text{ K}$ ,  $30 \text{ K}$  and  $4.2 \text{ K}$

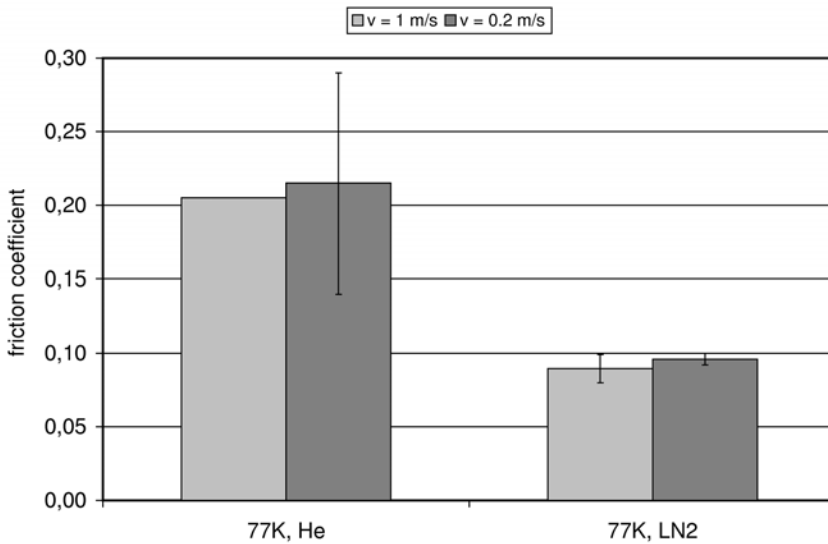


Figure 4.55: Friction coefficient of PTFE filled with 30% bronze and 10% CF at  $T = 77 \text{ K}$  in He-gas and in LN<sub>2</sub>

## 4 Results

### 4.2.4.1.3 Influence of the cryogenic liquid

Comparing the friction behaviour of bronze/CF filled PTFE in the three cryogenic liquids, a higher friction in LHe is found especially at high speed (*fig. 4.56*). At lower speed, the friction coefficient remains similar in the three cryogens.

While the influence of the speed is obvious in helium environment, this is not the case in LN<sub>2</sub>, where the friction coefficient of bronze/CF filled PTFE remains constant at  $v = 1$  m/s, 0.2 m/s and 0.06 m/s (*fig. 4.57*). That suggests that an optimal cooling is reached in LN<sub>2</sub> at low as well as at high speeds.

The same observations are seen with PEEK/CF filled PTFE composite. At low temperatures and low sliding speed, the friction coefficient is similar in LN<sub>2</sub> and in LH<sub>2</sub> (*fig. 4.58*). Concerning the Ekonol<sup>®</sup>/CF filled PTFE material, the coefficient of friction is higher in LHe than in LN<sub>2</sub>, but lower than the one measured in He-gas (*fig. 4.59*).

### 4.2.4.1.4 Influence of hydrogen environment at RT

Friction measurements of PTFE and PEEK composites were carried out at RT in air and in hydrogen. *Figure 4.60* indicates that the friction coefficient is much smaller for the three composites in hydrogen environment.

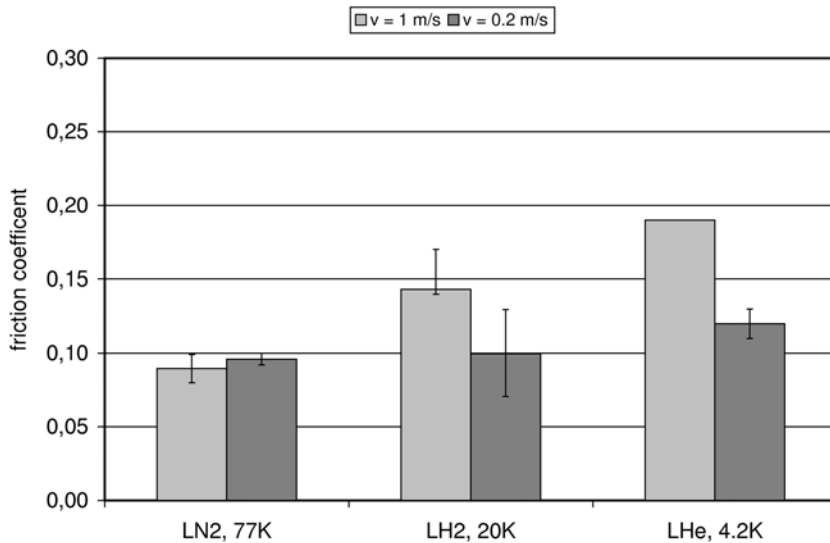


Figure 4.56: Friction coefficient of PTFE filled with 30% bronze and 10% CF in LN<sub>2</sub>, in LH<sub>2</sub> and in LHe



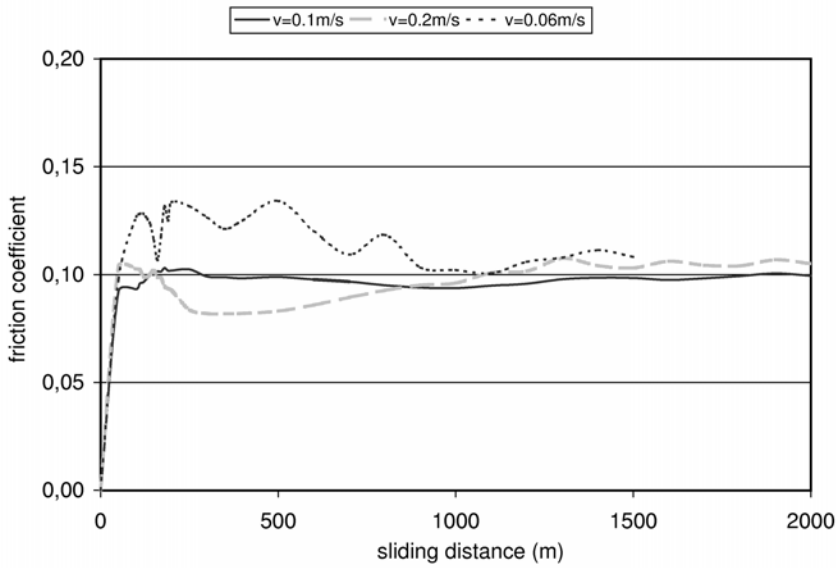


Figure 4.57: Friction coefficient of PTFE filled with 30% bronze and 10% CF in  $\text{LN}_2$

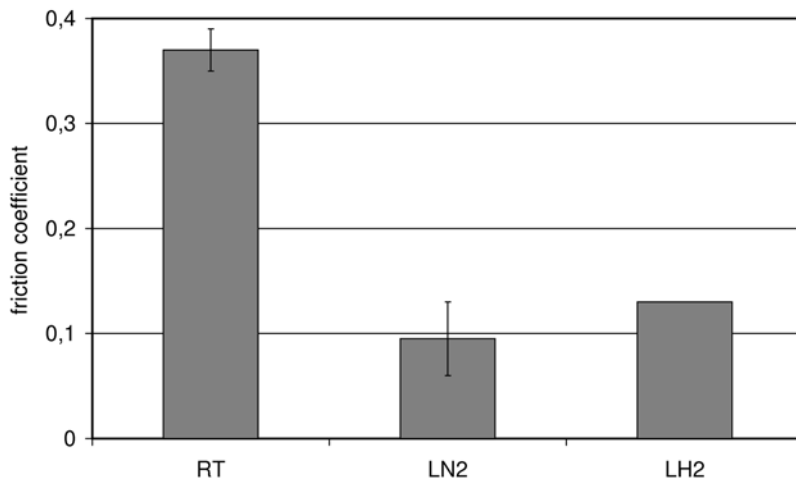


Figure 4.58: Friction coefficient of PTFE filled with 15% CF and 9% PEEK at RT in air, in  $\text{LN}_2$  and in  $\text{LH}_2$  ( $v = 0.2\text{ m/s}$ )

## 4 Results

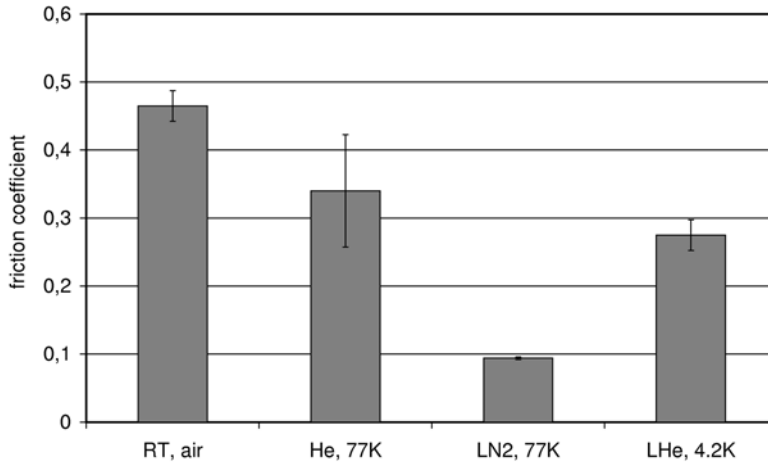


Figure 4.59: Friction coefficient of PTFE filled with 10% Ekonol<sup>®</sup> and 15% CF at RT in air, at  $T = 77\text{ K}$  in He-gas, in LN<sub>2</sub> and in LHe ( $v = 0.2\text{ m/s}$ )

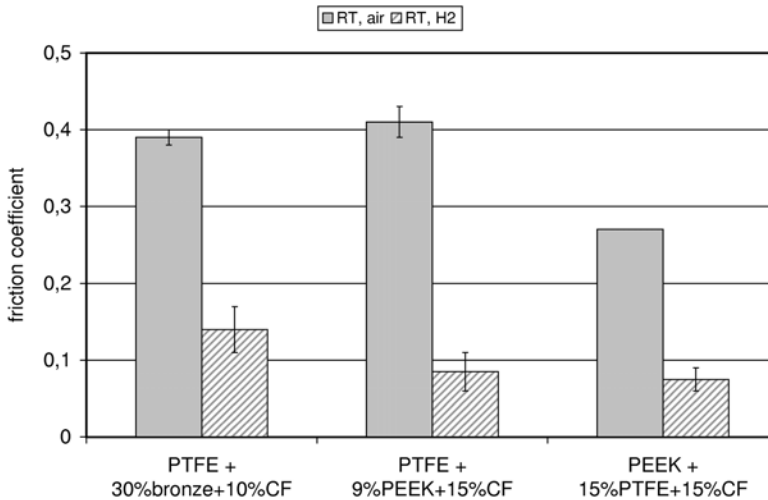


Figure 4.60: Friction coefficient of PTFE and PEEK composites at RT in air and in H<sub>2</sub> ( $v = 0.2\text{ m/s}$ )

## 4.2.4.2 Wear measurements

The wear volume of PTFE and PEEK composites was measured after the experiments at RT in air, in LN<sub>2</sub>, LH<sub>2</sub> and LHe (figs. 4.61 and 4.62). The results indicate that both composites wear much less either in LN<sub>2</sub> or in LH<sub>2</sub>. Furthermore, the PEEK composite has a smaller wear than the PTFE composite in all environments.

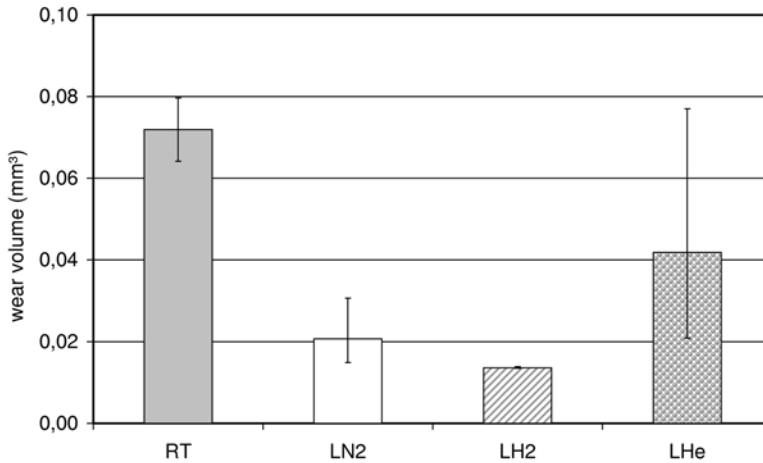


Figure 4.61: Wear volume of PTFE composite with 15% CF and 9% PEEK ( $v = 0.2$  m/s)

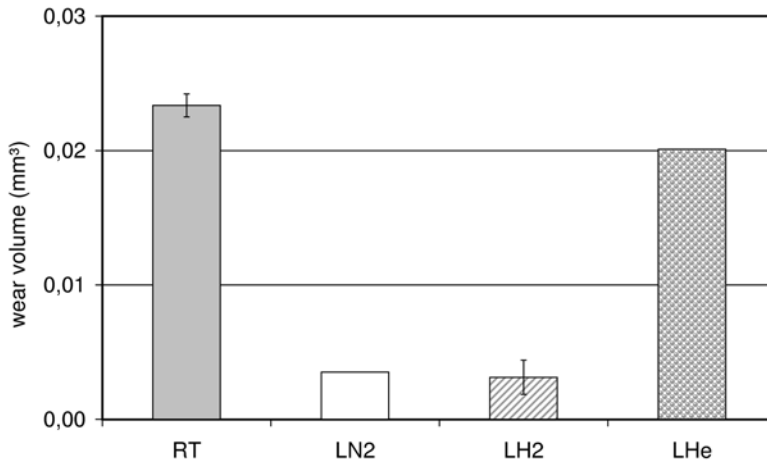


Figure 4.62: Wear volume of PEEK composite with 15% CF and 15% PTFE ( $v = 0.2$  m/s)

## 4 Results

### 4.2.4.3 Surface analyses

#### 4.2.4.3.1 Topography, analyses of the transfer film

The transfer film formed on the surface of the disc after the tests against bronze/CF filled PTFE were investigated by means of optical microscopy, profilometry, SEM and AFM.

At  $v = 1$  m/s, profile measurements and optical microscopy images show the important influence of the temperature as well as the environment on the topography (*fig. 4.63*). At room temperature in air, the transfer film is clearly visible (*fig. 4.63a*). It consists of a homogeneous film, 200 nm to 300 nm thick, with some 0.5  $\mu\text{m}$  thick lumps. At  $T = 77$  K in He-gas, the transfer is inhomogeneous (*fig. 4.63b*). The thin area consists of long PTFE lumps (*fig. 4.64a*). In the centre, the transfer film is thicker, up to 1.2  $\mu\text{m}$ . The experiments carried out in  $\text{LN}_2$  produced a much thinner transfer film (*fig. 4.63c*) that consists of scattered polymer particles. The average thickness is 100 nm. The transfer film built up in LHe is thicker compared to the one formed in  $\text{LN}_2$  (*fig. 4.63d*). The film consists of broad tracks, which are up to 1.5  $\mu\text{m}$  thick. The transfer film is brittle and shows many small wear debris at the edge as well as at the centre of the film (*fig. 4.64b*).

For the experiments carried out at  $v = 0.2$  m/s, profile measurements (*fig. 4.65*) indicate also a clear influence of temperature and environment. However, the topography of the disc is quite different from the one at  $v = 1$  m/s. Significant abrasive scarves are produced in  $\text{LN}_2$  (*fig. 4.66*) as well as in LHe.

The transfer film developed in  $\text{LH}_2$  at  $v = 1$  m/s consists of accumulations of particles (*fig. 4.67*). Broad scoring can be observed at the surface of the disc (*fig. 4.67a*). Similar observations of the transfer film can be made after the experiments at  $v = 0.2$  m/s (*fig. 4.68*). However, the scoring at lower speed is larger (*fig. 4.68a*). The transfer particles are partly broken (*fig. 4.68b*).

One of the major difference in  $\text{LH}_2$  is that the transfer film formed is extremely thin. AFM line scan indicated the contrast with  $\text{LN}_2$  and LHe at  $v = 0.2$  m/s (*fig. 4.69*).

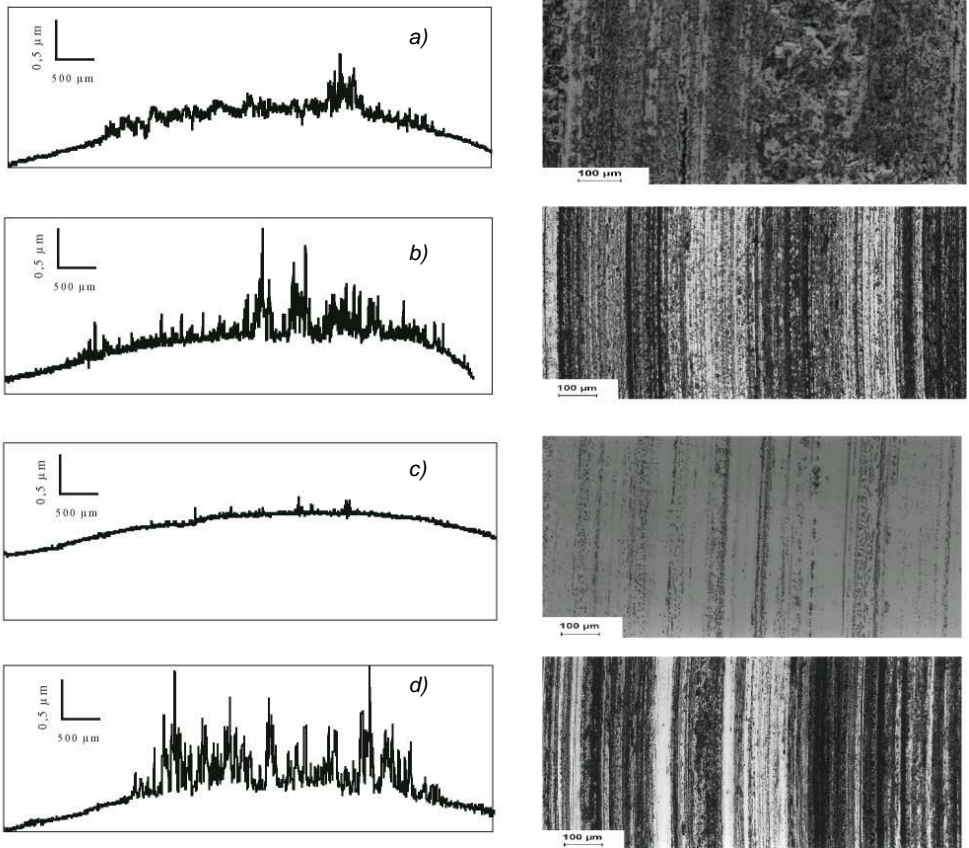


Figure 4.63: Profile and optical microscopy images of the transfer film formed on the disc after experiments against bronze/CF filled PTFE ( $v = 1$  m/s) a) at RT in air, b) in He-gas at  $T = 77$  K, c) in  $\text{LN}_2$ , and d) in LHe

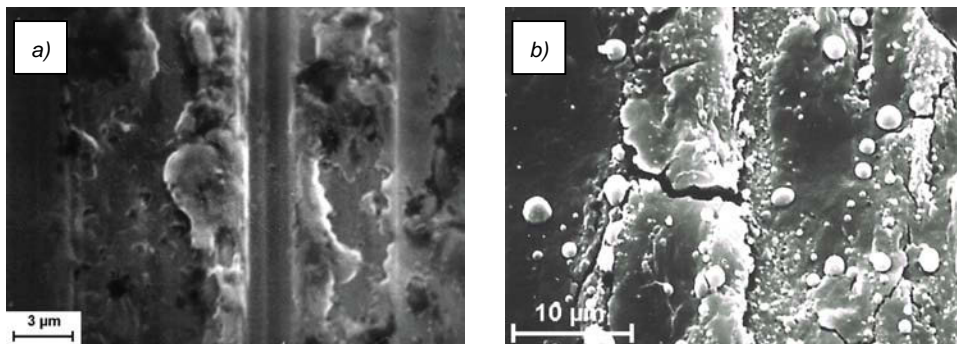
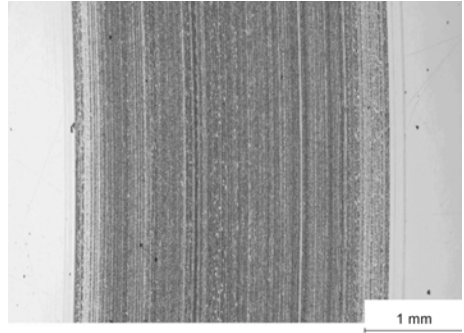
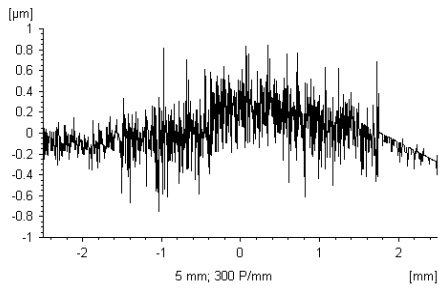


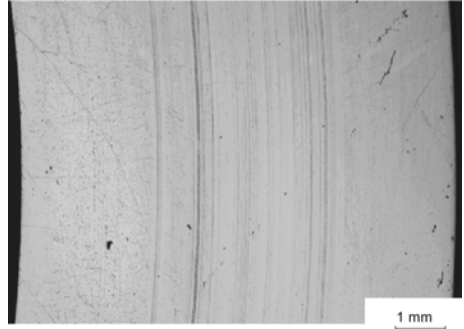
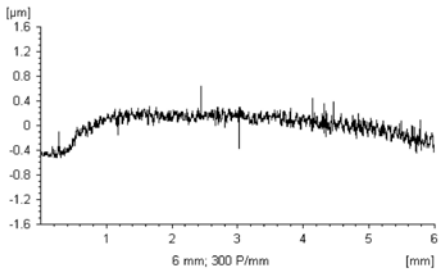
Figure 4.64: SEM images of the transfer film formed on the disc after experiments against bronze/CF filled PTFE ( $v = 1$  m/s) a) in He-gas at  $T = 77$  K and b) in LHe

## 4 Results

a)



b)



c)

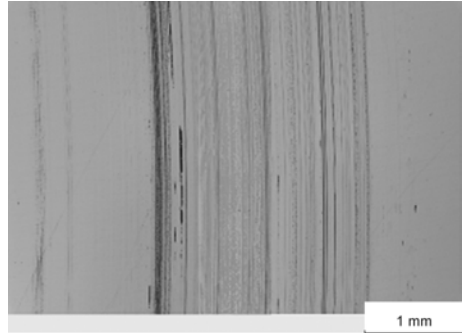
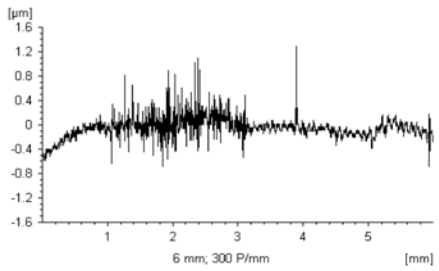


Figure 4.65: Profilometry measurements and optical microscopy images of the surface of the discs after tests against bronze/CF filled PTFE at  $v = 0.2 \text{ m/s}$  a) in air at RT, b) in  $\text{LN}_2$ , and c) in LHe

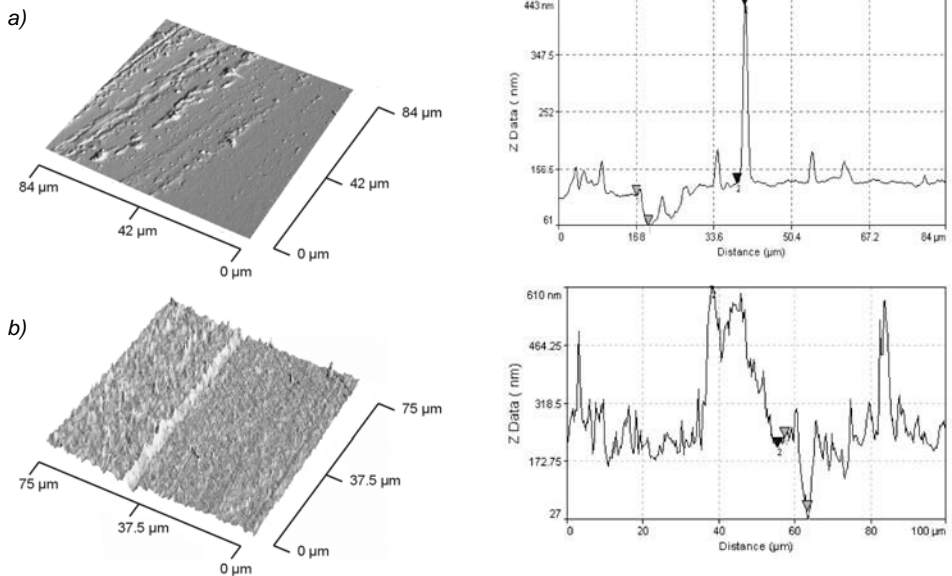


Figure 4.66: AFM images of the surface of the discs after the experiments against bronze/CF filled PTFE in  $\text{LN}_2$  at a)  $v = 1 \text{ m/s}$  and b)  $v = 0.2 \text{ m/s}$

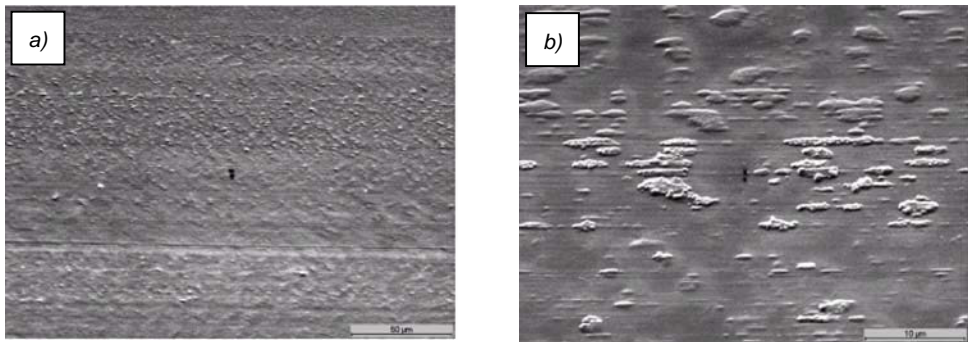


Figure 4.67: SEM images of the surface of the discs after the experiments against bronze/CF filled PTFE in  $\text{LH}_2$  at  $v = 1 \text{ m/s}$

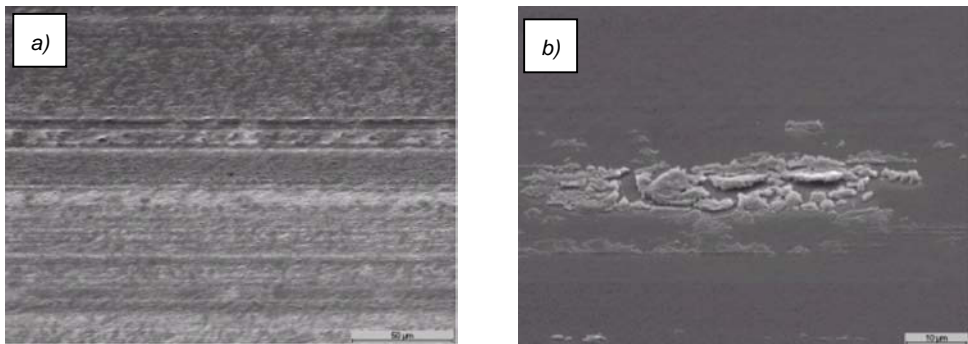


Figure 4.68: SEM images of the surface of the discs after the experiments against bronze/CF filled PTFE in  $\text{LH}_2$  at  $v = 0.2 \text{ m/s}$

## 4 Results

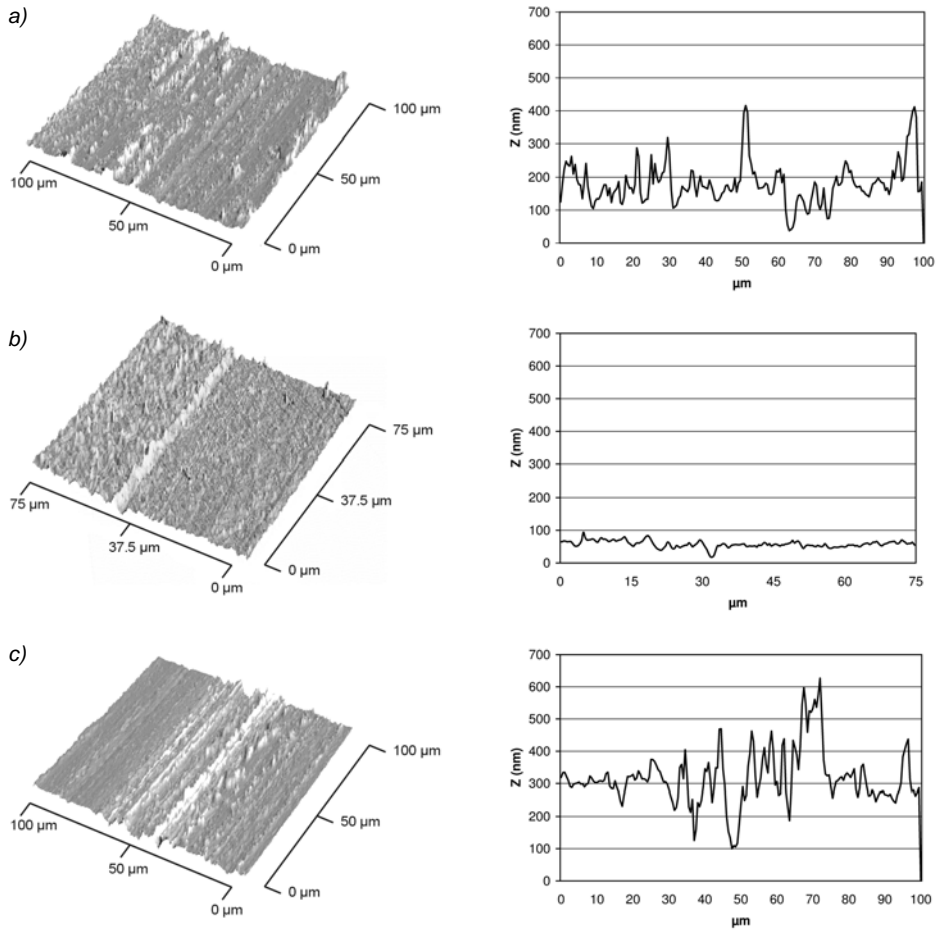


Figure 4.69: AFM images of the surface of the discs after tests against bronze/CF filled PTFE at  $v = 0.2 \text{ m/s}$  in a)  $\text{LN}_2$ , b)  $\text{LH}_2$  and c)  $\text{LHe}$



#### 4.2.4.3.2 Topography, analyses of the pins

Similarly to the transfer film analyses, a significant influence of the medium on the morphology of the surfaces of the pins was observed. The surface of the bronze/CF filled PTFE pin tested at  $v = 1$  m/s at room temperature is flat, bronze and CF particles are clearly visible (*fig. 4.70a*). The SEM images of the sample tested in LN<sub>2</sub> (*fig. 4.70b*) show that the bronze particles are partially covered with PTFE lumps, which are pulled out of the matrix.

The influence of the speed is particularly seen at the surface of the composite after the experiments carried out in LH<sub>2</sub> and in LHe. At  $v = 1$  m/s, PTFE filaments are seen to be present at the surface of the pin tested in LH<sub>2</sub> (*fig. 4.70c*), while powder-like wear debris are observed after the experiments in LHe (*fig. 4.70d*).

At  $v = 0.2$  m/s (*fig. 4.71*), similar observations of the pin surfaces are seen after the experiments at RT and in LN<sub>2</sub>. The surface of the pin tested in LH<sub>2</sub> presents some cracks and powder-like wear debris as well as the one tested in LHe.

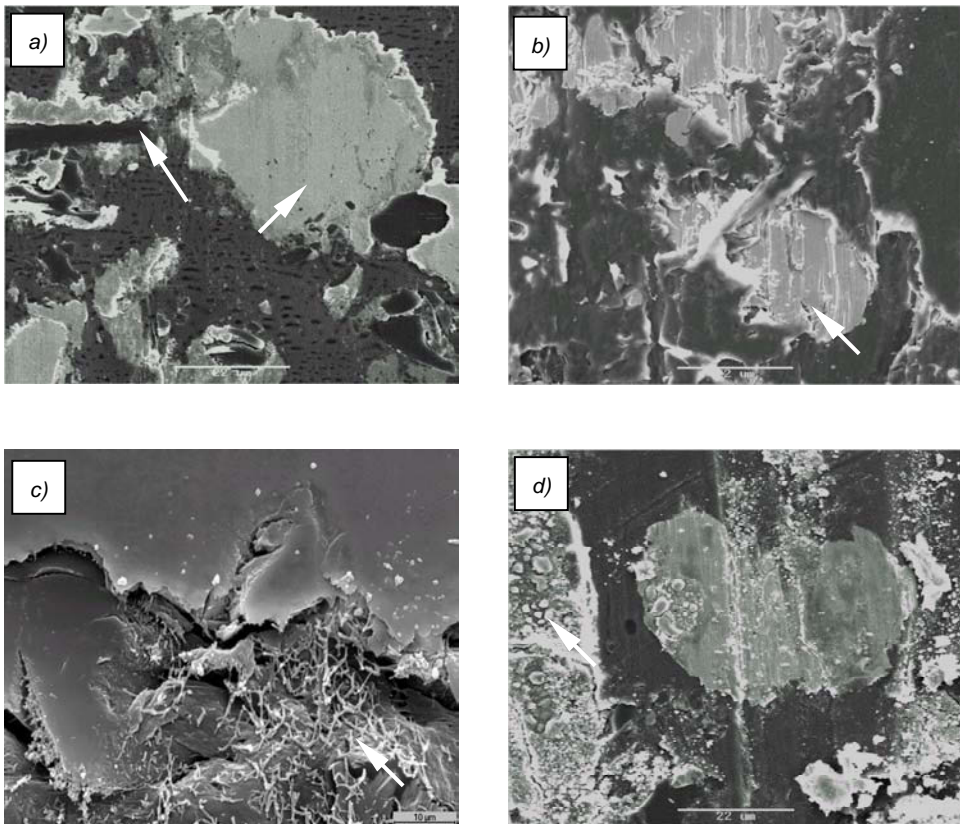


Figure 4.70: SEM images of the bronze/CF filled PTFE after experiments at  $v = 1$  m/s a) at RT, b) in LN<sub>2</sub>, c) LH<sub>2</sub> and d) LHe

## 4 Results

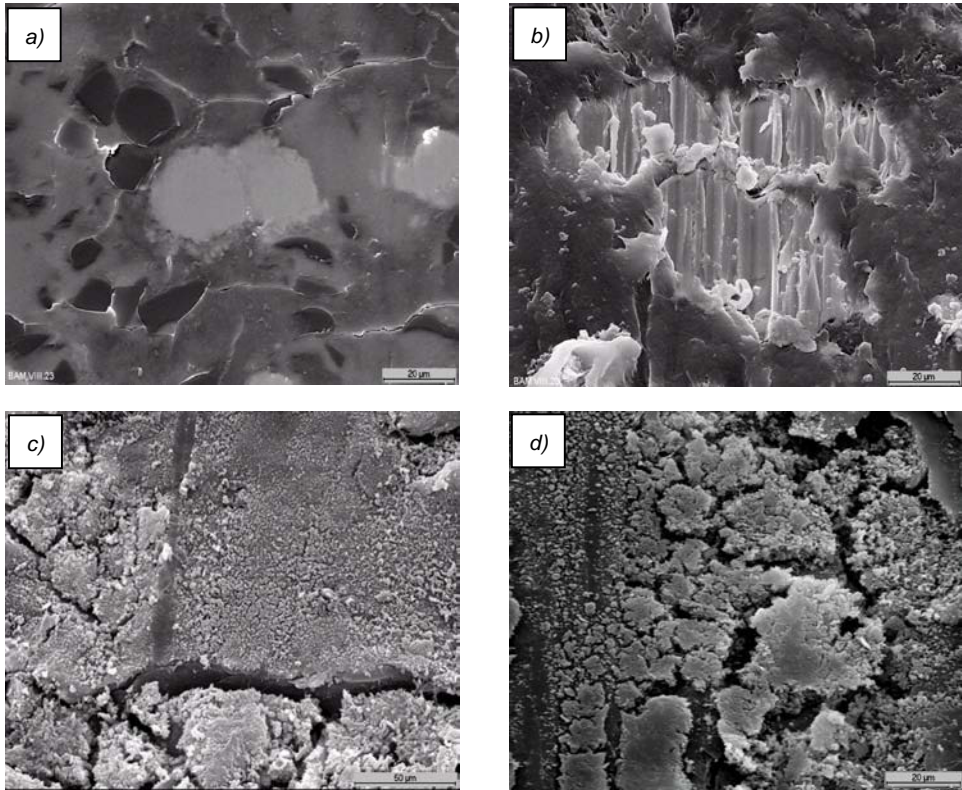


Figure 4.71: SEM images of the bronze/CF filled PTFE after experiments  
a) at RT, b) in LN<sub>2</sub>, c) LH<sub>2</sub> and d) LHe at  $v = 0.2$  m/s

### 4.2.4.3.3 Chemical analyses of the pin surfaces

EDX investigations were made after the experiments accomplished at RT, in LN<sub>2</sub>, LH<sub>2</sub> and LHe and for both sliding speeds.

On the bronze/CF filled PTFE composite, iron is detected after all the tests in addition to copper, tin, carbon and fluorine. No distinction of the chemical analysis of the wear debris could be found in the different environments. After the experiments in LN<sub>2</sub>, iron is detected on the bronze particle as well as isolated in the wear scar (*fig. 4.72*). EDX analyses carried out after the tests in LH<sub>2</sub> indicate that larger wear pieces consist mainly of bronze (*fig. 4.73*), whereas powder-like wear debris seem to contain mainly iron (*fig. 4.74*). After the tests in LHe, iron is also present on the surface of the pin, in particular on the wear scar (*fig. 4.75*).

EDX analyses of the wear debris with a light element detector reveal the presence of iron as well as fluorine (*fig. 4.76*). However, it is difficult to confirm the chemical structure of the debris. It can be either iron, PTFE or iron fluorides.

EDX analyses of PEEK/CF filled PTFE indicate also the presence of iron on the surface of the composites after RT experiments as well as after tests in cryogenic environments.

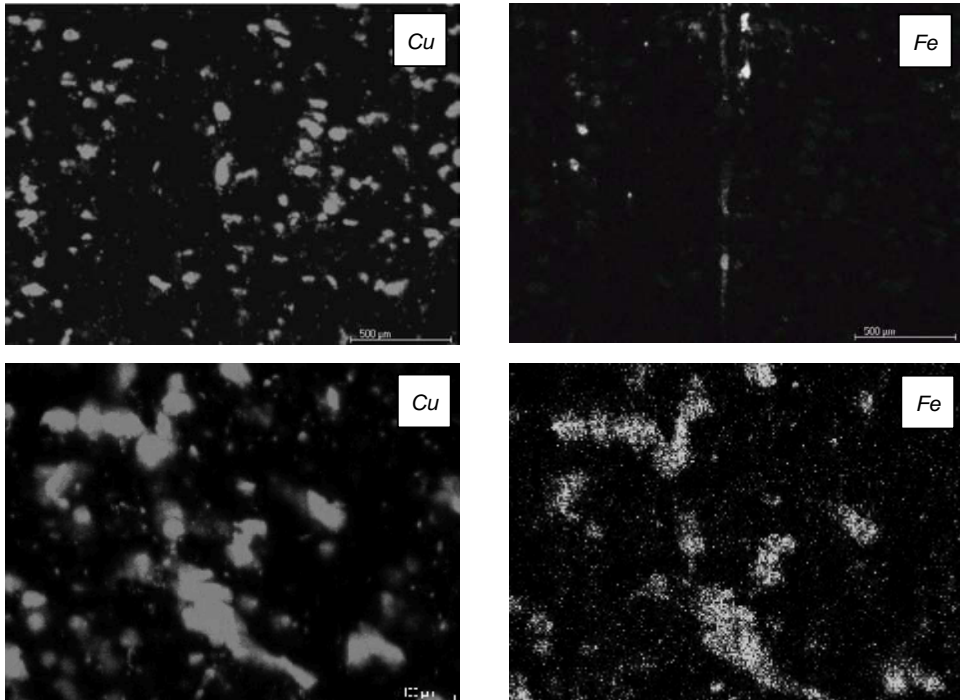


Figure 4.72: EDX mapping of bronze/CF filled PTFE after experiment in  $\text{LN}_2$  at  $v = 0.2$  m/s (at two different places)

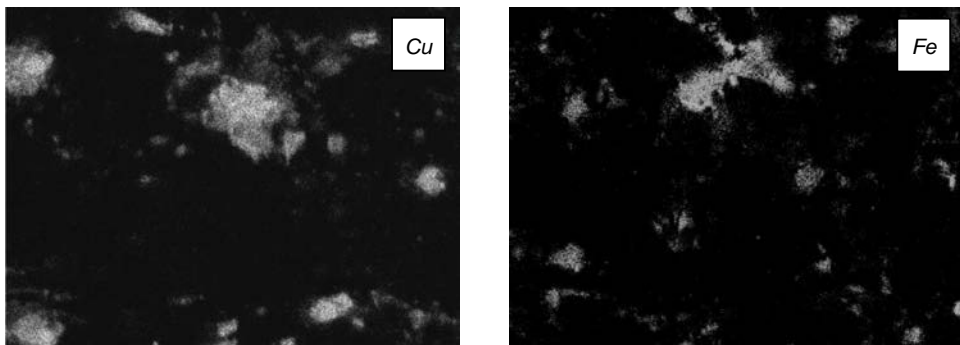


Figure 4.73: EDX mapping of bronze/CF filled PTFE after experiment in  $\text{LH}_2$  at  $v = 0.2$  m/s.

## 4 Results

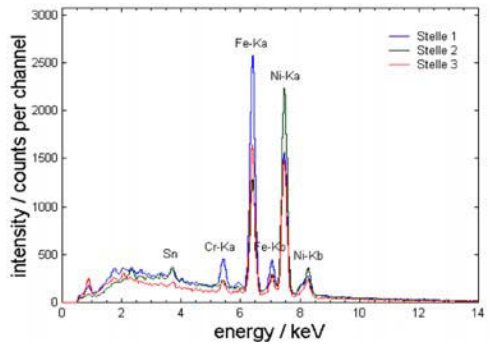
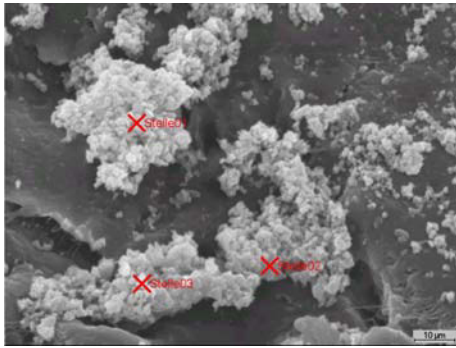


Figure 4.74: EDX spectrum of wear debris on bronze/CF filled PTFE after experiment in LH<sub>2</sub> at  $v = 0.2$  m/s.

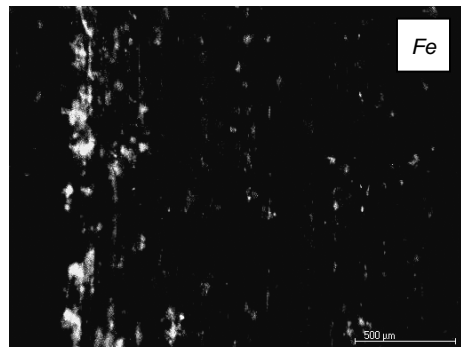
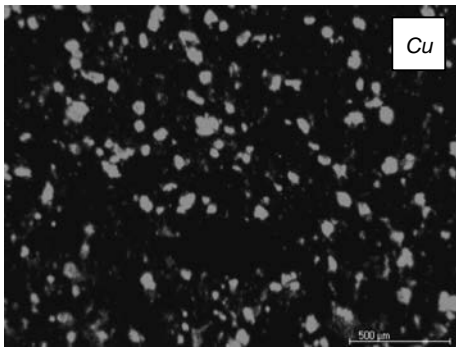


Figure 4.75: EDX mapping of bronze/CF filled PTFE after experiment in LHe at  $v = 0.2$  m/s.

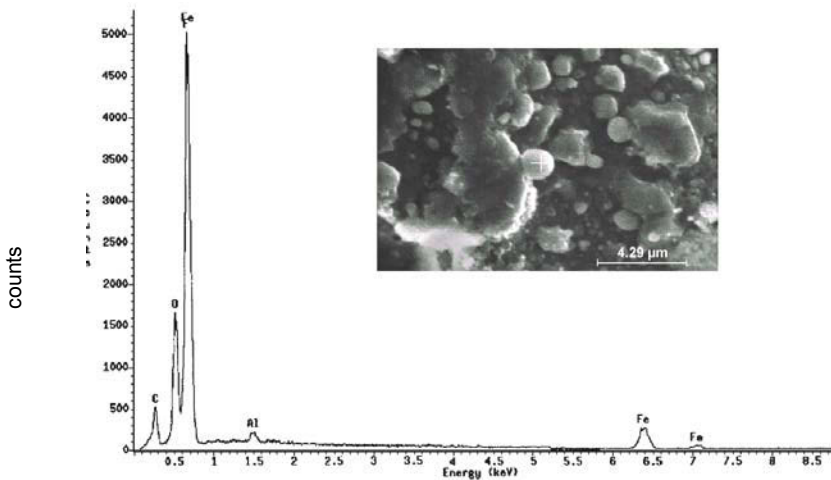


Figure 4.76: EDX spectrum of wear debris on bronze/CF filled PTFE after experiment in LHe at  $v = 1$  m/s.

#### 4.2.4.3.4 Chemical analyses of the transfer on the disc

To investigate the influence of the cryogenic liquids, XPS analyses of the transfer film were carried out after the experiments with bronze/CF filled PTFE at RT in air, in LN<sub>2</sub> and in LHe at  $v = 1$  m/s and in LN<sub>2</sub> and LH<sub>2</sub> at  $v = 0.2$  m/s. As comparison, further analyses were performed after the tests with Ekonol<sup>®</sup> filled PTFE in LN<sub>2</sub> and LH<sub>2</sub>.

*Figure 4.77* shows the spectra of the fluorine F(1s), carbon C(1s) and iron Fe(2p) peaks detected at the surface of the transfer film obtained after the experiments with bronze/CF filled PTFE at  $v = 1$  m/s. The F(1s) spectrum of the film grown at RT in air shows two peaks: one at 687.7 eV, characteristic for the fluoride in PTFE, and another one at 684 eV, which indicates the presence of a metal fluoride according to the NIST data base [NIST]. In the Fe(2p) spectrum, two overlapping peaks were noticed. The iron fluoride peak is at the same position as the ferric oxide peak (711 eV). Since iron fluoride (FeF<sub>2</sub>) was found by other authors [Cadm79, Gong90], it is reasonable to deduce that iron fluoride is also present in our experiment. Similar results were obtained for the film grown at  $T = 77$  K in LN<sub>2</sub>. The F(1s) spectrum shows two peaks at 688.6 eV (PTFE) and at 684.6 eV (metal fluoride). The Fe(2p) spectrum, however, shows two peaks at 711 eV and at 714.7 eV, which indicates the presence of FeF<sub>2</sub> or FeF<sub>3</sub> (714.7 eV). As for the XPS analysis of the film formed at  $T = 4.2$  K, the spectrum of F(1s) shows a larger percentage of the metal fluoride (peak at 684.8 eV) corresponding to a smaller C(1s) peak of PTFE at 292.3 eV. The Fe(2p) spectrum has a higher peak at 714.7 eV, which suggests the presence of FeF<sub>3</sub>.

XPS analyses performed after the experiments at  $v = 0.2$  m/s in LN<sub>2</sub> and in LH<sub>2</sub> with bronze/CF filled PTFE revealed similar results (*fig. 4.78*). F(1s), C(1s) and Fe(2p) spectra indicate the presence of iron fluorides in both cases. Furthermore the F(1s) spectrum of the transfer film produced in LH<sub>2</sub> presents a higher peak at 684 eV, which suggests that more iron fluorides are formed in LH<sub>2</sub> than in LN<sub>2</sub>.

XPS analyses of the transfer film formed with PTFE composite filled with 10% Ekonol<sup>®</sup> and 15 % CF did not detect any iron fluoride after the experiments in LN<sub>2</sub> nor in LH<sub>2</sub>.

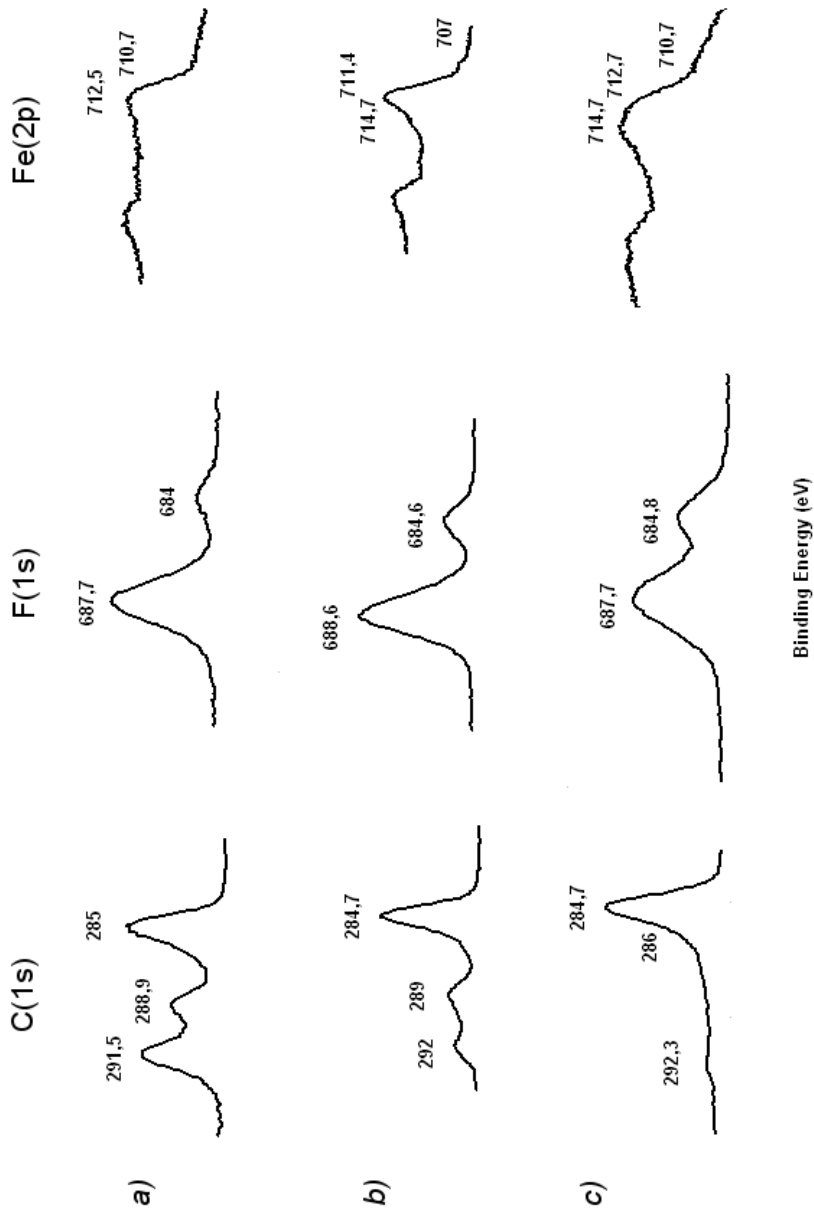


Figure 4.77: XPS analyses of the transfer film formed with bronze/CF filled PTFE on the steel disc after experiments at  $v = 1.0$  m/s; C(1s), F(1s) and Fe(2p) spectra at a) RT in air, b)  $T = 77$  K in LN<sub>2</sub> and c)  $T = 4.2$  K in LHe



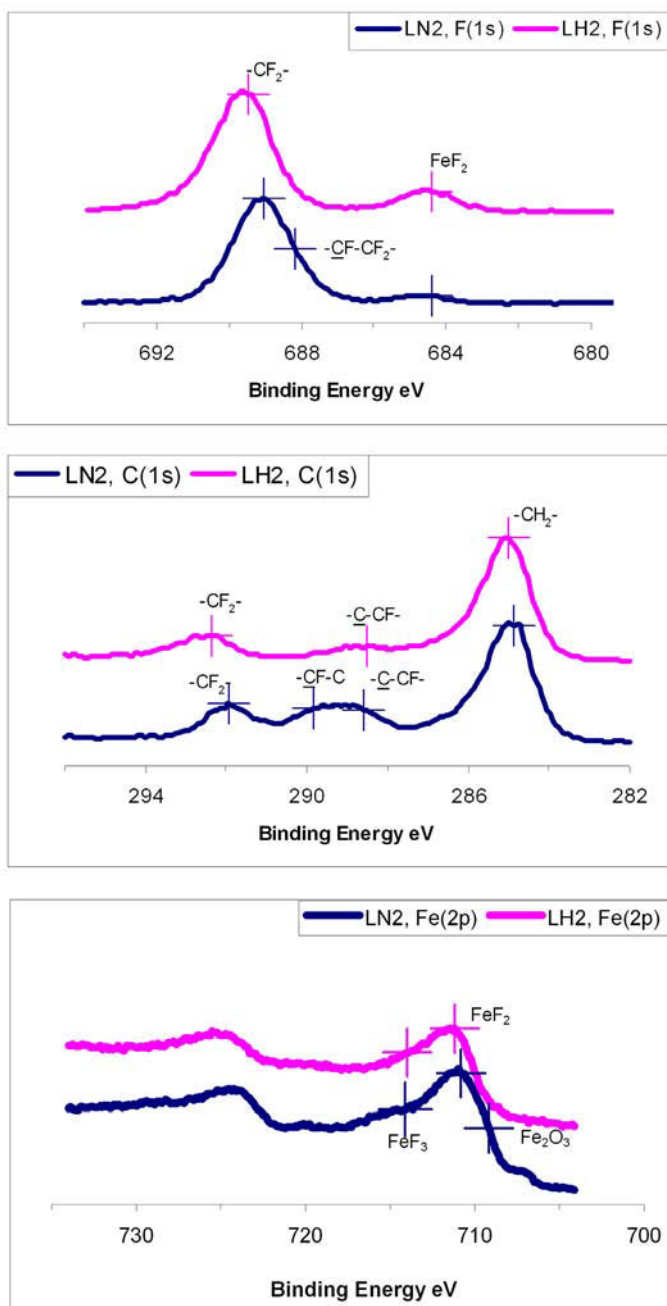


Figure 4.78: XPS analyses of the transfer film formed with bronze/CF filled PTFE on the steel disc after experiments in  $\text{LN}_2$  and  $\text{LH}_2$ ; C(1s), F(1s) and Fe(2p) spectra at  $v = 0.2$  m/s





## 5 Discussion

### 5.1 Material properties

#### 5.1.1 Thermophysical testings

The results of the thermophysical experiments confirm the temperature dependence of the polymer properties described in section 2.2.2. The specific heat  $c_p$  decreases proportionally with the temperature accordingly to the *table 2.4*.

Furthermore, over the experimental temperature range, the variations of integral and coefficient of thermal expansion are higher for PTFE than for PEEK. The main reason is that the experiments were carried out beneath the  $T_g$  of PEEK. Indeed, as described in [Hart94], thermal expansion can be considered as a thermally induced vibrational pressure against binding forces. When the volume available for the internal pressure of the vibration increases, the expansivity rises. At low temperatures and beneath  $T_g$ , molecular segments and side groups are frozen, which decreases the free volume and thereby the thermal expansion.

The thermal conductivity decreases slightly with temperature for both composites according to *table 2.7*. PTFE composite has a higher conductivity than the PEEK material due to its higher crystallinity.

#### 5.1.2 Thermal and environmental testings

##### 5.1.2.1 Thermal shock cycles

Thermal shock experiments lead to internal stresses at the interface between matrix and particles (*figs. 4.8 and 4.9*). This is due to the different thermal expansion coefficients between the components (*table 2.6*):

for PTFE  $-\Delta l / l_0 (293 \text{ K} \rightarrow 77 \text{ K}) = 1.7 \%$  , whereas

for copper  $-\Delta l / l_0 (293 \text{ K} \rightarrow 77 \text{ K}) = 0.30 \%$  .

However, the cryogenic liquids used in the experiments have not a significant influence on the results (*figs. 4.10 and 5.1*). The reason is that the thermal expansion of the components at  $T = 77 \text{ K}$  and  $T = 4.2 \text{ K}$  are similar (*table 2.6*):

for PTFE,  $-\Delta l / l_0 (293 \text{ K} \rightarrow 77 \text{ K}) = 1.7 \%$  and

$-\Delta l / l_0 (293 \text{ K} \rightarrow 4.2 \text{ K}) = 1.8 \%$  .

The results of the experiments carried out by heating up in water (process 1) show significant debonding of the short fibres and fillers from the matrix at the surface of the composites. These damages appear when using either  $\text{LN}_2$  ( $T = 77 \text{ K}$ ) or  $\text{LHe}$  ( $T = 4.2 \text{ K}$ ), with no major differences between the two experiments.

The thermal cycles carried out by dipping the samples in water (process 1) showed a much more damaged surface of the composite than by heating up the samples directly with warm air (process 2). This is certainly due to a more effective thermal shock by heating in water [Theil02c]. Water has indeed a higher specific heat capacity ( $c_p = 4.182 \text{ kJ/kgK}$  at

## 5 Discussion

$T = 293 \text{ K}$ ) than warm air ( $c_p = 1.009 \text{ kJ/kgK}$  at  $T = 333 \text{ K}$ ) [ETB03]. Moreover, it might be possible that despite the drying process, some traces of water still remain at the surface of the composite. This water would then freeze in the cryogenic liquid and could affect the free expansion of the matrix and fillers. This second explanation should be taken with precautions since the presence of water on the polymer surface after drying is not to be expected due to the hydrophobic properties of PTFE.

Thermal shock experiments carried out with PEEK composites did not lead to significant debonding of fibres as observed in the case of PTFE materials (*fig. 4.12*). This can be explained by a better adhesion between PEEK and carbon fibres than the one between PTFE and carbon fibres. PEEK has indeed a higher bond strength because it can crystallize on the fibre surface [Seife86], whereas PTFE has a low surface energy. Another reason is that PEEK has a smaller thermal expansion than PTFE (*table 2.6*):

$$\begin{aligned} \text{for PTFE} \quad -\Delta l / l_0 (293 \text{ K} \rightarrow 77 \text{ K}) &= 1.7 \% \text{ , whereas} \\ \text{for PEEK} \quad -\Delta l / l_0 (293 \text{ K} \rightarrow 77 \text{ K}) &= 0.9 \% \text{ .} \end{aligned}$$

This should lead to less internal stresses at the interface between matrix and fibres in PEEK composites.

### 5.1.2.2 Cryo-treatment

Cryo-treatment of polymer composites immersed in  $\text{LN}_2$  for 40 hours has also some influence on the surface of the composite (*figs. 4.13* and *4.14*). However, compared with the thermal shock experiments, the cooling and heating were performed slowly, with no intermediate medium such as water. Damages were still observed. This means that the long immersion time in  $\text{LN}_2$  has a similar effect as thermal shock experiments. During the cooling phase below the  $T_g$ , the polymer molecules get frozen and shrink. This state stays for 40 hours before the heating process starts slowly. In addition to the different thermal expansion coefficients within the composite, the debonding between the particle and matrix observed at the surface of the polymer can be due to the reorganization of the polymer chain during the heating phase up to RT. Reaching  $T_g$  ( $T = 170 \text{ K}$ ) PTFE slowly crystallizes, which leads to shrinkage of the matrix. However, this hypothesis could not be verified since the degree of crystallinity of the matrix could not be measured before and after the experiment.

### 5.1.2.3 Thermal ageing in hydrogen

Surface analyses of the composites after thermal ageing in hydrogen indicated similar effects as observed after the thermal shock experiments. Due to different coefficients of expansion between matrix and fibres, internal strains occurred at the interface between the components (*fig. 4.15*). Furthermore, the temperature of  $473 \text{ K}$  is above the highest transition temperature recorded for PTFE ( $T = 400 \text{ K}$ ). The polymer matrix becomes softer and expands. During the low cooling rate regime, the polymer molecules can reorganize to a state of higher crystallinity, producing a shrinkage of the matrix. But as for the cryo-treatment, this hypothesis could not be verified.

Hydrogen treatment at  $T = 473$  K leads to no changes in weight of the polymer composites, which suggests that no chemical reaction takes place between the medium and the composite.

### 5.1.3 Mechanical testings

Below the glass transition temperature and at low temperatures, molecules are frozen, which prevents molecular motions. This is why the YOUNG's moduli of PTFE- and PEEK-matrix composites are higher at  $T = 77$  K ( $E = 6.3$  GPa and  $E = 7.4$  GPa respectively) than at RT ( $E = 1.4$  GPa and  $E = 5.5$  GPa respectively) (fig. 4.16).

Compared to RT values, the results at  $T = 77$  K indicate that the YOUNG's modulus of the PTFE composite increases more than the one of the PEEK composite (figs. 4.17 and 4.18). This can be explained by the fact that at RT, PEEK is already below its glass transition ( $T_g = 416$  K). Therefore, the material behaviour of PTFE composites is expected to vary much more between RT and  $T = 77$  K than the material behaviour of PEEK composites. This can also clearly be seen in the SEM images made after the tensile experiments (figs. 5.2 and 5.3). Significant differences are observed in the PTFE-matrix composite (fig. 5.2) between RT and  $T = 77$  K: at RT, the PTFE-matrix is characterized by filaments, which indicates a more ductile behaviour of the matrix compared to the experiments at  $T = 77$  K. SEM images of PEEK present minor differences between the two temperatures (fig. 5.3).

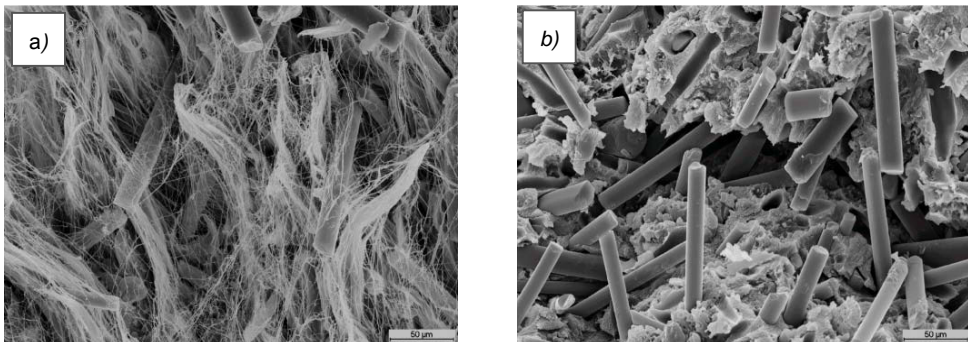


Figure 5.2: SEM images of PTFE composite filled with 15% CF and 9% PEEK after tensile tests a) at RT and b) at  $T = 77$  K

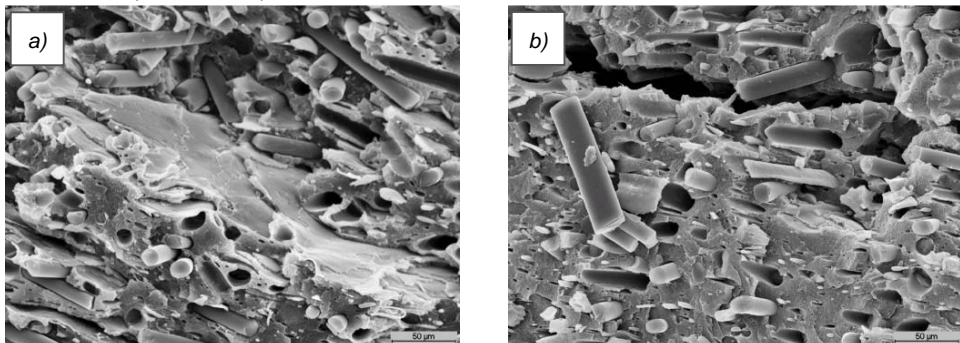


Figure 5.3: SEM images of PEEK composite filled with 15% CF and 15% PTFE after tensile tests a) at RT and b) at  $T = 77$  K

## 5 Discussion

### 5.1.4 Consequences for tribological applications

The purpose of these thermal and mechanical experiments was to obtain experimental data of PTFE and PEEK composites regarding their low temperature properties for a better understanding of their behaviour in tribological applications.

The results obtained give the following indications:

- Thermal conductivity decreases with decreasing temperature. This can reduce the evacuation of the frictional heat at the surface contact. Hot spots will be easier produced at low temperatures.
- Different coefficients of expansion within a composite lead to stresses at the interface between polymer matrix and fillers. This can facilitate the extraction of particles or wear debris from the matrix to the sliding contact.
- YOUNG's modulus increases with decreasing temperature. This will affect the tribological behaviour of the materials.
- The properties of PTFE composites are more affected at low temperatures than the ones of PEEK composites; the tribological behaviour of PTFE composites should therefore be more affected.

## 5.2 Tribological experiments

### 5.2.1 Influence of the thermal treatments on friction at RT

Generally speaking, no major changes in the friction behaviour were recorded for both composites after the thermal treatments. Some slight improvements are seen with the PTFE composite, whereas friction slightly increases for the PEEK composite (*figs. 4.21 to 4.23*).

As seen in section 4.1.2, thermal shock experiments lead to internal stresses at the interface between matrix and particles. Due to the shrinkage and expansion of the matrix, debonding between CF and the matrix appears, in particular with PTFE-matrix. Some CF pieces are loose at the surface of the PTFE-matrix, some others are even removed from the surface. CF are not well embedded in the matrix anymore. Before each tribological experiment, the pins are ground with an emery paper in order to produce a homogeneous surface parallel to the disc. This preparation can modify the surface by taking away possible debonded CF out of the surface. This can produce a rich PTFE layer at the surface of the composite, leading to a lower friction behaviour.

During the cryo- and thermal treatments, debonding also occurred at the surface of the PTFE composite as seen in section 4.1.2, but not as much as with thermal shock experiments. This can explain why in both cases, the friction coefficient of the PTFE composite does not decrease as much as after the thermal shock experiments.

Concerning the PEEK material, fewer debonding occurred between the CF and the PEEK-matrix. This can explain the relatively unchanged friction behaviour of the material after the thermal experiments.

It is noticeable that no major changes in friction behaviour occur after the heat treatment in hydrogen. This suggests that, in this experiment, hydrogen has not a significant influence on the material properties at RT.

## 5.2.2 Influence of the material composition at RT and at $T = 77$ K

### 5.2.2.1 PTFE and PEEK content

At RT, friction and wear depend on the percentage of PTFE. In this experiment, 5% of the solid lubricant gives the lowest friction (*fig. 4.24*) and 15% gives the lowest wear (*fig. 4.25*). This is in accordance with the results obtained by Lu [Lu95], who studied the influence of PTFE in PEEK composites. The reduction of friction at low PTFE contents can be explained with the microstructure of the materials. In PEEK-matrix composites, the surface of the pin presents a continuous phase of PEEK with dispersed PTFE particles. During sliding, these PTFE particles produced a homogenous film at the surface of the disc, which is responsible for low friction (*fig. 4.52*). In PTFE-matrix composites, hard PEEK particles and CF are present at the friction contact (*fig. 4.32*), which can destroy partly the thin PTFE film (*fig. 4.48*).

At  $T = 77$  K, the coefficient of friction of PTFE and PEEK composites decreases. The surfaces of the composites present fewer damages than after RT experiments, and CF particles are still buried in the matrix in most cases (*figs. 4.33, 4.35 and 4.37*), which indicates that the wear process of the matrix has been hindered. Polymer transfer is also reduced as indicated by the optical microscopy images (*figs. 4.49 and 4.53*). This can be explained by the low temperature properties of polymers. Below the glass transition of polymers, molecules get frozen, their mobility decreases and the hardness of the polymer increases accordingly. A direct consequence of this is that the real contact area ( $A_r$ ) is smaller than at RT.

Since the adhesion component of the friction force  $F_a$  is related to the real contact area  $A_r$  by the relation  $F_a = \tau_s A_r$  (equation 9), the corresponding friction decreases with decreasing  $A_r$ .

Furthermore, according to the equations 12 and 15, the YOUNG's modulus  $E$  is inversely proportional to the adhesion ( $\mu_a$ ) and deformation component ( $\mu_d$ ) of friction:

$$\mu_a \propto (E^{-1}), \quad (23)$$

$$\mu_d \propto (E^{-1}). \quad (24)$$

As the YOUNG's modulus increases at low temperatures (section 4.1.3), the deformation and adhesion components of friction decrease, which decreases the whole friction accordingly to the two models of friction described in section 2.1.3.

The schematic representation of the friction mechanism at RT proposed by Lu for PTFE/PEEK compounds can also be applied for composites with PTFE/PEEK/CF composites (*fig. 5.4*). Taking into account the above discussion, a similar representation is suggested in *figure 5.5* for the friction mechanism at low temperatures, which presents a much smaller area of contact than at RT.

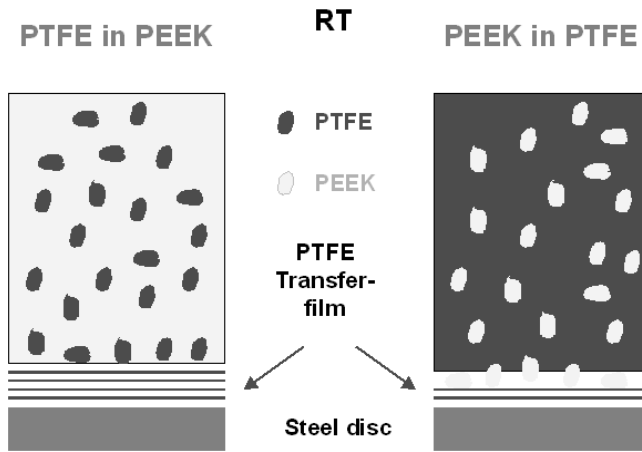


Figure 5.4: Friction mechanism of PTFE/PEEK compounds at RT [Lu]

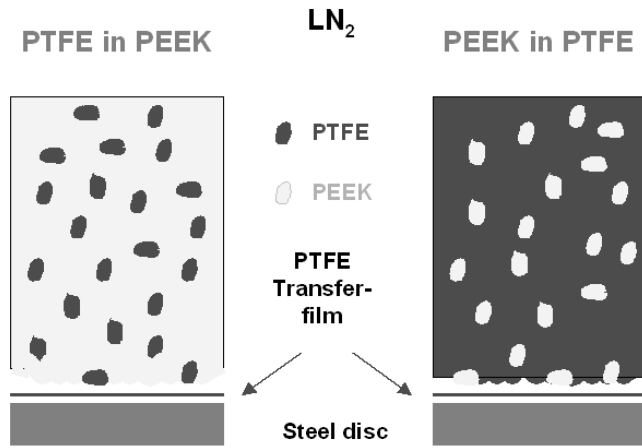


Figure 5.5: Friction mechanism of PTFE/PEEK compounds in LN<sub>2</sub>

### 5.2.2.2 Carbon fibre content

At RT, the friction coefficient of PTFE-matrix composites increases significantly with CF content (*fig. 4.27*). In this experiment, the optimal CF amount is 5%. Concerning wear, a maximum amount of 15% seems to be relevant in order to maintain good performances (*fig. 4.29*). Above 15%, the wear increases drastically. PTFE composites are characterized by a relative smooth surface and some scorings (*fig. 4.38*). These scorings on the surface of the composite in sliding direction can be due to the detachment of fibre fragments from the soft matrix. The addition of carbon fibres leads to more losses of CF fragments and debris at the friction contact (*fig. 4.38b*), which leads to abrasion of the composite surface. Increasing the CF content releases more fragments which contribute to higher wear.

At low temperatures in LN<sub>2</sub>, the PTFE-matrix wears out less. Due to the increase in hardness, PTFE still covers many CF. Consequently, CF are not so numerous at the surface as after RT experiments. Contrary to the thermal shock experiments, the composites remained immersed in LN<sub>2</sub> during the whole test. Thereby the matrix shrinks and binds the fibres better than at RT [Hart94], at least for the composite with low CF content (*fig. 4.39a*). At a higher CF content in PTFE-matrix composite filled with 20% Ekonol<sup>®</sup> (*fig. 4.39b*), detachments of CF particles are observed, which can be responsible for the slight increase of friction and wear (*figs. 4.27 and 4.29*).

Similar results were obtained by varying the CF content in PEEK-matrix composites (*fig. 4.28*). The friction increases slightly with increasing CF content after RT experiments. However, the influence of CF content on friction is not as significant at RT as for the PTFE composites. SEM images certainly indicate some more CF at the surface of the composite with 30% CF than in the case of 15% CF, but the worn surfaces do not differ significantly (*fig. 4.40*). This might be due to the better bonding of CF by the PEEK-matrix, which produces fewer fragment detachments than in the PTFE-matrix.

After the experiments in LN<sub>2</sub>, friction and surface analyses are almost independent of the CF content (*fig. 4.41*). The tribological behaviour of PEEK composites in LN<sub>2</sub> is mainly influenced by the low temperature properties of the matrix.

### 5.2.2.3 Fillers in PTFE and transfer film formation

Several theories on the mechanism of friction of PTFE composites at RT have been developed since many decades [Maki64, Tana73, Tana86, Gong90, Bisw92]. The effect of fillers on friction varies from study to study. In this work, the type of fillers does not influence significantly the friction behaviour of PTFE-matrix composites, but has a major influence on the wear.

After the experiments at RT, optical microscopy images of the surface of the disc tested against PTFE filled with CF and either bronze or PEEK show the presence of polymer transfer (*figs. 4.44 and 4.48*). The formation of this thin transfer film is produced by the destruction of the PTFE band structure which is due to the low activation energy of the slippage of lamellae in PTFE bands [Tana86]. This PTFE film is certainly responsible for the rather constant friction values obtained whatever the filler incorporated in the composite.

## 5 Discussion

Concerning the wear results, different values were obtained depending on the incorporated fillers (*fig. 4.31*). The wear obtained with Ekonol<sup>®</sup> fillers are similar to the one obtained with PEEK, due to the similar chemical structure of these two polymers. A significant improvement of the wear resistance was observed with the bronze filled composite at RT.

It is well known that the role of fillers on the wear mechanism of PTFE can be attributed to the load supporting action of the fillers due to the enrichment of the surfaces layers by fillers and fibres. This prevents the large scale destruction of PTFE banded structure [Tana73, Gong90]. In this experiment, SEM images of the worn pins show for all PTFE composites similar smooth surfaces rich in fillers and fibres (*figs. 4.32a* and *4.42*). No significant differences could be detected between the composites.

A major factor that can affect the wear behaviour of PTFE materials is the thermal conductivity of the composite, which can be improved by incorporating fibres or metal particles. As shown in *table 5.1*, the thermal conductivity of the bronze filled PTFE composite is much higher than in the case of Ekonol<sup>®</sup> filled PTFE. This leads to a better dissipation of the frictional heat at the friction contact and can contribute to the improvement of the wear resistance.

However, *figure 5.6* illustrates the influence of the thermal conductivity on the linear wear of Ekonol<sup>®</sup> filled PTFE composites with different amounts of CF. Apart from the composite with the highest CF content, linear wear is directly proportional to the thermal conductivity for RT as well as LN<sub>2</sub> experiments. This is in contradiction to the observations made above that compare bronze and Ekonol<sup>®</sup> fillers. This suggests that the thermal conductivity property of bronze filled PTFE is not the only factor influencing the wear resistance. Surface analyses of the discs give some other indications.

Indeed, after the experiments at RT, the transfer film developed by the bronze composite is more homogenous compared to the one developed by other composites (*figs. 4.44* and *4.48*). It is reasonable to suggest that the wear reduction property of bronze/CF filled PTFE composite can be associated with a better adhesion of the transfer film onto the counterface, which agrees with the theory proposed in [Baha92].

At low temperatures, the transfer of material onto the disc does not build a homogenous film as it does at RT as shown by the optical microscopy images and profile measurements (*figs. 4.45* and *4.47*). Only scattered particles are seen on the surface of the disc (*fig. 4.51*). The destruction of the PTFE band structure is hindered by the frozen state of the molecules, which prevents also the composite material from wearing out. Friction depends no more of the formation and adhesion of the transfer film, but more on the real surface in contact between pin and disc, as described above. In LN<sub>2</sub>, tribological behaviour of the polymer composites does not depend on the composition because of similar properties of thermoplastic materials at low temperatures (section 2.2.2.4).

Comparing the wear results of the PTFE composites in *figure 4.31*, the wear of bronze filled composite does not decrease at low temperatures. This may be due to the fact that the wear value at RT is already quite small.



Table 5.1: Thermal conductivity of PTFE composites [Klei01]

Material	Thermal conductivity [W/mK]
PTFE + 30% bronze + 10% CF	0.46
PTFE + 10% Ekonol <sup>®</sup> + 15% CF	0.27

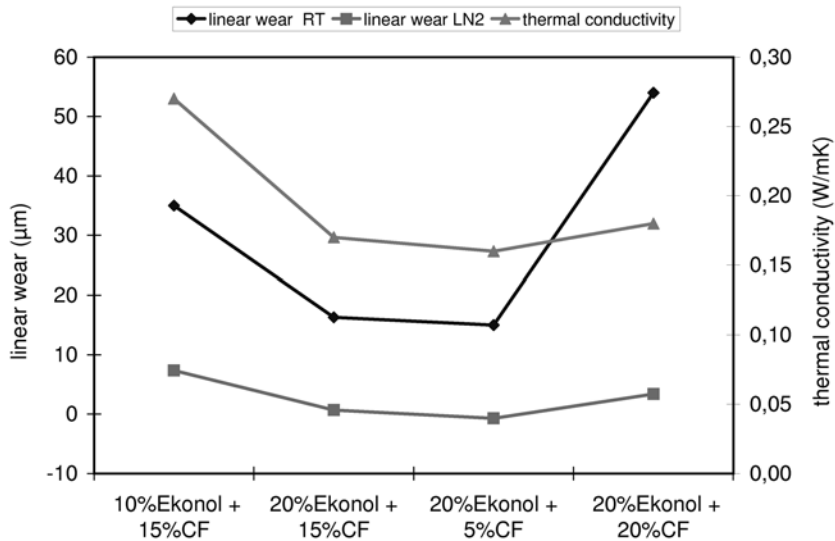


Figure 5.6: Linear wear [Theil02a] and thermal conductivity [Klei01] of PTFE composites

## 5.2.3 Influence of the cryogenic environment

### 5.2.3.1 Friction

As seen above, the coefficient of friction of PTFE and PEEK composites decreases from room temperature to  $T = 77$  K in LN<sub>2</sub> (fig. 4.24). This has been explained by the low temperature properties of polymer materials, in particular by the increased YOUNG's modulus. However, the temperature of the environment is not the only significant parameter to understand and explain the tribological behaviour of these composites in cryogenic media. The temperature at the friction contact is the main factor to consider. Since it was not possible in this study to determine this temperature, special attention was given to the physical - especially thermal - properties of the cryogenic media, which affects the temperature at the friction contact. A good example is given by the friction results at  $T = 77$  K comparing He-gas and LN<sub>2</sub> environments (fig. 4.55). Although both experiments are carried out at  $T = 77$  K, the coolant LN<sub>2</sub> has a better cooling efficiency than He-gas.

## 5 Discussion

Moreover, the decrease of friction with temperature of the cryogen is not observed down to extreme low temperatures. Indeed, a higher coefficient of friction is measured at  $T = 4.2$  K compared to the one at  $T = 77$  K in LN<sub>2</sub>, especially for the experiments carried out at high sliding speed (*fig. 4.56*).

This behaviour cannot be explained by the bulk structure of PTFE, whose lowest transition temperature is at about  $T = 170$  K, neither by the temperature dependence of its mechanical characteristics, because at  $T = 4.2$  K the hardness and mechanical properties should be slightly higher than at  $T = 77$  K according to [Hart94].

The influence of the diffusion of helium into materials has not been investigated here. However, this should not have a significant effect on the behaviour of the friction couple since at  $v = 0.2$  m/s, similar friction results are obtained in LN<sub>2</sub>, LH<sub>2</sub> and LHe.

The thermal properties of the cooling medium can be responsible in this case for a higher friction coefficient in LHe compared to LN<sub>2</sub>. Since the frictional heat rises the temperature at the contact area, especially for polymers with low heat conductivity, the heat transfer to the environmental medium is a significant factor to consider [Grad01b, Theil02a]. As soon as a relative motion occurs and generates frictional heat, the liquid in the contact area begins to evaporate, and bubbles appear. Thereby, by thermal conduction, convection and evaporation, the heat is extracted from the contact. This leads to an efficient cooling effect. During this bubble formation phase (nucleate boiling), the temperature difference between the contact area and environmental medium is relatively small, because the evaporation requires a large amount of heat. With increasing friction, the size and number of bubbles increase largely until finally reaching a vapour film at the contact area (film boiling). Since the heat transfer to a gaseous environment is much less efficient than to a liquid, the transition from nucleate to film boiling is accompanied by a steep temperature rise which can amount several hundred K. For free radiating heaters, the temperature increase as function of the heat flux density can be taken from boiling curves [Bren65]. The data from such curves cannot be transferred directly to the conditions in a frictional contact, which represents a confined geometry and forced-flow conditions, but they may serve as a rough estimation of the temperature conditions in the contact zone.

A direct measurement as well as a calculation of the actual temperature distribution in the contact zone are extremely complex and have not been carried out in this study. However, the heat flux density ( $q$ ) occurring at the sliding contact of area ( $A$ ) can be calculated as followed:

$$q = \frac{\mu F_N v}{A} . \quad (25)$$

*Figure 5.7* gives the heat flux density corresponding to the friction measurements carried out at  $v = 1$  m/s with the bronze/CF filled PTFE composite (from *figs. 4.54* to *4.56*).

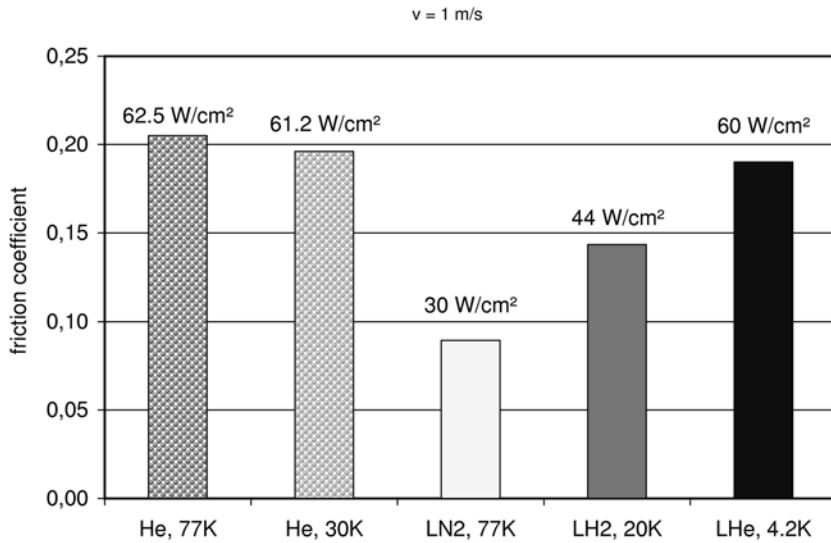


Figure 5.7: Friction coefficient of PTFE filled with 30% bronze and 10% CF in different cryogenic environments, and heat flux density developed for each experiment at  $v = 1 \text{ m/s}$

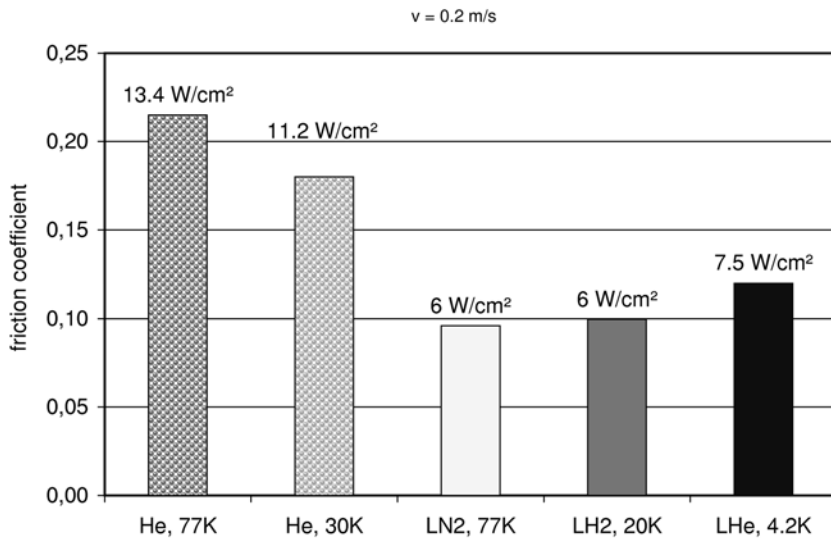


Figure 5.8: Friction coefficient of PTFE filled with 30% bronze and 10% CF in different cryogenic environments, and heat flux density developed for each experiment at  $v = 0.2 \text{ m/s}$

## 5 Discussion

In He-gas and LHe, no differences of the coefficient of friction appear at high speed ( $v = 1$  m/s). The calculated heat flux density ( $q_f$ ) in both cases is  $60 \text{ W/cm}^2$  for the bronze filled composite. Since for LHe the heat flux density at the onset of film boiling, i.e. the critical heat flux density ( $q_c$ ), is only  $1 \text{ W/cm}^2$  [Bren65], the contact area at  $60 \text{ W/cm}^2$  is far in the film boiling regime with a corresponding  $\Delta T$  of approximately 500 K for static free radiating heaters [Bren65]. In this case the entire contact is certainly surrounded by gas, which separates the hot contact zone from the surrounding cryogenic liquid. That means that the heat transfer at the friction contact is similar for each test in He-environment (at  $T = 77 \text{ K}$  and  $T = 4.2 \text{ K}$ ), and thus the same temperature leads naturally to the same coefficient of friction.

In  $\text{LN}_2$ , a heat flux density of  $30 \text{ W/cm}^2$  was calculated, which is just above the transition to film boiling for static free radiating heaters in  $\text{LN}_2$  [Bren65]. Because the rotating disc continuously transports liquid and provides a cold surface area in the contact zone, it can be assumed that this transition is shifted to higher heat fluxes and  $\Delta T$  is still within a range of 10 K. The low coefficient of friction and only small material transfer confirm this assumption.

In  $\text{LH}_2$ , the critical heat flux density ( $q_c$ ) is  $20 \text{ W/cm}^2$ , which is below the calculated  $q_f$  ( $46 \text{ W/cm}^2$ ).

At  $v = 0.2$  m/s (*fig. 5.8*), the heat flux density for  $\text{LN}_2$ ,  $\text{LH}_2$  and LHe reach only 6 to  $7.5 \text{ W/cm}^2$ , which is respectively below or near the critical values  $q_c$ . The similar friction behaviour in the three cryogenic liquids can be explained by comparing the critical heat flux density.

Friction measurements with other PTFE composites indicated similar friction behaviour as with the bronze/CF filled PTFE at low sliding speed in  $\text{LN}_2$  and  $\text{LH}_2$  (*fig. 4.58*). However, the friction coefficient of Ekonol<sup>®</sup> filled PTFE is higher in LHe than in  $\text{LN}_2$ . The lower heat conductivity of this composite could be responsible for the bad evacuation of the frictional heat developed in LHe, leading to the formation of gas bubbles at the contact area.

Hence, the tribological behaviour of the composites investigated in different environments can be partly explained by the thermal properties of the cryogenic media. As seen above,  $\text{LN}_2$  is an efficient coolant since friction stays constant whatever the sliding velocity (*fig. 4.57*). The hydrodynamic effect has not been considered, since the viscosity of the cryogens are too low to establish a hydrodynamic film of sufficient thickness to separate the two surfaces [Boze01]. However, a possible influence of the cryogenic fluid, in particular on the displacement of the wear particles from the sliding track can be considered. Indeed, powder-like wear debris were found on the surfaces of the pin (*figs. 4.70 and 4.71*) and disc (*fig. 4.64*) after testing in LHe and  $\text{LH}_2$ . Surface analyses after the experiments in  $\text{LN}_2$  at  $v = 0.2$  m/s show however less wear debris on the pin. This suggests that  $\text{LN}_2$  has an influence in removing wear particles from the surface, probably due to its relatively higher viscosity compared to LHe and  $\text{LH}_2$ .

### 5.2.3.2 Wear

The SEM images of the sample tested in LN<sub>2</sub> (*fig. 4.70b*) show that bronze particles are partially covered with PTFE lumps, which are pulled out of the matrix. As discussed above, the wear process of the polymer matrix is slowed down due to the fact that the molecular chains are frozen at  $T = 77$  K. This corresponds with the observations of few transfer of scattered polymer particles to the counterface produced in LN<sub>2</sub>.

After the experiments in LHe, both surfaces of the composite and of the polymer transfer onto the disc are characterized by some cracks and small wear particles (*figs. 4.71 and 4.64*). Powder-like debris are present on both surfaces, in particular in the case of the experiments performed at low speed.

After the tests in LH<sub>2</sub>, the pin surface shows similar characteristics as after the experiments in LHe: powder-like wear debris and scoring. At  $T = 20$  K and even more so at  $T = 4.2$  K, the polymer ductility may have reached its limit. During the tests, frictional heat rises the temperature at the contact surface, but this is moderated at low speed conditions.

Furthermore, the surface of the discs tested in LN<sub>2</sub>, LH<sub>2</sub> and LHe present strong abrasive wear scars at  $v = 0.2$  m/s. The fact that there are fewer deep scars at the surface of the disc after the experiments at  $v = 1$  m/s than in the case of  $v = 0.2$  m/s, points out that the wear process is mainly adhesive in the first case and more abrasive in the latter case. Low speed reduces the heat generated at the friction contact and thereby, the low temperature characteristics of the material are more dominant at low speed conditions.

However, according to *table 2.9* the hardness of the polymer at  $T = 77$  K is still lower than the one of the counterface. Surface analyses gave some hints regarding abrasive particles which can be involved in the wear process:

- CF fragments are present at the composite surface or between the two sliding contacts (*figs. 4.32 to 4.43*). These fragments are not totally detached from the matrix and may therefore affect much more the counterface than the composite itself.
- EDX analyses of the pin indicate the presence of iron on the worn surface after all the experiments (*figs. 4.72 to 4.76*). No distinction of the chemical analyses could be found in the different environments. Iron was detected on the bronze particles as well as isolated in the wear scar, in particular after the experiments in LN<sub>2</sub> and LHe at  $v = 0.2$  m/s. This confirms that material transfers from the disc onto the pin at RT as well as at low temperatures. The wear particles detected in cryogenic environments could be some iron oxides (Fe<sub>2</sub>O<sub>3</sub>, Fe<sub>3</sub>O<sub>4</sub> (600-800 HV)) [Jish94] or iron fluoride particles detected by XPS.
- Due to frictional heat and hot spots at the contact area some glass-like carbons can be produced by the degradation of polymers. These have a high hardness (up to 120 SH [Noda69, Bush91]) and could be responsible for the abrasion of the disc.

## 5 Discussion

Wear measurements carried out with rounded pins (*figs. 4.61 and 4.62*) confirm that the wear process was reduced in LN<sub>2</sub> and in LH<sub>2</sub> experiments. In LHe, both PTFE and PEEK composites worn much more, reaching almost the RT value for the PEEK material. With rounded pins, the frictional heat developed at the contact area is much higher than the one produced with flat pins, leading to the evaporation of LHe at the contact zone.

### 5.2.3.3 Chemical analyses of the transfer film

XPS analyses of the transfer film developed with bronze/CF filled PTFE composite indicate the presence of iron fluorides down to  $T = 4.2$  K. After the experiments at  $v = 1$  m/s, it was also observed that the percentage of fluorine in PTFE decreases at the surface of the transfer in LHe, and respectively, the percentage of the metal fluoride increases (*fig. 4.77*). This could be due to the fact that iron fluorides build up at the steel surface, within the first few runs of the test [Mule01]. Subsequently PTFE transfers on the top of this tribochemical layer. Similar structured layers of the transfer film were observed at room temperature by other researches [Gong90, Blan93]. At  $T = 4.2$  K the transfer film is characterized by small cracks and wear debris (*fig. 4.64*), which could belong to the upper PTFE layer and to the iron fluoride layer.

However, XPS analyses carried out after the experiments with Ekonol<sup>®</sup> filled PTFE did not detect any iron fluorides at the surface of the disc. This may suggest a certain influence of the bronze on the formation of fluorides, possibly acting as a catalyst in this chemical reaction.

In order to estimate the influence of hydrogen environment on tribochemical reactions, XPS analyses were performed after the experiments carried out at  $v = 0.2$  m/s in LN<sub>2</sub> and in LH<sub>2</sub>. Iron fluorides were detected at the surface of the discs in both cases (*figs. 4.78*). The larger F(1s) peak at 684eV in LH<sub>2</sub> suggests that the transfer film produced in LH<sub>2</sub> contains more iron fluorides than the one produced in LN<sub>2</sub>. This could be due to the reducing characteristics of hydrogen [Theil03]. The native oxidized film of the disc is easily removed by hydrogen, which could facilitate the chemical formation of iron fluorides on the fresh metal surface. NOSAKA expressed similar assumptions [Nosa99].

The exact tribochemical reactions at the surface of the disc are quite difficult to determine since the samples had to be transported in a desiccator within a short time from the cryotribometer to the XPS chamber. This could affect the composition of the surface layer by the presence of oxide in air. However, some suggestions can be made regarding the results obtained above, taking into account the work carried out by JINTANG [Jint00], who studied the tribochemical effects in formation of polymer transfer film of PTFE against metal at RT in air. Due to mechanical and thermal stresses during tribological tests, polymer molecules are submitted to frictional heat and shear strain, which produces chain fragments. PTFE decomposes and radicals are produced. These radicals can react either with oxygen from the environment (at RT in air) or from the oxide layer at the surface of the metal (in nitrogen or helium environment) or directly with the fresh metal surface that has been reduced by hydrogen.

Possible chemical reactions, suggested for RT experiments in [Jint00], are extrapolated in *figure 5.9* to LH<sub>2</sub> test conditions. In our experiment, iron fluoride formation was promoted in hydrogen environment. Furthermore, peroxide radicals (-CF<sub>2</sub>CF<sub>2</sub>OO•) have a good adhesion to metal surfaces because of their strong polarity. This could explain the topography of the disc observed by means of AFM. Indeed the transfer film in hydrogen was found to be extremely thin compared to the one produced in the other environments. Peroxides developed in LN<sub>2</sub>, LHe and even more in air, would be responsible for the good adhesion of the transfer material to the disc. It is reasonable to suggest that the formation of metal-oxygen-polymer complex promotes the adhesion to the steel disc as reported in other studies [Burk81, Park91].

Surface analyses of the disc after the experiments in hydrogen at RT show more transfer than after the tests in LH<sub>2</sub>. However, the transfer is not as homogenous as after the experiments at RT in air (*fig. 5.10*). This confirms the lack of adhesion of the transfer film in hydrogen environment.

In this study the relation between the presence of metal fluorides and the tribological performance was not obvious. However, fluoridation of metal surfaces with formation of metal fluoride layers is used in recent space application studies to improve the tribological performance of cryogenic turbo pump bearings [Nosa00]. This point should be investigated further, in particular with in-situ XPS in the tribometer.

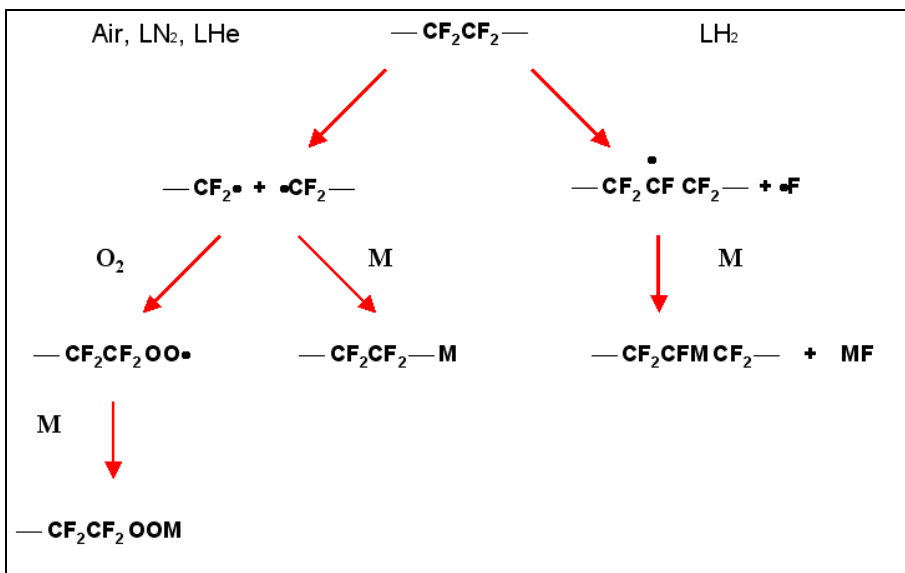
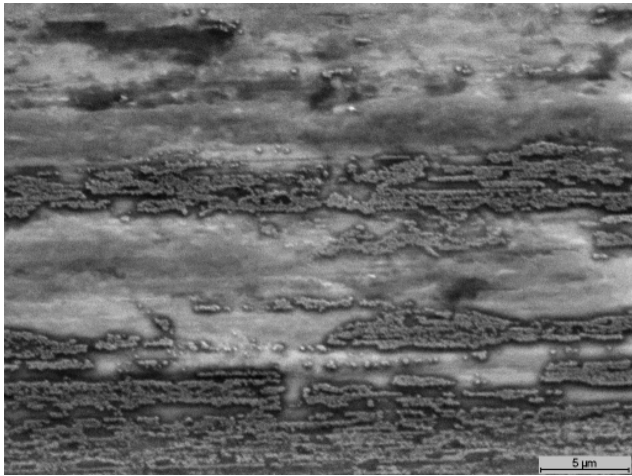


Figure 5.9: Possible chemical reactions produced at the surface of the steel disc during the tribological experiment against PTFE composite [Jint00], extrapolated to other environmental test conditions

## 5 Discussion



*Figure 5.10: SEM image of the surface of the disc after the experiment against bronze/CF filled PTFE at RT in  $H_2$  ( $v = 0.2$  m/s)*



## 6 Conclusion

Many new technologies are based on applications in extreme conditions, such as at low temperatures or in hydrogen environment. Components of cryotechnical machines with interacting surfaces in relative motion like bearings, seals or valves are critical parts. These applications involve new material requirements, in particular regarding their operability and reliability. To fulfil this demand, materials with low friction and good mechanical properties are prime candidates. This is why the tribological behaviour of PTFE- and PEEK-matrix composites filled with carbon fibres (CF) was investigated at cryogenic temperatures and in hydrogen.

Initially, because of the temperature-dependent characteristics of polymer materials, thermal and mechanical properties of these composites were investigated at low temperatures. Specific heat, thermal expansion and thermal conductivity were measured for the two composites. Particular attention was given to the thermal effect in composites with regard to the compatibility of the components and the different thermal coefficients of expansion between matrix and fillers. Thermal shock experiments between room temperature (RT) and  $T = 77$  K, and between RT and  $T = 4.2$  K as well as cryo- and hydrogen treatments were carried out with PTFE- and PEEK-matrix composites. Different coefficients of thermal expansion within the composite produce stresses at the interface between polymer matrix and particles in these experiments. This leads to debonding of the short fibres from the matrix, particularly with PTFE composites. Tribological experiments at RT after the thermal treatments indicated no significant influences on the friction coefficient, but free particles at the friction contact can induce more abrasiv wear.

Tensile tests with PTFE and PEEK composites indicate that YOUNG's modulus increases at  $T = 77$  K compared to RT for both materials due to the fact that below the glass transition temperature, molecular chains are frozen. This improvement at low temperatures is however moderate for PEEK composite which is already under its glass transition at RT.

In the main investigation, tribological experiments were carried out at first with several PTFE and PEEK composites to observe the influence of the matrix, fillers and fibres on the friction and wear performances at  $T = 77$  K comparing to RT.

At low temperatures, the coefficient of friction of CF filled PTFE and PEEK composites is much smaller than the one at room temperature. Wear is hindered and polymer transfer onto the disc does not build a homogenous film as it does at RT. Only scattered particulates are seen at the surface of the counterface. It was shown that the low temperature properties of the polymer improve the tribological behaviour of these composites, in particular due to the higher YOUNG's modulus at  $T = 77$  K.

Whereas at RT friction and wear depend strongly of the CF content, the quantity of fillers and fibres does not have a significant effect at low temperatures. At  $T = 77$  K, the tribological behaviour of PTFE and PEEK composites is mainly influenced by the matrix. PEEK composites have a better tribological performance than PTFE materials especially regarding the wear resistance. Therefore, for applications at successively RT and low temperatures, it is recommended to take the composites which have the optimal performances at RT.

## 6 Conclusion

Furthermore, the influence of the cryogenic medium was investigated with selected composites. Experiments were carried out in LN<sub>2</sub> ( $T = 77$  K), LH<sub>2</sub> ( $T = 20$  K) and LHe ( $T = 4.2$  K), as well as in helium at  $T = 77$  K and hydrogen at RT.

Generally, friction and wear of PTFE and PEEK composites decrease at low temperatures. However, this decrease is not proportional to the temperature of the cryogenic environment, but depends on the temperature at the friction contact. The thermal properties of the cryogenic medium have a significant influence on the tribological performance of the polymer composites, particularly since the thermal conductivity of the polymer decreases.

Experiments at  $T = 77$  K indicate a much better tribological behaviour in LN<sub>2</sub> than in helium gas due to a better cooling efficiency of the cryogenic fluid compared to the gas. In cryogenic liquid, the tribological performances of PTFE and PEEK composites decrease with decreasing temperature. Due to the low heat of evaporation of helium, a small frictional heat in LHe produces a gas environment at the contact area. The generation of a gaseous film around the friction contact decreases significantly the cooling ability of the environment. Moreover, the better cooling efficiency of LN<sub>2</sub> and LH<sub>2</sub> compared to LHe is accentuated by the lower thermal conductivity of helium.

Due to the lower frictional heat at low sliding speed, the effect of low temperatures on the tribological behaviour of these composites was more clearly detected in these conditions, with a change in wear mechanism from mainly adhesive to more abrasive.

Furthermore, LN<sub>2</sub> is an efficient coolant since friction stays constant whatever the sliding velocity. It is also suggested that LN<sub>2</sub> has an influence in removing wear particles from the surface, probably due to its relatively higher viscosity. Indeed, surface analysis of worn composites and discs indicated much less wear debris after the experiments in LN<sub>2</sub>.

EDX analysis of the pin indicates the presence of iron on the worn surface after the experiments at RT as well as in LN<sub>2</sub>, LH<sub>2</sub> and LHe. XPS analysis of the transferred material indicates the presence of iron fluorides down to  $T = 4.2$  K. XPS results suggest that these fluorides lay directly at the surface of the disc and are covered by a layer of PTFE.

Whereas thermal ageing in hydrogen (three hours at  $T = 473$  K) did not significantly affect the tribological behaviour of PTFE and PEEK composites, the influence of hydrogen was particularly seen after the tribological experiments performed in LH<sub>2</sub> on the surface of the disc. Compared with air, nitrogen or helium environments, the adhesion of the transfer is hindered in hydrogen. The reduction effect of hydrogen may have an influence on the tribochemical reactions which appear during sliding, enhancing the formation of iron fluorides, but no influence of the metal fluorides on the tribological performance could be determined in this study.

This work showed that PTFE and PEEK composites are suitable at cryogenic temperatures and also in hydrogen environment. PEEK materials have some advantages regarding their lower wear and their better resistance to thermal shock. Experiments in LN<sub>2</sub> give the best friction and wear performance at low as well as at high sliding speed. Therefore, results from systematic low temperature investigations, which are usually performed in LN<sub>2</sub>, should be taken with precautions since they are not applicable to all cryogenic environments. The behaviour of these composites in LHe does not benefit from the low temperature properties of polymers due to the low heat of evaporation of LHe. Laboratory experiments should be carried out with the same test conditions as for the applications foreseen in LH<sub>2</sub> and especially in LHe.

Although the tribological behaviour of PTFE and PEEK composites is much improved in LH<sub>2</sub> compared to RT experiments, it is recommended to carry out further investigations regarding the long-term effect of hydrogen environment on possible long-term property changes of the materials which may lead to failure in tribosystems.

In this study the relation between the presence of metal fluorides and the tribological performance was not obvious. However, fluoridation of metal surfaces with formation of metal fluoride layers is used in recent space application studies to improve the tribological performance of cryogenic turbo pump bearings [Nosa00]. Therefore further chemical in-situ analyses are recommended in order to measure the exact influence of these metal fluorides on the tribological performance of polymer composites.



## References

- [Ahlb89] AHLBORN K.: *Mechanische Eigenschaften von kohlenstoff-faserverstärkten Thermoplasten für die Anwendung in der Tieftemperaturtechnologie*. Dissertation Uni. Karlsruhe (TH) 1989.
- [Ahlb91] AHLBORN K.: *Cryogenic Mechanical Response of Carbon Fibre Reinforced Plastics with Thermoplastic Matrices to quasi-static Loads*. Cryogenics 31, 1991.
- [Baha92] BAHADUR S., GONG D.: *The Action of Fillers in the Modification of the Tribological Behaviour of Polymers*. Wear 158: 41-59, 1992.
- [Blan93] BLANCHET T., KENNEDY F., JAYNE D.: *XPS Analysis of the Effect of Fillers on PTFE Transfer Film Development in Sliding Contacts*. Tribol. Trans 36(4): 534-544, 1993.
- [Bisw92] BISWAS S.K., VIJAYAN K.: *Friction and Wear of PTFE – a Review*. Wear, 158: 193-211, 1992.
- [Boze01] BOZET J.L.: *Modelling of Friction and Wear from Designing Cryogenic Valves*. Tribol. Intern. 34: 207-215, 2001.
- [Boze93] BOZET J.L.: *Type of Wear for the pair Ti6Al4V/PCTE in Ambient Air and in Liquid Nitrogen*. Wear 162-164: 1025-1028, 1993.
- [Bren65] Brentari E.G: Smith RV: Adv. in Cryogenic Eng. 10: 325, 1965.
- [Brew66] BREWE D.E., SCIBBE H.W., ANDERSON W.J.: *Film Transfer Studies of Seven Ball Bearing Retainer Materials in 33 K Hydrogen Gas at 0.8 million DN Value*. NASA Tech. Note D-3730, 1966.
- [Bris86a] BRISCOE B.J.: *Interfacial Friction of Polymer Composites. General Fundamental Principles*. In: K. FRIEDRICH (Ed.): *Friction and Wear of Polymer Composites*, Elsevier, 1986.
- [Bris86b] BRISCOE B.J., YAO L.H., STOLARSKI T.A.: *The Friction and Wear of PTFE-PEEK Composites: An Initial Appraisal of the Optimum Composition*. Wear 108: 357-374, 1986.
- [Bris90] BRISCOE B.J., TWEEDALE P.J.: *A View of Polymer Composite Tribology*. In: ROHATGI P.K., BLAU P.J., YUST C.S. (Ed.): *Tribology of Composite Materials*, Conference Proceedings, Oak Ridge, TN., 1990.
- [Bryd72] BRYDSON J.: *The Glass Transition, Melting Point and Structure*. In: A. Jenkins (Ed.), *Polymer Science* Vol. 1, pg. 193-247, 1972.
- [Burk81] BURKSTRAND J.M.: *Metal-Polymer Interfaces: Adhesion and X-Ray Photo Emission Studies*. J. Appl. Phys. 52: 4795-4800, 1981.
- [Bush91] BUSHAN B., GUPTA B.K.: *Materials, Coatings and Surface Treatments*. In: MCGRAW-HILL: *Handbook of Tribology*, New York, 1991.

## References

- [Cadm79] CADMAN P., GOSEEDGE G.M.: *The Chemical Nature of Metal-Polytetrafluoroethylene Tribological Interactions as Studied by X-Ray Photoelectron Spectroscopy*. Wear 54: 211-215, 1979.
- [Canf98] CANFER S.J., EVANS D.: *Properties of Materials for Use in Liquid Hydrogen Containment Vessels*. Advances in Cryogenic Engineering (Materials) 44, 1988, Plenum Press, New York.
- [CF03] Database on Material Properties, 2003. <http://www.matweb.com>
- [Clar83] CLARK A.F.: *Thermal Expansion*. In: R.P. Reed, A.F. Clark (Eds.): *Materials at Low Temperatures*. ASM, Metals Park 1983.
- [Czic86] CZICHOS H.: *Introduction to Friction and Wear*. In: K. FRIEDRICH (Ed): *Friction and Wear of Polymer Composites*, Elsevier, 1986.
- [Czic92] CZICHOS H., HABIG K.H.: *Tribologie Handbuch, Reibung und Verschleiß*. Vieweg, 1992.
- [DWV04] The German Hydrogen Association 2004. <http://www.hyweb.de/h2cars>
- [Ekon03] Saint-Gobain Product Informations, 2003. <http://www.ekonol.com>
- [ETB03] Database for Technical Applications, 2003. <http://www.Engineeringtoolbox.com>
- [Evan79] EVANS D.C., LANCASTER J.K.: *The Wear of Polymers*. Wear 13: 85-139, 1979.
- [Flöc99] FLÖCK J., FRIEDRICH K., YUAN, Q.: *On the Friction and Wear Behaviour of PAN- and Pitch-Carbon Fibre Reinforced PEEK Composites*. Wear 225-229: 304-311, 1999.
- [Frey81] FREY H., HAEFER R.: *Tiefemperaturtechnologie*. VDI-Verlag, 1981.
- [Frie92] FRIEDRICH K., KARGER-KOCSIS J., SUGIOKA T., YOSHIDA M.: *On the Sliding Wear Performance of Polyethernitrile Composites*. Wear 158: 157-170, 1992.
- [Frie95] FRIEDRICH K., LU Z.P., HÄGER A.M.: *Recent Advances in Polymer Composites' Tribology*. Wear 190: 139-144, 1995.
- [Fusa90] FUSARO R.L.: *Self-Lubricating Polymer Composites and Polymer Transfer Film Lubrication for Space Applications*. Tribol. Intern. 23: 105-122, 1990.
- [Gard86] GARDOS M.N.: *Self-Lubricating Composites for Extreme Environmental Conditions*. In: *Friction and Wear of Polymer Composites (Friedrich, K.), Composites Materials Series, (Pipes, R.B.)*, vol. 1, pg. 397-447, Elsevier, 1986.

- [Geis00] GEISS G.: *Einfluss von Tieftemperatur and Wasserstoff auf das Versagensverhalten von Glasfaser-Verbundwerkstoffen unter statischer und zyklischer Belastung*. Dissertation, Uni. Karlsruhe (TH) 2000.
- [Glae74] GLAESER W.A., KISSEL J.W., SNEDIKER D.K.: *Wear Mechanisms of Polymers at Cryogenic Temperatures*. Polymer Sci & Technology. 5B: 651-662, 1974.
- [Gong90] GONG D., ZHANG B., XUE Q., WANG H.: *Effect of Tribochemical Reactions of Polytetrafluoroethylene Transferred Film with Substrates on its Wear Behaviour*. Wear 137: 267-273, 1990.
- [Gong91] GONG D., XUE Q., WANG H.: *ESCA Study on Tribochemical Characteristics of Filled PTFE*. Wear 148: 161-169, 1991.
- [Grad01a] GRADT T., BÖRNER H., SCHNEIDER T.: *Low Temperature Tribometers and the Behaviour of ADLC Coatings in Cryogenic Environment*. Tribology Intern. 34: 225-230, 2001.
- [Grad01b] GRADT T., BÖRNER H.: *Einführung in die Tieftemperatur-Tribologie*. In: *Gleitverschleiß polymerer Verbundwerkstoffe zwischen Raumtemperatur und 4,2 K*. BAM-Sonderheft 3, 2001.
- [Haeg93] HÄGER A.M., DAVIES M.: *Short-Fibre Reinforced, High-Temperature Resistant Polymers for a Wide Field of Tribological Applications*. In K. FRIEDRICH (Ed): *Advances in Composite Tribology*, Elsevier, 1993.
- [Haeg97] HÄGER A.M.: *Polyaryetherketone für den Einsatz in Gleitlagern und Gleitelementen*. Shaker Verlag, Aachen, 1997.
- [Hart94] HARTWIG G.: *Polymer Properties at Room and Cryogenic Temperatures*, Plenum Press, 1994.
- [Hart97a] HARTWIG G., HÜBNER R.: *Fatigue Behaviour of Fiber Composites at Low Temperatures*. Adv. Cryog. Eng. Materials 42: 155-159, 1997.
- [Hart97b] HARTWIG G., HÜBNER R.: *Overview of the Fatigue Behaviour of Fibre Composites at Low Temperatures*. In: *Proc. of the 16<sup>th</sup> Intern. Cryogenic Conf / Intern. Cryogenic Mater. Conf.*, Kitakyushu, Japan 1996, pg. 1977-1980, Elsevier, 1997.
- [Hart98] Hartwig G.: *Properties of Fibre Composites (F2)*. In: B. SEEBER (Ed.): *Handbook of Applied Superconductivity*, pg. 1007-1065 Uni Geneva, 1998.
- [Hein84] HEINICKE G.: *Tribochemistry*. Akademie-Verlag, Berlin, chapter 4.5, 1984.
- [Hüb01] HÜBNER W., MULET G., BERNDEN O.: *Investigations in Materials Behaviour in Cryogenic Tribosystems for Formulation of Safety Regulations*. In: PROC. OF THE 4<sup>TH</sup> INT. SYMP. ON HYDROGEN POWER, vol. 2, pg. 397-401. 2001.
- [Hüb98] HÜBNER W., GRADT T., SCHNEIDER T., BÖRNER H.: *Tribological Behaviour of Materials at Cryogenic Temperatures*. Wear 216: 150-159, 1998.

## References

- [Indu99] INDUMATHI J., BIJWE J., GHOSH AK., FAHIM M., KRISHHARAJ, N.: *Wear of Cryo-treated Engineering Polymers and Composites*. *Wear* 225-229: 343-353, 1999.
- [Jint00] JINTANG G.: *Tribological Effects in Formation of Polymer Transfer Film*, *Wear* 245: 100-106, 2000.
- [Jint97] JINTANG G., SHAOLAN M., JINZHU L., DAPENG F.: *Tribochemical Effects of some Polymers/Stainless Steel*. *Wear* 212: 238-243, 1997.
- [Jish94] JISHENG E., GAWN D.T.: *Tribological Performance of Bronze-filled PTFE Facing for Machine Tool Slideways*. *Wear* 176: 195-205, 1994.
- [Kase75] KASEN M.B.: *Cryogenics* 15: 701-702, 1975.
- [Kens81] KENSLEY R.S., MAEDA H., IWASA Y.: *Transient Slip Behaviour of Metal/Insulator Pairs at 4.2K*. *Cryogenics* 21: 479-489, 1981.
- [Kinl87] KINLOCH A.J.: *Adhesion and Adhesives: Science and Technology*. Kluwer Academic Publishers, 1987.
- [Klei01] KLEIN P., FRIEDRICH K., MULET G., HÜBNER W.: *Untersuchungen zum Verschleißverhalten ausgewählter PTFE-Werkstoffe bei tiefen Temperaturen*. In: *Gleitverschleiß polymerer Verbundwerkstoffe zwischen Raumtemperatur und 4,2 K*. BAM-Sonderheft 3, 2001.
- [Klei05] KLEIN P.: *Tribologisches Eigenschaftsprofil kurzfaserverstärkter Polytetrafluorethylen/Polyetheretherketon-Verbundwerkstoffe*. Dissertation Uni. Kaiserslautern, expected in 2005.
- [Lee85] LEE L.-H.: *Polymer Wear and its Control*. Ed. Lee, ACS, Washington DC, 1985.
- [Lu95] LU Z.P., FRIEDRICH K.: *On Sliding Friction and Wear of PEEK and its Composites*. *Wear* 181-183: 624-631, 1995.
- [Lub66] Lubrication (Tribology) Education and Research. *A Report on the Present Position and Industry's Needs*. Her Majesty's Stationery Office. London. 1966.
- [Maki64] MAKINSON K.R., TABOR F.R.S.: *The Friction and Transfer of Polytetrafluoroethylen*. In: *Proceedings of the Royal Society of London*, vol. 281, 1964.
- [Mich91] MICHAEL P.C., RABINOVICH E., IWASA Y.: *Friction and Wear of Polymeric Materials at 293, 77 and 4.2 K*. *Cryogenics* 31: 695-704, 1991.
- [Mich94] MICHAEL P.C., IWASA Y., RABINOWICZ E.: *Reassessment of Cryotribology Theory*. *Wear* 174: 163-168, 1994.
- [Moul83] MOULDER J.C., HUST J.G.: *Compatibility of Materials with Cryogenics*. In: R.P. Reed, A.F.Clark (Ed.): *Material at low Temperatures*. ASM, Metals Park, 1983.



- [Mule01] MULET G., HÜBNER W., KLEIN P, FRIEDRICH K.: *Tribologische Eigenschaften ausgewählter PTFE-Werkstoffe bei tiefen Temperaturen*. BAM-Sonderheft 3, 2001.
- [Nish97] NISHIJIMA S.: *Cryogenic Properties of Advanced Composites and their Applications*. In: *Proc. 16<sup>th</sup> Intern. Cryogenic Conf./Intern. Cryogenic Mater. Conf., Kitakyushu, Japan 1996*, P1, pg. 19-26, Elsevier, 1997.
- [NIST] NIST Scientific and Technical Database, 2003. <http://srdata.nist.gov/xps>
- [Noda69] NODA T., INAGAKI M., YAMADA S.: *Glass-like Carbons*. *Journal of non-crystalline Solids* 1: 285-302, 1969.
- [Nosa00] NOSAKA M., KIKUCHI M., KAWAI N., KIKUYAMA H: *Effects of Iron Fluoride Layer on Durability of Cryogenic High-Speed Ball Bearing for Rocket Turbopumps*. *Tribology Trans.* 43(2), 163-174, 2000.
- [Nosa88] NOSAKA M., OIKE M., KAMIJO K., KIKUCHI M., KATSUTA H.: *Experimental Study on Lubricating Performance of Self-Lubricating Ball Bearings for Liquid Hydrogen Turbopumps*. *Lubric. Eng.*44: 30-44, 1988.
- [Nosa99] NOSAKA M., WIKUCHI M., OIKE M., KAWAI N.: *Tribo-characteristics of Cryogenic Hybrid Ceramic Ball Bearing for Rocket Turbopumps: Bearing Wear and Transfer Film*. *Tribo. Trans.* 42 (1) : 106-115, 1999.
- [Park91] PARK J.M., MATIENZO L.J., SPENCER D.F.: *Adhesion and XPS Studies on a Fluoropolymer-Metal Interface*. *J. Adhesion Sci. Technol.* 5(2): 153-163, 1991.
- [Reed83] Clark A.F. (Ed.): *Materials at Low Temperatures*. Reed R.P., ASM, Metals Park, 1983.
- [Sana97] SANADA K., SHINDO Y., HORIGUCHI K.: *Non Linear Fracture Behaviour of G-10 Woven Glass-Epoxy Laminates at Liquid Nitrogen Temperature*. In: *Proc. 16<sup>th</sup> Intern. Cryogenic Conf, Kitakyushu, Japan 1996*, P3, 1981-1984, Elsevier, 1997.
- [Sefe86] SEFERIS, J.C., VELISARIS C.N: *Crystallisation Kinetics of Polyetheretherketone (PEEK) Matrices*. *Polym. Eng. Sci.* , 26 : 1574-1581, 1986.
- [SNR] SNR Wälzlager Hauptkatalog. Klett Druck 1987.
- [Song93] SONG J., EHRENSTEIN G.W.: *Friction and Wear of Self-Reinforced Thermoplastics*. In K. FRIEDRICH (Ed): *Advances in Composite Tribology*, Elsevier, 1993.
- [Spin98] SPINADEL E., GAMALLO F., NUNEZ G., SPINADEL F., CERVINO M.: *Hydrogen Energy Progress XII*. In: *Proc.12th World Hydrogen Energy Conf. Buenos Aires, June 1998*, vol. 1, pg. 369, 1998.
- [Suh73] SUH N.P.: *The Delamination Theory of Wear*. *Wear* 25:111, 1973.

## References

- [Suzu97] SUZUKI T., USAMI S., TSUKAMOTO H., OTSUKA M.: *Effects of Friction on Shear/Compressive Strength of High-Density GFRP at Low Temperature*. In: *Proc. 16<sup>th</sup> Intern. Cryogenic Conf, Kitakyushu, Japan 1996*, P3, pg. 1985-1988, Elsevier, 1997.
- [Svir81] SVIRIDYONOK A., KHOLODILOV O.V.: *A Study of the Morphology of Friction-Transferred Products of Polymers*. ASLE Trans. 25(3) : 286-390, 1981.
- [Tabo81] TABOR D.: *Friction- The Present State of Our Understanding*. Trans. ASME, 103 : 169-179, 1981.
- [Taka97] TAKAO T., NEMOTO T., KONDA H., KASHIMA D.T., YAMANAKA A.: *Frictional Characteristics of High Strength Polyethylene Fiber Reinforced Plastics*. In: *Proc. 16<sup>th</sup> Intern. Cryogenic Conf, Kitakyushu, Japan 1996*, P3, pg. 1993-1996, Elsevier, 1997.
- [Tana73] TANAKA K., UCHIYAMA Y., TOYOOKA S.: *The Mechanism of Wear of Polytetrafluoroethylene*. Wear 23: 153-172, 1973.
- [Tana86] TANAKA K.: *Effect of Various Fillers on the Friction and Wear of PTFE-Based Composites*. In: K. Friedrich (Ed.): *Friction and Wear of Polymer Composites*, Elsevier, 1986.
- [Theil02a] THEILER G., HÜBNER W., GRADT T., KLEIN P., FRIEDRICH K.: *Tribological Behaviour of PTFE-composites against Steel at Cryogenic Temperature*. Tribol. Intern. 35: 449-458, 2002.
- [Theil02b] THEILER G., HÜBNER W., GRADT T., KLEIN P., FRIEDRICH K.: *Influence of low Temperatures and Environmental Media on the Frictional Characteristics of PTFE Composites*. In: *Proc. 19<sup>th</sup> Int. Cryogenic Engineering Conf., ICEC 19, Grenoble, France, 22-26 July 2002*, pg. 717-720, 2002.
- [Theil02c] THEILER G., MEINE K., HÜBNER W., KLEIN P., FRIEDRICH K.: *Thermal Shock Cycle Experiments between Room and Cryogenic Temperatures on Polymer Composites*. In: *Proc. 19<sup>th</sup> Int. Cryogenic Engineering Conf., ICEC 19, Grenoble, France, 22-26 July 2002*, pg. 729-732, 2002.
- [Theil03] THEILER G., HÜBNER W., KLEIN P., FRIEDRICH K.: *Oberflächencharakterisierung von Paarungen PTFE-Komposit/Stahl nach tribologischer Beanspruchung in LN<sub>2</sub>, LH<sub>2</sub> und LHe - Rolle der Kältemittel-*. In: *Proc. 2<sup>nd</sup> Symposium IVW-BAM 2003*, pg. 17-23, BAM Tagungsbericht 2003.
- [Wiss59] WISSANDER D.: *Wear and Friction of filled PTFE Compositions in Liquid Nitrogen*. ASLE transactions 2 (1), 1959.

## Curriculum Vitae

Name Géraldine Elisabeth Theiler, born Mulet  
 Date of Birth 23.05.70 in Rennes, France  
 Nationality French  
 Family Status Married, 1 child

### Education

09/76 - 06/81 Primaire du champs l'Evêque, Bruz  
 09/81 - 06/85 Collège P. Brossolette, Bruz  
 09/85 - 06/88 Lycée Bréquigny, Rennes  
 08/88 - 05/89 Halls High School, Knoxville, TN, USA. High School Diploma (05/89)  
 09/89 - 06/90 Lycée la Poterie, Rennes. Baccalauréat „C“ (07/90)

### Qualifications

09/90 - 06/92 University of Science, Rennes.  
 Two year degree in maths, physics and chemistry. D.E.U.G „A“  
 (Diplôme d'Etudes Universitaires Générales) (06/92)  
 09/92 - 06/95 Ecole Louis de Broglie, Rennes.  
 Engineering School; three year programme in automated production  
 science, computer science, electrical engineering with a specialisation  
 in material science. Diplôme d'Ingénieur (06/95)

### Trainings

09/93 PSA Peugeot Citroën, Rennes  
 12/93 - 04/94 Sagem SA, Fougères  
 07/94 National Laboratory, Oak Ridge, TN, USA  
 09/94 - 01/95 Legris SA (R&D), Rennes

### Work Experience

01/96 - 12/99 Federal Mogul - Research Centre Rugby, England  
 • Project leader in the Polymer Tribology Department  
 Federal Mogul - Deva GmbH, Stadtallendorf, Germany (2/99-12/99)  
 • Secondment in R&D as development Engineer  
 01/00 - 09/04 Federal Institute for Materials Research and Testing (BAM), Berlin,  
 Germany  
 • Scientist in the laboratory VIII.12: Fretting; Microtribology;  
 Cryotribology

Berlin, May 2005



